Studies on Blends of Natural Rubber and Ethylene-Vinyl Acetate Copolymer with Special Reference to Effects of Crosslinking Systems

THESIS SUBMITTED TO
THE MAHATMA GANDHI UNIVERSITY
IN PARTIAL FULFILMENT OF THE REQUIREMENTS
OF
THE DEGREE OF
DOCTOR OF PHILOSOPHY
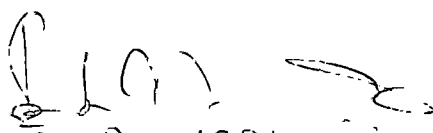UNDER THE FACULTY OF SCIENCE
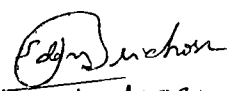
BY
ALEX T. KOSHY, M. Sc.,

SCHOOL OF CHEMICAL SCIENCES
MAHATMA GANDHI UNIVERSITY
KOTTAYAM, KERALA
INDIA

DECEMBER, 1991

D E C L A R A T I O N

This is to certify that the thesis entitled **Studies on blends of natural rubber and ethylene-vinyl acetate copolymer with special reference to effects of crosslinking systems** is an authentic record of the research work carried out by **Mr. Alex. T. Koshy** under our joint supervision and guidance, during the period from March 1988 to December 1991, in partial fulfilment of the degree of Doctor of Philosophy, under the Faculty of Science of Mahatma Gandhi University. The work presented in this thesis has not been submitted for any other degree or diploma earlier. It is also certified that **Mr. Alex. T. Koshy** has fulfilled the course requirements and passed the qualifying examination for the Ph.D. degree of this University.

23 Dec 1991
DR. SABU THOMAS
Lecturer
School of Chemical Sciences
Mahatma Gandhi University
Kottayam-686631

23/12/1991
DR. BABY KURIAKOSE
Deputy Director
Rubber Research Institute of India
Kottayam-686009

·in carrying out this work. The co-operation extended by the Documentation Officer and Staff of the RII Library is acknowledge with thanks.

I express my sincere thanks to the Faculty Members and the Scholars, especially to Mr. Kuruvilla Joseph, of School of Chemical Sciences of Mahatma Gandhi University for the whole-hearted help given to me.

I am thankful to University authorities for granting the junior research fellowship for my research work.

The strenuous effort put by Mr. Mathews T. Itty and Mr. K.A. James for making the drawing neat and legible is gratefully acknowledged.

The encouragement and co-operation from my parents and brothers are also acknowledged.

Alex T. Koshy
23 Dec: 1991.
ALEX T. KOSHY

P R E F A C E

Elastomer blends have gained a lot of interest recently. The major objectives of this approach are property modification and cost dilution. Currently a lot of research is being carried out in this field. However, not much systematic study has been made on the effect of blend ratio and different crosslinking systems of blends based on natural rubber (NR) and ethylene - vinyl acetate copolymer (EVA). In this thesis, the melt flow behaviour, extrudate morphology, degradation characteristics, miscibility, crystallization behaviour, effect of silica, vulcanisation kinetics and mechanical properties of NR-EVA blends are discussed, with special reference to the effects of blend ratio and crosslinking system.

The subject matter of the thesis has been presented in eight chapters.

The first Chapter consists of a brief review of the earlier work in the field of elastomer blends and the scope of the present work.

The experimental techniques and the details of the equipments used are described in Chapter II.

Chapter III contains the results of the studies on the morphology, vulcanisation kinetics and mechanical properties of NR-EVA blends.

The miscibility and crystallization behaviour of NR-EVA blends are discussed in Chapter IV.

Chapter V contains the results of the studies on the melt flow behaviour and extrudate morphology of NR-EVA blends.

The effect of filler on mechanical and dynamic mechanical properties of the blends is discussed in Chapter VI of the thesis.

Chapter VII discusses the degradation behaviour of NR-EVA blends under the influence of heat, ozone and γ-radiation.

Chapter VIII deals with the effects of blend ratio and fillers on the cell structure and properties of microcellular sheets made of NR-EVA blends.

GLOSSARY OF TERMS

A_p :   Cross-sectional area of the plunger

DCP   :   Dicumyl peroxide

d_c :   Diameter of capillary

d_e :   Diameter of extrudate

EVA   :   Ethylene-vinyl acetate copolymer

G   :   Elastic shear modulus

F   :   Force on plunger

z   :   Weight fraction of the filler in the vulcanisate.

HDPE   :   High density polyethylene

IPN   :   Interpenetrating network

IR   :   Isoprene rubber

l_c :   Length of the capillary

Mrad   :   Mega rad

NMR   :   Nuclear magnetic resonance

NR   :   Natural rubber

n'   :   Flow behaviour index

1,2 PB   :   Thermoplastic 1,2 polybutadiene

PBR   :   Polybutadiene rubber

PE   :   Polyethylene

PP   :   Polypropylene

phr   :   Parts per hundred of resin/rubber

PVC   :   Poly(vinyl chloride)

Q	:	Volumetric flow rate
rpm	:	Revolutions per minute
S_R	:	Recoverable shear strain
T_g	:	Glass transition temperature
Tm	:	Temperature of melting
TPE s	:	Thermoplastic elastomers
UTM	:	Universal testing machine
V_r	:	Volume fraction of rubber
V_{rf}	:	Volume fraction of filled vulcanisate
V_{ro}	:	Volume fraction of unfilled rubber
%	:	per cent
η	:	Shear viscosity
τ	:	Shear stress at wall
$\dot{\gamma}_w$	:	Shear rate at wall
$\dot{\gamma}_{wa}$	:	Apparent shear rate at wall
$\tau_{11} - \tau_{22}$	:	Principal normal stress difference

C O N T E N T S

CHAPTER 1 – INTRODUCTION

Materials having rubber like properties at room temperature are called elastomers. Rubbers are macromolecular substances capable of passing, under the effect of vulcanisation, from a predominantly plastic state to a predominantly elastic state. Rubbers have a glass transition temperature lower than the temperature at which they are used and are composed of long flexible molecules which are randomly agglomerated and entangled. When chemical bonds are introduced between neighbouring molecules by vulcanisation, the raw rubber is converted into a technically utilizable material; which is capable of large reversible deformations within a broad range of temperature and which does not dissolve but only swells in solvents. From the technological point of view, the following properties of rubber are important[1].

. Elasticity - The ability to undergo large, reversible deformation on application of relatively small stress. The flexibility combined with elasticity is a characteristic property of rubber.

. Ability to accumulate a considerable amount of input energy during deformation, with low hysteresis.

. Considerable chemical resistance.

. Under suitable conditions, rubber has a long service life.

. Rubber compounds can be processed by relatively simple operations to give different products.

. The products are relatively inexpensive.

1.2 REASONS FOR BLENDING ELASTOMERS

In recent years, research and developmental activities in the field of polymer science and technology have been concentrated more on the modification of existing polymeric materials rather than on synthesizing new polymers. The easiest method to develop polymer compositions having the required properties involves physical blending of two or more polymers. All materials attract interest on the basis of their property - processing - cost-performance relationship. The most important concept in polymer blends is additivity of properties. By this we mean that when a polymer is mixed with another polymer, the resulting blend has a property which is the weighed average properties of the individual polymers. Modulus is one of such properties that is expected to obey some additivity relationship[2]. For blends the weighing functions of the composition will be sensitive to the morphology. A very intriguing possibility, although less frequently observed, is synergism in property. Here we refer to a situation where some property, such as tensile strength, for the blend is higher than that of the pure components. The success of a new material depends on several factors such as combination of properties and cost dilution. For example, when we blend a high thermal resistant polymer having poor process-ability with another polymer having good processability and poor thermal stability, the resulting blend may be useful for certain applications for which both the individual polymers are unsuitable.

Similarly, when a costlier polymer is blended with a cheaper one it may reduce the properties to a level still acceptable for a particular application. At the same time it will bring the cost of the blend to a range which is competitive in the market. Thus blending is an attractive means to engineer a material so that the user does not have to pay for more than he needs. This is the most driving force for developing products from elastomer blends.

1.2.1 Problems associated with blending

There are great many problems that should be discussed in connection with elastomer blends. The most important among these include the following[3].

1. It is rare for different polymers to be compatible at molecular level and almost all combinations of polymers are in fact not in a form of solutions one within the other, the blend being in a non-uniform mixture.

2. Ingredients such as vulcanising agent and accelerator are not homogeneously distributed in the two coexisting phases and because of this imbalance, the relative rates of crosslinking in the two phases will be different.

3. Non-equilibrium is readily produced in the case of fillers such as carbon blacks and consideration must be given to the mixing procedure for effective distribution and dispersion of fillers in the components of the blends.

4.   Viscosity and solubility mismatch of the polymers lead to wide variation in size of the dispersed phase. This affects the properties of the blend.

1.3 COMMERCIALLY SUCCESSFUL BLENDS BASED ON ELASTOMERS

Even though there are so many problems associated with the preparation and use of elastomer blends, several blends have been successfully developed to meet diverse performance requirements. For example, blends of NR or SBR with polybutadiene rubber (BR) are used in tread compounds to achieve better abrasion resistance and wet skid characteristics[4]. Similarly blends of NR and SBR are commonly used in footwear applications. In cables, blends of EPDM and EVA offer good electrical properties combined with weathering and ageing characteristics. Blends of nitrile rubber and PVC or blends of EPDM and NR are used for better ozone resistance[5]. To introduce thermoplastic processing characteristics, NR or EPDM is blended with PP or HPDE and such blends[6] have been commercialised in the production of thermoplastic elastomers .

The effect of high curing temperature on physical properties of blends of BR with NR is discussed by Glanvelle[7]. The heat stability imparted by cis-BR when blended with NR or SBR is confirmed by Svetlik[8]. Similar improvements in thermal properties are claimed for blends of emulsion BR with NR by Mc Call[9]. Addition of cis-BR is reported to decrease the tensile strength and modulus

of NR vulcanisates and to increase its elasticity and abrasion resistance[10]. Flannigan[11] commenting on the future consumption of SBR, reports that blends with highly unsaturated EPDM could lead to new applications. The tread-wear and wet skid resistance of SBR 1500 series and their blends are delt with by Kienle[12]. The hard rubber polyblends of SBR and butyl rubber vulcanised with sulphur have been studied in detail by Meltzer[13]. According to Meltzer's report, T_g was found to increase with degree of vulcanisation and dual or stepwise transition from glassy to rubbery characteristics of polyblends was found in all mixes. Reversion occurred on over cure and the temperature coefficient of vulcanisation of SBR-butyl blends was also calculated[14]. Sutton[15] reported that blends of EPDM with NR, SBR, NBR or CR gave compounds having good ozone and ageing resistance and good compression set characteristics. Stake[16] compared laboratory studies of tyre tread compounds based on SBR-EPDM and SBR-BR-EPDM blends with field performance. Results of the tests of heat ageing, groove cracking and abrasion resistance compared with those of SBR and SBR/BR controls indicated that the EPDM blends can be used in treads without antioxidants.

In blends with NR for the innerliners of tubeless tyres two characteristics of butyl rubber which are particularly advantageous are its damping properties[17] and impermeability[18]. Blends of chloro-butyl with nitrile rubber were studied in an attempt to develop vulcanisates having the desirable properties of the components at

lower cost[19]. EPDM-NBR blends have also been considered for obtaining moderate resistance to oils and ozone combined with an acceptable level of general mechanical properties[20]. A blend of flurosilicone and silicone can be easily bonded using flurosilicone adhesive, has better processing and technological properties and is cheaper than flurosilicone itself[21].

1.4 STUDIES ON ELASTOMER BLENDS

Properties of elastomer blends depend on several factors and a thorough understanding of these parameters is essential to predict the behaviour of elastomer blends. These include morphology, compatibility, interfacial adhesion, dispersion and distribution of ingredients, cure characteristics, melt flow behaviour and the method used for blend preparation. The influence of the above parameters on the properties of elastomer blends is briefly discussed in the following sections.

1.4.1 Morphology of polymer blends

Major factors which govern the morphology of polymer blends are (1) component ratio, (2) melt viscosity, (3) rate of shear and (4) presence of additives such as fillers and plasticizers. Apart from the above, the morphology of polymer blends also depends on the thermodynamic properties of the components (e.g., their Gibb's free energy of mixing and the surface tension) and on

parameters characterising the mixing process (e.g., the velocity gradient profile, mixing time and heat transfer during mixing and solidification of the polymer blend).

Danesi and Porter[22] have shown that for the same processing history, the composition ratio and melt viscosity difference of the components determine the morphology. Where the blend components have similar melt viscosities, the resultant morphology is a very fine and a uniform distribution of the minor component in the major one, no matter which one is the minor component. When the components have different melt viscosities, the morphology of the resultant blend depends on whether the minor component has a lower viscosity than the major one. If the minor component has a lower viscosity this component will be finely and uniformly dispersed with domains oriented in the sheared direction. In contrast, the minor component will be coarsely dispersed in essentially spherical domains if its viscosity is higher than that of the major constituent.

Morphology of different polymer blends has been studied by various researchers[22,23-31]. Baer[24] found mechanical and dynamic properties to be dependent mainly on the particle size of the dispersed phase and independent of the processing methods. Studies conducted by Miller[27], on blends of polypropylene and uncross-linked EPDM rubbers of varying molecular weight, crystallinity and viscosity, established correlation between rubber type and extent of dispersion in the final blends. Cimmino and coworkers[28] have

studied the morphology - composition relationship in binary polyamide - rubber blends. Yang and coworkers[29] have reported the compatibility of polypropylene with ethylene - propylene - diene rubber, polybutadiene rubber and styrene-butadiene rubber through characterisation of blend morphology. Studies conducted by Danesi and Porter[22] using phase contrast microscopy on EPDM-PP blends revealed that the elastomer phase formed the dispersed phase at lower concentrations. The dispersed particles of the rubber phase have undergone deformation under high shear stress. De and co-workers[31] have studied the morphology of NR-PP blends by preferential etching of the NR phase.

1.4.2 Interpenetrating network

An interpenetrating polymer network (IPN) consists of a co-continuous interlocking network of respective constituents[32,33]. IPN can be made simultaneously or sequentially. A simultaneous IPN is formed from the polymerisation and crosslinking of premixed monomers or linear pre-polymers. During network formation, the tendency for phase separation is promoted by the increasing molar mass of the constituents. But, provided the time scale for segregation is long relative to the crosslinking reactions, interpenetrating network can be achieved. In a sequential IPN one network is established prior to the formation of the second. Phase separation is more extensive than in simultaneous IPN, but co-continuity is still achieved. All rubber blends formed by mixing and crosslinking are regarded as

IPN. Semi IPN is often used in reference to an IPN in which one component remains uncrosslinked. From the structure of IPN it is expected that mechanical performance will be additive with regard to the component properties. Interlocked networks can transfer greater mechanical properties than a completely phase separated morphology.

1.4.3 Compatibility and compatibilizers

Compatibility can be defined in its strict sense as molecular miscibility. Compatibility can also be defined in industrial scene as a property of blends which has a relative ease of fabrication and a resistance to gross phase separation during cooling down from the homogeneous or heterogeneous molten mixture. In order to reduce this phenomenon, compatibilizers are used. A compatible blend of an incompatible polymer pair can be prepared by using a block or a graft copolymer as the compatibilizer. In a phase separated system the chain segments of the copolymers will diffuse into each phase and thereby the interfacial energy decreases. The copolymer prevents the coalescence of individual phases. For achieving compatibility without the addition of compatibilizers it is needed that functional groups are placed in or along the main chain of both polymers which show mutual attraction. Examples of such systems are blends of poly-chloroprene (CR) and epoxidised natural rubber (ENR), ternary systems such as ENR-XNBR-CR and NBR-ENR-PVC which were reported by De and coworkers[34,35].

1.4.4 Distribution of compounding ingredients

An important factor for obtaining acceptable vulcanisate properties in a rubber blend is the development of a satisfactory network structure in each phase. During mixing, curative more often make first contact with the lower viscosity phase, since it tends to occupy the outer regions of the flowing rubber mass. According to Leblanc[36] the curative locates within the continuous phase since the lower viscosity component tends to become the continuous phase. Generally the details of the mixing scheme will affect the distribution of curatives. Since the levels of sulphur and accelerators typically employed in rubbers are above their solubility limits curative migration can occur[37-40]. Owing to the higher solubility of sulphur in unsaturated elastomers and greater affinity of many accelerators for more polar rubbers[37,41-43], significant difference in crosslink density of the phases of rubber blends can result. In addition to this, if the rate of vulcanisation varies considerably between elastomers of the blend, depletion of the curative in the faster curing component can cause its migration and further enhance the cure imbalance[44]. This problem is usually observed in blends of dissimilar rubbers. Preblending of curative into the respective elastomers before blending the rubbers can improve the crosslink distribution[36]. This will also prevent prevulcanisation (scorch) problems. Cure imbalance can be overcome by chemical modification of accelerators so that their solubilities in the components of the rubber blend will be nearly equal and also by direct attachment

of the curative to the polymer chain[45-47].

Distribution of fillers and various processing aids in a multi-component rubber blends can also be non-uniform. This will also influence the properties. Extensive investigation in this area has demonstrated the preferential uptake of carbon black by certain rubbers, the unsaturated rubbers exhibiting the greatest affinity for carbon black[48]. During mechanical mixing of carbon black with unsaturated elastomers, sufficient interaction, primarily chemisorption occurs to prevent any subsequent transfer of the black. If the method of mixing is less vigorous or involves rubbers of higher saturation, transfer of the carbon black to phases with which it is more compatible can occur.

Oils, resins and other compounding ingredients can also, of course, have differing affinities for the phases of the blend. Their non-uniform distribution as well as post-mixing migration have been reported[48-50].

1.4.5 Cure rate incompatibility

There is an increased technological interest in the use of blends of various dissimilar rubbers. But, there are technological problems which are frequently the result of some type of mutual incompatibility which can exist between dissimilar elastomers. Three types of incompatibility have generally been noted. They are incompatibility due to viscosity mismatch, which prevents or greatly delays the

formation of intimate blends[51,52], thermodynamic incompatibility which prevents the mixing on the molecular scale[53,54] and in-compatibility due to cure rate mismatch[55-58]. In cure rate mismatch, the curative which is available in a composition is consumed by the faster curing component. The cure rate incompatibility happens when both the elastomers are vulcanised by the action of the same curing ingredients. The reaction rates of two elastomers are significantly different due to the solubility difference of the curative in elastomers. This behaviour is shown by blends which contain two elastomers which have wide difference in unsaturation.

1.4.6 Melt flow behaviour

In most industrial scale applications, polymer blends are made by melt mixing process. Hence studies of their rheological properties are of paramount importance. Further more, these properties govern the processability of any given blend. From the rheological point of view, the polymer blends are very complex systems. It is known that blending of polymers of different types produces heterogeneous systems. The dispersion medium and dispersed phase may differ greatly in their molecular structure and in the level of molecular interaction, resulting in polymeric blends having different rheological behaviour. It has been reported[59] that flow of polymer blends should be regarded as the combined flow of materials of differeing viscosity. From earlier studies[60.61], it has been concluded that blends of

polymers of similar chemical structure show viscosity which is similar to or greater than the additive values. But blends of elastomers of different chemical structure generally have a lower viscosity than the individual components of the blend.

Flow properties of polymer blends have been studied by various researchers[61-67]. Goettler and coworkers[65] have shown that olefinic thermoplastic vulcanisates behave like highly filled fluids during flow and their viscosity follows the Power law model over a wide range of shear rates and temperatures. The crosslinked blends give lower extrudate swell compared with the uncrosslinked blends. Scanning electron microscopy studies of the extrudates of thermoplastic guayule rubber (GR)-HDPE blends showed that at higher shear rates the sizes of the GR domains decreased[66]. The viscosity of the blends was found to be a non-additive function of the viscosity of the components and it was always lower than that predicted by simple linear additivity. The formation of a sheath and core type configuration during extrusion, with the component of lower viscosity forming the sheath was also observed. The rheological behaviour of EPDM-PP blends has been studied in detail by Danesi and Porter[22]. Melt flow behaviour of NR-PP blends has been reported by Kuriakose and De[23]. The melt flow behaviour of EVA-PP blends has been studied by Thomas et al.[67].

1.4.7 Methods for blending

When two polymers are mutually insoluble, blends may be produced which are macroscopically homogeneous and have useful properties. This is possible when the mechanical mixing is sufficiently intense so that the viscosities after mixing are high to prevent gross segregation. High shearing force is required to blend high molecular weight elastomers. This is usually carried out in open roll mills, internal mixers, or extruders. With regard to open roll mills, attention has been called to the desirability of similar polymer viscosities for ease of dispersion and to the mastication of NR prior to blending with synthetic rubbers[68].

Shundo et al.[69] compared the use of roll mills and banbury mixers in the preparation of NR-SBR blends and found the mills to furnish uniform compositions. On the other hand, Hess et al.[70] have reported more wider distributions of polymer zone-size in mill mixes than banbury mixes, confirming less critical nature of banbury blending procedures reported by other research groups[66,68].

1.5 CHARACTERISATION OF BLENDS

Various methods are used to characterise polymer blends. These methods are effective in understanding the morphology, miscibility, phase transition, and similar characteristics of the blends.

1.5.1 Electron microscopy

The most direct method of examining the structure of a multi-phase polymeric system is the direct observation under the electron microscope. When there is difference in unsaturation, staining techniques (eg. with OsO_4 or RuO_4) have been used to enhance the contrast. In elastomer blends a method known as ebonite method[71] is followed which makes use of the preferential reaction of one of the rubber phases with sulphur and zinc, to effect a large increase in electron density. The other method consists of swelling in a particular solvent to get phase contrast[72]. The blend is immersed in a solvent, stretched and subsequently observed under the electron microscope after evaporation of the solvent. The phase which was more swollen will thin out by streching.

1.5.2 X-ray and light scattering

Irradiation of matter usually gives rise to scattering of a portion of the incident intensity, where both the energy and propagation vector of the scattered wave may differ from that of the incident radiation. The angular dependence of the elastic scattering provides morphological information. Elastic light, X-ray and neutron scattering all result from the heterogeneities in the structure of the irradiated material. In a homogeneous system, thermal fluctuations in density and composition are responsible for the scattering. In multiphase polymer blends the angle dependence of the scattering

reflects the size and spacial distribution of the phases and so it can be applied to the study of the morphology of rubber blends. There is an extensive literature devoted to methods of analysing scattering data from multiphase system[73,74].

1.5.3 Thermal analysis (glass transition characteristics)

The degree of homogeneity in elastomer blend is assessed by the measurement of the temperature of transitions from rubbery to glassy state. This can be accomplished with a variety of methods, including calorimetry and dynamic mechanical measurements as well as less common techniques such as dilatometry and radio thermal luminescence. The observation of distinct transitions corresponding to the respective components of the blend indicates the existence of a multiphase structure. The presence of a single transition shows phase homogeneity. If the T_g's are close they may appear as single broad transition. Dynamic mechanical analysis of a homogeneous blend shows a single transition.

1.5.4 Nuclear magnetic resonance spectroscopy

There are a number of NMR methods used to determine the structure of polymer blends. If the components of a blend have different glass transition temperatures, proton NMR can be utilised to assess the phase structure of the blend by taking advantage of the rapid decrease of proton-proton coupling with nuclear separation[75-78]. At a temperature intermediate between the glass

transition temperatures of the components, observation of only a single broadline width is an evidence of spacial homogeneity on a scale of about one nanometer. Use of ^{13}C NMR helps to understand the molecular motions in a miscible blend. NMR imageing of solids is an increasingly popular technique which have applications to polymer blends. Recently, it has been used to characterise the phase sizes with a spacial resolution of less than 50 μm in immiscible mixtures containing polybutadiene[78].

1.5.5 Fluorescence

Fluorescence techniques provide a sensitive probe of polymer morphology. If the two components of the blend are labelled with donor and acceptor fluorophores respectively, non-radiative energy transfer is possible. The efficiency of this energy transfer is strongly dependent on the distance between the fluorophores. Phase separation will suppress the interaction. Measurement of the relative fluorescence intensity of the donor and acceptor, can therefore reveal the spacial proximity of the blend components[79-81]. A some what related technique relies on the quenching of a labelled species by the second component of a blend to reduce the fluorescence intensity when the morphology is homogeneous[82-84]. Upon phase separation the quenching is reduced, effecting an increased intensity.

1.6 ETHYLENE-VINYL ACETATE COPOLYMERS

1.6.1 Synthesis and structure

Ethylene-vinyl acetate copolymers can be produced to cover
a complete range of co-monomer ratio from 99:1 (ethylene:vinyl
acetate) to 1:99. These materials are produced commercially by three
different basic polymerisation methods. They are continuous bulk,
solution and emulsion polymerisation. Only the first two of these
are used commercially to produce copolymers having 5 to 50%
vinyl acetate content. These materials are classified as thermoplastic
elastomers (TPEs). Emulsion polymerisation is used to produce
copolymers containing   60-99% vinyl acetate and these cannot be
classified as thermoplastic elastomers[85]. The thermoplastic rubbery
behaviour is associated with the polyethylene crystallinity which
provides physical crosslinks that melt at moderately elevated
temperature. The structure of ethylene-vinyl acetate copolymer is
given below:

$$\left[\begin{array}{c} -CH_2-CH_2-CH_2-CH-CH_2-CH_2- \\ | \\ O \\ | \\ C=O \\ | \\ CH_3 \end{array} \right]$$

Ethylene   Vinyl acetate
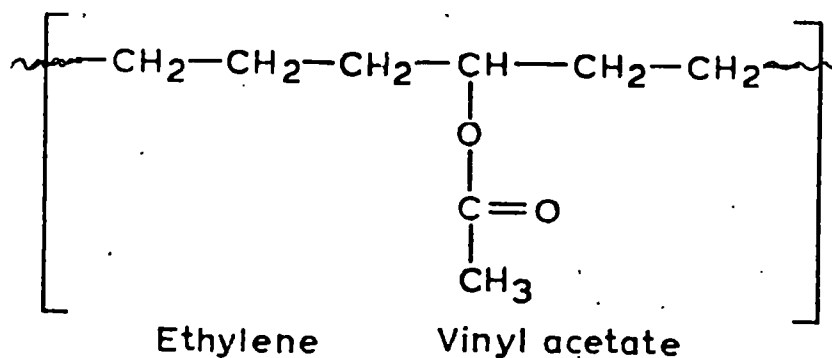
1.6.2 Structure-property relations

The properties of EVA copolymers can be varied over a wide range by controlling the co-monomer ratio, molecular weight and other structural features. This has made possible a diversity of end uses unparalleled by many other polymers. The first effect due to the relatively bulky nature of the acetoxy side chain, is a reduction in the ability of the polymer chains to close pack and form crystalline regions often referred to as crystallites.

Crystallinity is of supreme importance in controlling properties for particular end use and is very largely responsible for the unparalleled versatility of these products. On increasing crystallinity, properties such as modulus, surface hardness, tensile yield strength, and chemical resistance are increased, while impact strength, optical clarity, gas permeability, environmental stress crack resistance, coefficient of friction, retention of mechanical strength at higher filler loading and compatibility with other polymers are decreased.

The second over riding effect of vinyl acetate content results from the polar nature of the acetoxy side chain. Thus as the vinyl acetate content increases, the polarity of the copolymer increases. This gives rise to a number of interesting and important properties such as dielectric loss factor and compatibility with polar polymers.

Similar to other polymers, the average molecular weight has a major influence on properties of EVA. As the molecular weight

increases, the viscosity, softening point, environmental stress crack resistance, impact strength, tensile strength at break, stiffness, resistance to chemicals etc. increases. The molecular weight distribution also affects properties. EVA copolymers of broad molecular weight distribution will have relatively high viscosity at very low shear stresses. But at high shear stresses the flow will be significantly easier than EVA having a narrow molecular weight distribution.

1.6.3 Blends based on EVA

The semi-crystalline nature and polarity enable EVA copolymers to form compatible blends with many other polymers. An especially important outlet is for the improvement of environmental stress cracking resistance of PE, particularly for sheathing of telephone cables[85]. The mechanical properties of EVA-PE blends have been reported by Kovacs and Kallo[86]. The compatibility of these blends was studied by scanning electron microscopy. An optimum composition in terms of mechanical properties was established. Blends of block copolymers are also widely used in shoe soling in which EVA copolymers confer improved processability and ozone resistance to the rubber[85].

Wide compatibility of EVA with other polymers also leads to its use as the base polymer in universal masterbatches for incorporating various additives into other polymers such as nylon,

PVC and rubbers[85]. Blends of EVA with PVC have been studied by Mensel[87], Matsuo[88] and by Terselins and Ranby[89]. Their studies indicated that addition of EVA improved the impact strength, ageing resistance and weathering performance for outdoor applications. Incorporation of 10 parts by weight of EVA to PVC gave a hetero-geneous two phase system[90]. The EVA domains were dispersed in PVC matrix. EVA polymers having high molecular weight are preferred for blending with other polymers for high mechanical strength. The low molecular weight grades are used as lubricants or processing aides in a wide variety of polymers such as nylon, PVC, high impact PS, ABS and PP[85]. De and coworkers[91] reported on the morphology and mechanical properties of thermoplastic EVA-PP blends. The mode and the state of dispersion of EVA copolymers in polyamide blends have been reported by Martuscelli et al.[92].

1.7.1 Structure and properties of natural rubber (NR)

Chemically NR is a polymer of isoprene units linked together at 1-4 positions and arranged in cis-configuration as shown below:

$$CH_3 \qquad H$$
$$\diagdown C = C \diagup$$
$$\diagup \qquad \diagdown$$
$$\sim\!-CH_2\!-\!CH_2 \qquad CH_2\!-\!CH_2\!-\!\sim$$
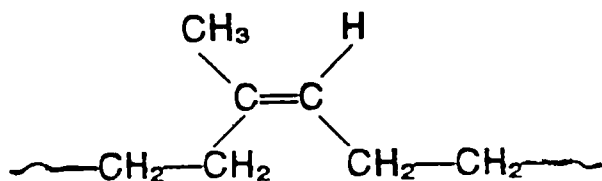
The molecular weight ranges from 3 to 10 lakhs. Due to its wide molecular weight distribution it has good processability. It is having good green strength and tackiness. On stretching it can undergo strain induced crystallisation which provides very high gum strength. The gum strength of NR ranges from 20-30 MPa at normal temperature. The strength drops rapidly with increase in temperature but is still better than many other elastomers. Natural rubber has excellent abrasion resistance, especially under mild abrasive conditions. Its high resilience, good resistance to flexing and fatigue together with low hysteresis make natural rubber useful in applications where cyclic stressing is involved. Its high green strength and tackiness are made use of in fabricating rubber products and in adhesives. However, due to the presence of a very reactive double bond in the main chain, it is susceptible to attack by oxygen, ozone etc. and has very poor resistance to high temperature.

1.7.2 Blends based on natural rubber

Natural rubber is blended with synthetic rubbers for a wide variety of purposes. One important example[93] is the blend of NR with polybutadiene rubber (BR). BR is blended with NR to achieve better processing characteristics and improved wear properties. Baker et al.[94] reported that upto 20 per cent of natural rubber may be introduced into a chloroprene rubber formulation without serious change in oil resistance. Blending of natural rubber with EPDM helps

to improve the ozone resistance of NR[65,95]. Blends of thermoplastics such as isotactic polypropylene and high density polyethylene and NR couple the superior processability characteristics of thermoplastics and service properties of elastomers[6]. The auto-adhesion between the elastomers can be improved by blending synthetic rubbers with NR. The tackiness increases with NR content of the blend.

1.8 SCOPE OF THE WORK

From the forgoing discussions it is evident that much work have been done to understand the processing characteristics and physical properties of every successful blend developed so far. When new elastomer blends are developed or such blends are tried for new applications, a detailed study on all aspects concerning the preparation, properties etc. are thoroughly investigated. Usually the components for blending are selected considering the properties to be achieved and compatibility of the components with respect to molecular and vulcanisation characteristics. As elaborated in the previous section, the mechanical properties of NR are excellent. However its resistance to ageing and ozone attack are poor which precludes its application in many critical areas. EVA copolymer possesses excellent ozone, weather and stress crack resistance. Its processing characteristics are more similar to those of thermoplastic materials. Hence it is expected that we may be able to couple the good properties of both these polymers through the process of blending. However, detailed studies on various aspects such as

processability, morphology, vulcanisation system, effect of degrading agents, reinforcement by fillers etc. are essential to develop successful blends from these two polymers. Even though NR-EVA blends are being used in some areas like footwear, no systematic study covering the above aspects has been reported so far. Hence this thesis work aims at investigating the above mentioned aspects of NR-EVA blends. Special emphasis has been made to investigate the effect of different cure systems on the processing, mechanical and dynamic mechanical properties of the blends.

1.9 OBJECTIVES OF THE WORK

NR and EVA are indigenously available at reasonable price. If we can develop blends having the prominent properties of NR and EVA, such blends may find application in areas where costly and imported elastomers are used at present. For achieving this objective detailed investigation on the following aspects were necessary.

1.9.1 Morphology

In a two-phase polymer blend, it has been established that the phase having largest proportion becomes the continuous phase, when both polymers are of similar viscosity at the temperature and shear rate of mixing. But at equal concentration, the polymer with lower viscosity tends to become the continuous phase. This

morphology is common with all heterogeneous polymer blends of two mutually incompatible components. Most of the elastomer blends show similar morphological features. The main physical factors that control the final morphology of the blends are component ratio, their intrinsic melt viscosity, rate of shear during melt mixing etc. Natural rubber (NR) possesses higher melt viscosity than ethylene-vinyl acetate copolymer (EVA). Therefore morphological studies of their blends are essential in order to understand the composition at which each phase becomes continuous. Since the properties of the blends are highly dependent on phase continuity, morphological studies of NR-EVA blends are necessary.

1.9.2 Vulcanisation characteristics

In blends, cure rate incompatibility is due to the difference in the solubilities of the curatives in the elastomers and also due to difference in rate of vulcanisation of the two components even when they have the same level of curatives. Natural rubber can be crosslinked using sulphur. But EVA cannot be crosslinked using sulphur because of its saturated backbone structure. Peroxides can be used for vulcanising both NR and EVA. Hence the effectiveness of a mixed crosslinking system, which contains both sulphur and peroxide, is worth to be examined in NR and EVA blends. In order to select an effective cure system for a particular blend ratio, studies of parameters such as cure time, cure rate index, activation energy, first order rate constant etc. are to be carried out.

1.9.3 Melt flow behaviour

A reliable knowledge of the melt flow characteristics of the blends over a wide range of shear rates or stresses and temperature is of paramount importance in predicting the flow characteristics during processing. Elastomers exhibit highly non-Newtonian flow behaviour and hence the melt viscosities are highly sensitive to rate of shear. NR and EVA possess different melt viscosities. In order to standardise the processing conditions for their blends, for any particular application, the effect of shear stress at different temperatures on the viscosity is to be understood. The elastic parameters such as die swell, principal normal stress difference, shear modulus, recoverable shear strain etc. are also highly essential to explain the ultimate properties of the products obtained from such blends. The above information can be obtained only through a detailed study of the rheology of the blends.

1.9.4 Effect of fillers

Fillers are used in rubber compounds for reinforcement, for modifying the processing characteristics and also to reduce the cost. Fillers are important to reduce the shrinkage and to increase the modulus and hardness. The blends prepared from NR and EVA can be used for making coloured articles. Normally we can use non-black, reinforcing fillers, such as silica for this. The reinforcement activity of the filler in blends depends on the affinity of the filler towards

each component of the blend and also on the distribution and dispersion of the filler in each phase of the blend. Hence a detailed study on the effect of filler on the mechanical properties is essential for suggesting the correct proportion and type of filler for a particular blend based on NR and EVA.

1.9.5 Degradation behaviour

In recent years, the effect of degrading agents on polymeric materials has been studied with a view to developing such materials for use under degrading conditions. Natural rubber has poor ageing resistance. But EVA has got an excellent ageing characteristics due to its saturated structure. For developing a product from their blend, the behaviour of the blend towards different degrading agents such as heat, ozone, oxygen and gamma radiation is to be understood.

1.9.6 X-ray, thermal and dynamic mechanical properties

Miscibility is an important factor which governs the ultimate property of a blend. EVA is crystalline and NR is crystallizable. The mechanical properties of these two materials are very much dependent on this factor. X-ray, DSC and DMTA methods are highly useful to study the miscibility and change of crystallinity in polymer blends. Hence in NR-EVA blends also the above characteristics are studied to correlate the changes in properties with blend ratio and type of cure system.

1.9.7 Cell structure of microcellular sheets

Blends of NR and EVA already find application in footwear because of light weight and good abrasion resistance characteristics. However, the properties of microcellular soles depend on the cell structure besides other parameters such as blend ratio, and filler loading. A detailed study on the above parameters is required to develop quality products such as microcellular sole based on NR-EVA blends. The results of such studies will be useful in developing products that meet standard specifications prescribed by national and international organisations.

CHAPTER II – EXPERIMENTAL TECHNIQUES

The details of the materials used and experimental techniques adopted in the present investigation are given in this Chapter.

II.1 MATERIALS USED

II.1.1 Natural rubber

The natural rubber (NR) used was crumb rubber, as obtained from the Rubber Research Institute of India, Kottayam. This rubber satisfied the Bureau of Indian Standard specifications for ISNR-5 grade natural rubber. The specification parameters and their limits for the ISNR-5 grade natural rubber are given in Table II.1. Since the basic properties such as molecular weight, molecular weight distribution and the contents of non-rubber constituents of natural rubber are affected by clonal variation, season, use of yield stimulants and methods of preparation[95,96], rubber from the same lot has been used in a particular experiment.

II.1.2 Ethylene-vinyl acetate copolymer

The ethylene-vinyl acetate copolymer (EVA) used was having 18 per cent vinyl acetate content and was obtained from Exxon Chemical Company, Houston, USA. The properties of Exxon EVA 218 are given in Table II.2.

II.1.3 Rubber chemicals

Accelerator dibenzothiazyl disulphide (specific gravity 1.50, melting point 170°C) was obtained from M/s Indian Explosives Limited, Rishra, India. Dicumyl peroxide having 40 per cent active

ingredient (specific gravity 1.55) was obtained from M/s Peroxides India Limited, Madras, India. Diethylene glycol (specific gravity 1.117, distillation range below $230^{\circ}C$) and styrenated phenol (specific gravity 1.04) was of chemically pure grade.

II.1.4 Fillers

Silica (INSIL VN_3) used in the present study was supplied by Degussa A.G., West Germany. The approximate composition and properties of INSIL VN_3 are given below:

Feature	Amount
1. Drying loss	○55%
2. Ignition loss	5%
3. SiO_2 (dry ban)	97%
4. Specific gravity	2.0

Clay and calcium carbonate used for the study are having specific gravity of 2.6 and 2.62 respectively. Both were commercially available grades.

II.1.5 Other chemicals

Zinc oxide (specific gravity - 5.5), stearic acid (specific gravity 0.92) and elemental sulphur (specific gravity - 1.9) used in the present study were chemically pure grade.

II.1.6 Special chemicals

The blowing agent used was Azodicarbonamide (ADC). It is a fine yellow powder with an average particle size of 2 to 10 microns and a decomposition temperature of 160°C. On decomposition, the gas evolution is around 190 to 200 cc at NTP and the composition of gas evolved is nitrogen 65%, carbon monoxide 24%, ammonia 5% and carbon dioxide 5%.

II.1.7 Solvents

Benzene and xylene used were of analytical grade.

II.2 PREPARATION OF THE BLENDS

II.2.1 Composition of the blends

The composition of blends of NR and EVA prepared for evaluation under the present study is given in Table II.3. The NR:EVA ratio has been varied from 0 to 100.

II.2.2 Cure systems

The dosage of curing agents has been selected as shown in Table II.4. The curing systems were based on sulphur, peroxide and a mixed one consisting of sulphur and peroxide.

II.2.3 Designation of the blends

The blend ratios are designated by A, B, C, D, E, F, G,

H, I, J as indicated in Table II.3. The subscript 1, 2 or 3 denote sulphur, peroxide and mixed cure system , respectively. Blend containing silica has an additional letter 'S' and loading of silica is indicated by S_0, S_{15}, S_{30}, and S_{45} for 0, 15, 30 and 45 phr of silica, respectively. For example, B_3S_{45} indicates 10:90 EVA:NR blend having mixed cure system and 45 phr of silica.

II.2.4 Blending and compounding

Blends of NR and EVA were prepared in a laboratory model intermix (Shaw Intermix KO) set at a temperature of 80°C and a rotar speed of 60 rpm. NR was masticated for 2.0 min and then blended with EVA for additional 2.5 min. The final temperature of the blend inside the intermix was in the range of 110° to 120°C, depending upon the blend ratio. The blends were compounded in a two roll laboratory mill (150 cm x 30 cm) at a friction ratio of 1:1.25 according to the formulations given in Table II.4.

II.2.5 Time for optimum cure

Optimum cure time at 160°C was determined using Monsanto Rheometer (R-100). The optimum cure time corresponds to the time to achieve 90 per cent (t_{90}) of the cure maximum torque.

II.2.6 Moulding of test samples

The sheeted out compound was compression moulded in a steam

heated hydraulic press at 160°C and the moulding pressure was 10.5 MPa. Test samples for all the physical tests were moulded out using aluminium foils in between the mould surfaces and the compound to reduce shrink marks and stickiness of the vulcanisate.

II.2.7 Compounding of microcellular sheet

Intermix was set at a speed of 60 rpm and an initial chamber temperature of 80°C. Total mixing time was 6 min. The blend was mixed for 2 min and then fillers and other ingredients were added and mixed for 2 min. Then blowing agent and curative were added and mixing continued for another two more min. The mix was dumped at the end of 6 min. The mixes had the formulation given in Table II.6.

II.2.8 Moulding of microcellular sheet

Moulding was carried out in a hydraulic press having steam heated platens at 160°C. The moulding pressure was 10.5 MPa. The mould was loaded with 3 per cent excess compound than the mould volume. When the compound was sufficiently cured (80 per cent of the maximum cure), the press was opened quickly and the sheet expanded out of the mould by itself in all directions. The excess material flown out was trimmed immediately after the removal from the mould to avoid bending of sheets.

II.2.9 Post curing

Post curing will complete the cure of precured sheets and will help in attaining the maximum physical properties. In the present experiments the post curing time given was 3 h at 80°C in a thermostatically controlled hot air oven.

II.3 PHYSICAL TEST METHODS

For parameters described below, at least four specimens per sample were tested for each property and the mean values are reported.

II.3.1 Modulus, Tensile strength and Elongation at break

These three parameters were determined according to ASTM D-412-80 test method, using dumb-bell shaped test pieces. The test pieces were punched out from the moulded sheets using C-type die, along the mill grain direction of the vulcanised sheets. The thickness of the narrow portion of specimen was measured using a dial gauge. The specimens were tested in a Zwick Universal Testing Machine (UTM) model 1474, at 25±2°C and at a cross -head speed of 500 mm per minute. The elongation at break, modulus and tensile strength were recorded on a strip chart recorder. The machine has a sensitivity of 0.5 per cent of full scale load.

II.3.2 Tear resistance

The tear resistance of the sample was tested as per ASTM D-624-81 test method, using unnicked 90° angle test specimens which were punched out from the moulded sheets, along the mill grain direction. This test was also carried out in the Zwick UTM, at a cross-head speed of 500 mm per minute and at 25±2°C. The tear strength values are reported in kN/m.

II.3.3 Hardness

The hardness of the samples was measured as per ASTM D-2240-81 test method using a Shore A type Durometer, which employed a caliberated spring to provide the indenting force. Since the hardness reading decreased with time after firm contact between the indentor and the sample, the readings were taken immediately after the establishment of firm contact.

II.3.4 Abrasion resistance

The abrasion resistance of the samples was tested using a DIN Abrader. It consisted of a drum on to which a standard abrasive cloth is fixed. The drum is rotated at a speed of 40±1 rpm and total abrasion length is 42 meters. Sample having a diameter of 16±0.2 mm and a thickness of 6 to 10 mm, is kept on a rotating sample holder. Usually 10 N load is applied. Initially a pre-run was given for the sample and then its weight taken. The weight

after the final run was also noted. The difference in weight is the abrasion loss. It is expressed as the volume of the test piece getting abraded away by its travel through 42 m on a standard abrasive surface. The abrasion loss was calculated as follows:

$$V = \frac{\Delta m}{\rho}$$

where Δm = mass loss

ρ = density

V = abrasion loss

II.3.5 Rebound resilience

Dunlop Tripsometer (BS 903, Part 22, 1950) was used to measure rebound resilience. The sample was held in position by applying vacuum. It was conditioned by striking the indentor six times. The temperature of the specimen holder and the sample was kept constant at 35°C. Rebound resilience was calculated as follows:

$$\text{Rebound resilience \%} = \frac{1 - \cos \theta_2}{1 - \cos \theta_1} \times 100$$

where θ_1 and θ_2 are the initial and rebound angles, respectively. θ_1 was 45° in all cases.

II.3.6 Compression set

The samples (1.25 cm thickness and 2.8 cm diameter) in

duplicate, compressed to give 25 per cent deflection were kept in an air oven at 70°C for 22 h (ASTM D-395-71, Method B). After the heating period, the compression was released; the samples were cooled to room temperature for half an hour and final thickness was measured. The compression set was calculated as follows:

$$\text{Compression set (\%)} = \frac{t_0 - t_1}{t_0 - t_s} \times 100$$

where t_0 and t_1 are the initial and final thickness of the specimen and t_s is the thickness of the spacer bar used.

II.4   MELT FLOW STUDIES

II.4.1   Equipment details

The melt flow studies were carried out using a capillary rheometer attached to a Zwick UTM model 1474. The extrusion assembly consisted of a barrel, made of hardened steel mounted on a special support, underneath the moving cross-head of a Zwick UTM. A hardened steel plunger, which is accurately ground to fit inside the barrel is held to the load cell extension. An insulating ring thermally isolates the barrel from the rest of the machine and prevents heat losses due to conduction. The capillary is inserted at the bottom of the barrel and is locked using a clamping device. The capillary is made of Tungsten carbide. The barrel was heated using a three zone temperature control system. The difference between

the successive temperature zones in the barrel was kept at 5°C and the temperature of the lower zone, where the capillary is located, is taken as the test temperature.

The moving cross-head of the Zwick UTM runs the barrel at a constant speed irrespective of the load on the melt, maintaining constant volumetric flow rate through the capillary. The cross-head speed can be varied from 0.5 mm/min to 500 mm/min giving shear rates ranging from 3 s^{-1} to 3000 s^{-1} for a capillary of L/D = 40. Forces corresponding to specific plunger speeds were recorded on a strip chart recorder. These values were converted to shear stresses.

II.4.2 Test procedure

Sample for testing was placed inside the barrel which was maintained at the test temperature. The sample was forced down to the capillary using the plunger attached to the cross-head. After a warming up period of three minutes the melt was extruded through the capillary at pre-selected speeds of cross-head. The melt height in the barrel before extrusion was kept the same in all experiments and machine was operated to give ten different plunger speeds. Each plunger speed was continued until the recorded force was stabilised, before changing to the next speed. Forces corresponding to specific plunger speeds were recorded. The force and cross-head speed were converted into apparent shear stress (τ_w) and shear rate ($\dot{\gamma}_{wa}$) at

the wall by using the following equations involving the geometry of the capillary and the plunger:

$$\tau_w = \frac{F}{4A_p \, (l_c/d_c)}$$

$$\dot{\gamma}_w = \frac{(3n' + 1)}{4n'} \quad \frac{32Q}{\pi d_c^3}$$

F   =   Force applied at a particular shear rate.

A_p =   Cross sectional area of the plunger.

l_c =   Length of the capillary.

d_c =   Diameter of the capillary.

Q   =   Volume flow rate.

n'   =   Flow behaviour index, defined by $d(\log \tau_w)/d(\log \dot{\gamma}_{wa})$.

$\dot{\gamma}_{wa}$ =   Apparent wall shear rate.

$\dot{\gamma}_w$ =   Actual shear rate at wall.

n' is determined by regression analysis of the values of τ_w and $\dot{\gamma}_{wa}$ obtained from the experimental data. The shear viscosity η was calculated as

$$\eta = \tau_w / \dot{\gamma}_w$$

The shear stress at the wall need be corrected as suggested by Bagely[97]. But this correction factor diminishes as the length

to diameter ratio increases and for a capillary having L/D ratio 40, it is assumed that the correction factor is negligible. The following assumptions were also made for the analysis of the data.

1. There is no slip at the capillary wall.

2. The fluid is time independent.

3. The flow pattern is constant along the capillary.

4. The flow is isothermal.

5. The material is incompressible.

6. The flow properties are independent of hydrostatic pressure.

II.4.3 Extrudate swell

Extrudate swell was expressed as the ratio of the diameter of the extrudate to that of the capillary used. The extrudate emerging from the capillary was collected without any deformation. The diameter of the extrudate was measured after 24 h rest period using a WILD Stereomicroscope model M 650 at several points on the extrudate. The average value of ten readings was taken as diameter (d_e) of the extrudate and swelling index was calculated as (d_e/d_c) where d_c is the diameter of the capillary. For each sample, the extrudate swell at two different shear rates was determined.

II.5 DEGRADATION STUDIES

II.5.1 Ozone cracking

The apparatus used for studying ozone cracking was ozone test

chamber manufactured by MAST Development Company. The chamber provides an atmosphere with a controlled concentration of ozone and temperature. Ozone concentration used was 50 pphm which is generated by an UV quartz lamp. The test was carried out as per ASM (D-1149-81) specification. The temperature of test was 37.5°C.

II.5.2 Radiation studies

Test samples (2±0.2 mm thick) were irradiated with γ -rays from a ^{60}Co source in a Gamma chamber. The samples were irradiated for different radiation doses at a dose rate of 0.321 Mrad/h in air at room temperature. The mechanical properties were measured before and after irradiation.

II.5.3 Thermal ageing

Test samples (2±0.2 mm thick) were aged at 70°C for 4 days, 7 days and 10 days in an air oven. The tensile and tear strengths were measured before and after ageing.

II.6 DETERMINATION OF VOLUME FRACTION OF RUBBER

The volume fraction of rubber, V_r, in the solvent swollen specimen of gum and filled samples was determined using equilibrium swelling method. Xylene was the solvent used. The samples were allowed to swell at 35±0.1°C in xylene, placed inside squadishes and kept immersed in a thermostatically controlled water bath.

Swollen samples were taken out after 1, 2, 3, 5, 9, 14, 24, 36 and 48 h of immersion in xylene and the surface blotted with filter paper and then quickly weighed in stoppered weighing bottles. It was observed that 48 h were required in most of the cases to attain equilibrium swelling. Samples were then dried in an air oven set at 70°C, for 24 hours, and then in vacuum. The dried samples were weighed accurately after cooling in a desiccator. Three test pieces were taken for each sample to ensure reproducibility. The V_r values were calculated using the method reported by Ellis and Welding[98]. The equations used for calculating the V_r values are given below:

$$V_r = \frac{(D - FT)\rho_r^{-1}}{(D - FT)\rho_r^{-1} + A_o\rho_s^{-1}}$$

Where T = Initial weight of the test specimen.

   D = De-swollen weight of the test sample.

   F = The weight fraction of the insoluble component.

   A_o = Weight of the absorbed solvent, corrected for swelling increment.

   ρ_r = Density of rubber.

   ρ_s = Density of solvent.

From the experimental data, the value of A_o can easily be calculated as described below:

The weight fraction of the solvent absorbed at any time 't' is given by

$$W_t = \frac{S_t - T}{T}$$

where S_t is the swollen weight of the sample at any time 't'. If the equilibrium time is taken as 'X' hours, the percentage increment d_x after 'X' hours is calculated from the equation:

$$d_x = \frac{100 \ (W_x - W_o)}{W_o}$$

where W_o is the weight of the solvent absorbed per gram of the sample without swelling. W_o is obtained from a plot of W_t against t by extrapolating the straight line to zero time. The value of A_o is then given by

$$A_o = A_x \ (1 - \frac{d_x}{100})$$

where A_x is the weight of the solvent absorbed after 'X' hours immersion and is equal to $(S_x - D)$. S_x is the swollen weight of the sample after 'X' hours.

II.7 MORPHOLOGY

For studying the morphology of the blends the natural rubber phase of the uncrosslinked blends was extracted using benzene. The solvent was changed after every 6 h. After 7 days of immersion, the sample was dried in an air oven at $40\pm1^\circ C$. The extracted edge of the sample was examined under a JOEL 35C model Scanning Electron Microscope.

II.7.1 Scanning Electron Microscope

Scanning Electron Microscopy (SEM) has been successfully used for studying the failure surfaces of rubber composites[99]. It has also been found to be a valuable tool in studying the phase morphology of high impact strength blends of PP and EPDM[100]. In using the SEM, the sample preparation is quite simple unlike in other microscopes and it presents a physical picture of the phase structure of the blends under investigation. But care should be taken to keep the sample undisturbed, in dust free atmosphere after the extraction of one phase. Due to the non-conducting nature of the rubber and plastic surfaces, the extracted surface shall be coated with a conducting material such as gold or copper.

II.8 DYNAMIC MECHANICAL PROPERTIES

The dynamic mechanical properties of NR-EVA blends were measured using a dynamic mechanical analyser (Polymer Laboratories

DMTA MK-II), consisting of a temperature programmer and a controller. It measures dynamic modulus (both storage and loss moduli and damping of the specimen under oscillatory load as a function of temperature. The experiment was conducted at a strain amplitude of 64 µm and a frequency of 10 Hz. The heating rate of the samples was 1°C/min. Liquid nitrogen was used to achieve sub-ambient temperature. The mechanical loss factor tan δ and dynamic moduli (E', E") were calculated with a micro computer.

II.9   VULCANISATION KINETICS

The kinetics of vulcanisation was evaluated using Rheometer 100. The range of temperature selected was 160°C to 190°C. The angle of oscillation of rotor was 3° and the frequency was 100 cycles/min.

II.10   THERMAL ANALYSIS

Thermal analysis were carried out using a Perkin Elmer DSC4 differential scanning calorimeter (DSC). DSC was calibrated with ultra-pure Indium. The glass transition temperature (T_g) was recorded at the half height of the corresponding heat capacity jump. The samples were inserted into the DSC-4 apparatus at room temperature and immediately heated to 200°C at the rate of 40°C/min and kept for one minute at this temperature. The samples were quenched to -110°C at the rate of 320°C/min. The DSC scan was made from -110°C to 80°C at the rate of 10°C/min. The T_g values reported in Chapter V were those recorded during the second scan.

II.11 X-RAY ANALYSIS

X-ray diffraction patterns of the samples were recorded with a Philips X-ray diffractometer (Type PW 1840) using Ni filtered CuK_α radiation from a Philips X-ray generator (Type PW 1729). The angular range was 9 to 35° (2 Θ). The samples were of the same thickness and the same area were exposed. The operating voltage and the current of the tube were kept at 40 KV and 20 mA, respectively throughout the entire course of investigation.

The degree of crystallinity and d values have been determined from this study. The X-ray diffraction patterns of the samples were separated into two parts, crystalline and amorphous by taking natural rubber as fully amorphous. The areas under the crystalline and amorphous portions were measured in arbitrary units and the degree of crystallinity (X_c) and the amorphous content (X_a) of the samples were measured using the relation

$$X_c = \frac{I_c}{I_c + I_a}$$

$$X_a = \frac{I_c}{I_c + I_a}$$

I_c and I_a represent the integrated intensity corresponding to the crystalline and amorphous phases, respectively.

II.12 TESTING OF MICROCELLULAR SHEETS

II.12.1 Determination of compression set

Compression set is the difference between the original thickness and that after the application of a specified load for a specified period of time and is expressed as percentage of the initial thickness of the sample.

The test piece having diameter 30 ± 0.2 mm and thickness 9.5 ± 0.2 mm was conditioned at $27\pm1^{\circ}C$ and 65 per cent relative humidity for 24 h. Thickness of each test piece at the centre was measured using a gauge. The test pieces were then placed between the parallel plates of the Wallace constant stress compression set apparatus and a load of 140 ± 1 kg was applied for 24 h. When the test was over, the samples were removed and allowed to recover. After recovery period of one hour the thickness of the samples was noted. Compression set was calculated using the formula:

$$\text{Compression set (\%)} = \frac{(t_0 - t_1)}{t_0} \times 100$$

where t_0 = initial thickness in mm.

t_1 = final thickness in mm.

II.12.2 Determination of split tear strength

It is the maximum load required split off a test piece of specific size, which was separated at a constant speed of 75 mm per minute.

Four rectangular pieces of size 25 x 100 x 7 ± 0.2 mm were cut out along and across the moulded sheet. The test piece was prepared by splitting the sample midway between the top and bottom surface for a distance of 30 mm from one end and thus forms two tongues at the end.

The two tongues of test pieces were clamped between the jaws of the Zwick UTM, Model 1474 and allowed to separate at a constant rate of 75 mm/min. Mean of maximum load of the four samples was taken as the split tear strength.

II.12.3 Determination of heat shrinkage

It is the reduction in length that may occur to a sample of specified size when it is kept in a heating chamber maintained at 100±1°C for one hour.

Sample of size 150 x 25 x 15 mm was cut from the sheet after splitting all the sides of the sample. The test piece was conditioned at 65±5 per cent relative humidity and a temperature of 27±2°C for 24 h prior to testing.

Length of the test piece was measured to the nearest 0.1 mm and placed in a heating chamber maintained at $100\pm1^{\circ}C$ for one hour. The test piece was then removed from the heating chamber and allowed to cool for 2 h at $27\pm2^{\circ}C$. Length of the test piece was again noted. Heat shrinkage was calculated using the equation

$$\text{Heat shrinkage, \%} = \frac{(L_0 - L_1)}{L_0} \times 100$$

where L_0 = Length before heating in mm.

L_1 = Length after heating in mm.

II.12.4 Determination of relative density

A sample of size 50 x 50 mm was cut from vulcanised and post cured microcellular sheets. The test pieces were conditioned at 65 ± 5 per cent relative humidity and a temperature of $27\pm2^{\circ}C$ for 24 h prior to testing. After conditioning the mass, length, breadth and thickness of the samples were noted.

Relative density was then calculated as follows:

$$\text{Relative density} = \frac{M}{L \times B \times T}$$

where M = Mass of the test piece in grams after conditioning.

L = Length of the test piece after conditioning.

B = Breadth of the test piece after conditioning.

T = Thickness of the test piece after conditioning.

II.12.5 Determination of hardness

Hardness is measured as the resistance offered by the material for the indentation of a pointer of specified dimension attached to a :precalibrated: spring and is expressed as a number. Test piece of size 50 x 50 mm was conditioned at 65±5 per cent relative humidity and a temperature of 27±2°C for 24 h. Hardness was then measured using Shore-A Durometer. The result is expressed directly in Shore-A.

II.12.6 Determination of abrasion resistance

Abrasion loss is expressed as the volume of the test piece getting abraded by its travel through 42 m on a standard abrasive surface. This is expressed by the following equation:

$$V = \frac{\Delta m}{\rho}$$

V = Volume loss

Δm = mass loss

ρ = density

Abrasion test was conducted using DIN abrader which was described in Section II.3.4.

Die cut sample of specified dimension was fixed on the sample holder and a load of 5 N was applied. Sample holder with the samples was allowed to travel through the specified distance. After giving an initial surface smoothening run, the weight of the sample was noted. Then the test run was conducted and the weight was again noted. From the difference in weight, the abrasion loss was calculated.

II.12.7 Determination of flex life

In this method, the number of flexing cycle required for the sample with an initial cut of definite size to grow to a definite length and for failure, are determined. Ross flexing machine is used to determine the cut growth of microcellular samples. The machine allows the pierced flexing area of the test specimen to bend freely over a rod of 10 mm diameter by an angle 90°. The machine runs at 100±5 cycles per minute. One end of the test specimen is clamped firmly to a holder .arm and the other end is placed on two rollers which permit a free bending movement of the test specimen during each cycle.

Sample was given a cut of 2.50±0.02 mm in length at the centre of the flexing face at a definite length of 62.0±1.0 mm from the clamping side. Test piece was having a length of 150 mm, width 25.0±1.0 mm and a thickness of 6.30±0.2 mm. Test specimens were clamped to the holder arm of the flexing machine in such a position that when specimens were flexed at 90° the cuts were at the centre point of the arc of the flexure.

Adjustable top roller is let down till it touches the specimen and permits the specimen to travel freely between rollers. Frequent observations were made for determining the rate of increase in cut length.

Observations were taken for

1. Number of cycles required for propagation of the initial crack by 100 per cent.

2. Extent of crack growth after 100,000 cycles.

II.12.8 Determination of room temperature shrinkage

It is the percentage linear shrinkage that occurs to the sample after keeping the sample at 27±2°C for two weeks. Test pieces of size 125 x 5 x 15 mm were cut from the sample after splitting off all the sides. It was then conditioned in an atmosphere of 65±5 per cent relative humidity and at a temperature of 27±2°C for 24 h prior

to testing. Initial length of the test piece was noted to the nearest of 0.1 mm. The test piece was placed in a chamber maintained at $27\pm2^{\circ}C$ for 2 weeks. It was then removed and its length noted. Room temperature shrinkage was calculated and expressed as

$$\text{Shrinkage, \%} = \frac{L - L_1}{L_0} \times 100$$

L_0 = Original length of the test piece in mm.

L_1 = Length of the test piece in mm after 2 weeks.

II.12.9 Cell structure study by SEM

The SEM observations of the microcellular sheets were made using a JOEL 35C model scanning electron microscope. Cell structure was examined using a thin sample cut from the centre of the micro-cellular sheets. The surface to be examined was then sputter coated with gold. It was then observed using SEM and photomicrographs of the cells were taken and compared.

Table II.1. Specifications for ISNR-5 grade natural rubber.

Parameters	Limit	Actual value
Dirt content (% by Mass, Max)	0.05	0.03
Volatile matter (% by Mass, Max)	1.0	0.70
Nitrogen content (% by Mass, Max)	0.7	0.40
Ash content (% by Mass, Max)	0.6	0.48
Initial plasticity (Po, Min)	30.0	40.0
Plasticity Retention Index (PRI, Min)	60.0	75.0

Table II.2. Properties of Exxon EVA 218.

Property	Test method (ASTM)	Value
Melt flow index (g/10 min)	1238	1.7
Density (g/cm^3)	792	0.939
Vicat softening point ($^\circ$C)	1525	64
Vinyl acetate content (%)	--	18

Table II.3. Composition of the blends.

Ingredients	A	B	C	D	E	F	G	H	I	J
EVA	0	10	20	30	40	50	60	70	80	100
NR	100	90	80	70	60	50	40	30	20	0

Table II.4. Formulation of the compounds.

	Sulphur system (1)	DCP system (2)	Mixed system (3)
Polymer	100.0	100.0	100.0
Zinc oxide	5.0	5.0	5.0
Stearic acid	1.5	1.5	1.5
Styrenated phenol (Antioxidant)	1.0	1.0	1.0
Dibenzothiazyl disulphide	0.8	--	0.8
Dicumyl peroxide (40% active)	--	4.0	4.0
Sulphur	2.5	--	2.5

Table II.5. Formulation of the silica filled compounds.

Ingredient	S_0	S_{15}	S_{30}	S_{45}
Polymer	100.0	100.0	100.0	100.0
Zinc oxide	5.0	5.0	5.0	5.0
Stearic acid	1.5	1.5	1.5	1.5
MBTS	0.8	0.8	0.8	0.8
Sulphur	2.5	2.5	2.5	2.5
Dicumyl peroxide (40% active)	4.0	4.0	4.0	4.0
Styrenated phenol	1.5	1.5	1.5	1.5
Precipitated silica (INSIL VN_3)	0.0	15.0	30.0	45.0
Naphthenic oil	0.0	1.5	3.0	4.5
Diethylene glycol	0.0	1.0	1.5	2.0

Table II.6. Formulation for microcellular sole compounds.

Material	F'	G'	H'	I'	J'	Calcium carbonate					Clay				
						G'_1	G'_2	G'_3	G'_4	G'_5	G''_1	G''_2	G''_3	G''_4	G''_5
Natural rubber (NR)	50	40	30	20	0	40	40	40	40	40	40	40	40	40	40
Ethylene-vinyl acetate (EVA)	50	60	70	80	100	60	60	60	60	60	60	60	60	60	60
Zinc oxide	3.5	3.5	3.5	3.5	3.5	3.5	3.5	3.5	3.5	3.5	3.5	3.5	3.5	3.5	3.5
Stearic acid	1	1	1	1	1	1	1	1	1	1	1	1	1	1	1
Zinc stearate	2.0	2.0	2.0	2.0	2.0	2.0	2.0	2.0	2.0	2.0	2.0	2.0	2.0	2.0	2.0
Styrenated phenol	1	1	1	1	1	1	1	1	1	1	1	1	1	1	1
Calcium carbonate	75	75	75	75	75	45	60	75	90	105	-	-	-	-	-
China clay	-	-	-	-	-	-	-	-	-	-	45	60	75	90	105
Paraffinic oil	3.0	3.0	3.0	3.0	3.0	1.8	2.4	3.0	3.6	4.2	1.8	2.4	3.0	3.6	4.2
Dicumyl peroxide	4	4	4	4	4	4	4	4	4	4	4	4	4	4	4
Diethylene glycol	-	-	-	-	-	-	-	-	-	-	0.9	1.2	1.5	1.8	2.1
Azodicarbonamide (ADC)	5.5	5.0	4.5	4.0	3.0	5.0	5.0	5.0	5.0	5.0	5.0	5.0	5.0	5.0	5.0

CHAPTER III   –   A.   MORPHOLOGY

B.   KINETICS OF VULCANISATION AND MECHANICAL
PROPERTIES OF NR-EVA BLENDS.

Part of the results described in this Chapter has been published in the Indian Journal of Natural Rubber Research, 3(2): 77-81, 1990.

Elastomer blends have the advantage that a wide range of properties can easily be obtained by varying the composition of the blends. Properties of elastomer blends depend not only on the size of the dispersed phase but also on the difference in the rates of vulcanisation of the components and on the extent of cure of each phase. To select a blend ratio and a crosslinking system suitable for a particular application, a clear understanding of the change in physical properties with blend ratio and crosslinking systems is essential. While NR can be vulcanised using sulphur, EVA is not vulcanisable by sulphur due to its saturated backbone structure. But both these polymers can be cured by using peroxides. However in a blend of the two, the extent of cure undergone by each phase shall depend on the distribution of the curative in each phase and also on the rate of cure of the individual polymers. The morphology of the blend will also exert a strong influence on the distribution of the curative and on the physical properties of the vulcanisates.

This chapter of the thesis consists of the results of a systematic study conducted on the morphology of uncrosslinked NR-EVA blends and on the effects of three crosslinking systems namely, sulphur, peroxide and a mixed cure system consisting of sulphur and peroxide on the vulcanisation kinetics and mechanical properties of the blends. This chapter has been divided into two parts.

In Part A, the change in morphology of the uncrosslinked blends with the change in blend ratio of the components is discussed. Part

B contains the results of the studies on the effects of three cross-linking systems on vulcanisation kinetics and mechanical properties of the blends.

A.   MORPHOLOGY

III.A Morphology of the Blends

Figure III.A.1 is the photomicrograph of the blend G, the composition of which is 60:40 EVA:NR. The holes seen on the surface are formed by extraction of the NR phase. At this blend ratio NR remained as dispersed particles in the EVA matrix. The size of the dispersed particles is also small compared with its size in those blends which contained a higher proportion of NR. As the proportion of NR in the blend is increased to 50 per cent (blend F), the size of the holes has increased several fold (Figure III.A.2). The boundary of EVA separating the holes has narrowed down to a thin layer. When the EVA:NR ratio is 40:60 (blend E) this narrow boundary layer is seen broken, since it is unable to withstand the forces due to the swelling of the NR phase (Figure III.A.3). It is possible that in blends E and F, both NR and EVA formed continuous phases because of the higher proportion of the NR phase and the lower melt viscosity of the EVA phase. The photomicrograph of the 30:70 EVA:NR blend showed particles of EVA remaining on the benzene extracted surface (Figure III.A.4) which indicated that EVA formed the dispersed phase when its proportion is below 40 per cent and

NR formed the dispersed phase when its proportion was 40 per cent or below. In blend ratios 40:60 and 50:50 EVA:NR both the polymers remained as continuous phases leading to a sponge-like interpenetrating structure for the blend.

B. KINETICS OF VULCANISATION AND MECHANICAL PROPERTIES

A general equation for the kinetics of a first order chemical reaction can be written as

$$\ln (a-x) = -kt + \ln a \qquad \ldots\ldots(1)$$

where a = initial reactant concentration,

   x = reacted quantity at time 't', and

   k = first order reaction rate constant.

The rate of crosslink formation is usually monitored by measuring the torque developed during the course of vulcanisation by using a curometer and the torque values thus obtained are proportional to the modulus of the rubber. Hence if a physical property such as modulus is being measured rather than the change in reactant concentration, then the following substitutions can be made:

$$(a-x) = (M_\alpha - M) \qquad \ldots\ldots(2)$$

$$a = (M_{\infty}-M_0) \qquad \qquad \ldots\ldots(3)$$

where M_{∞} = maximum modulus,

M_0 = minimum modulus, and

M = modulus at time 't'.

Substituting torque values for modulus, we get

$$(a-x) = (M_h-M_t) \qquad \qquad \ldots\ldots(4)$$

where M_h = the maximum torque developed, and

M_t = the torque at time 't'

If the reaction is of first order, a plot of ln (M_h-M_t) against 't' should give a straight line whose slope will be the specific reaction rate constant 'k'. Typical plots of ln (M_h-M_t) vs 't' of the blends E_1, E_2 and E_3 are shown in Figure III.B.1. A straight line graph in each case indicates that the reaction is of first order.

To find out the activation energy of the vulcanisation reaction, the modified Arrhenius equation is used

$$t_{90} = Ae^{E/RT} \qquad \qquad \ldots\ldots(5)$$

$$\log t_{90} = \log A + \frac{E}{2.303 \ RT} \qquad \qquad \ldots\ldots(6)$$

where E -- activation energy,

t_{90} = time in minutes to attain 90% of maximum torque, and

T = absolute temperature °K.

A plot of log t_{90} vs 1/T gives a straight line, from the slope of which E is calculated. Typical plots of log t_{90} vs 1/T for the blends E_1, E_2 and E_3 are shown in Figure III.B.2.

III.B.1 Kinetic factors and cure characteristics

The activation energy (E), the first order specific rate constant (k) and the optimum cure time (t_{90}) of the blends at 160°C are given in Table III.1. For all the three types of cure systems studied, the activation energy for vulcanisation increased and the first order rate constant decreased with increase in the proportion of EVA in the blend. The higher E and lower K values for the compounds J_2 and J_3 compared with those of compounds A_2 and A_3 are due to the fact that EVA has a saturated backbone structure and is less reactive than NR. The increase in E and decrease in k of the sulphur cured blends with over 30 per cent EVA are expected, as EVA cannot be vulcanised by sulphur and the sulphur which is dispersed in the EVA phase migrates to the NR phase as the reaction progresses. Between DCP and the mixed cure system, the latter showed lower E and higher k values. While the differences in E were prominent in blends having higher proportions of EVA, the differences between the k values were more evident in blends

containing higher proportions of NR. Sulphur is known to act as a co-agent in peroxide vulcanisation of elastomers. It is also possible that most of the sulphur remained in the NR phase because of its higher solubility[101]. The higher k values of the mixed cure system compared with those of the DCP cure system can be due to these reasons. These observations are further supported by the optimum cure time of the blends at 160°C. The effect of sulphur in activating peroxide is evident from the lower cure time of the pure EVA compound having the mixed cure system (J_3) compared with that of the DCP cured compound (J_2). While the change in cure time with increase in the proportion of EVA in the blend was only marginal in the DCP cured blends, it was quite significant in the case of blends which contained sulphur and the mixed cure system. The mixed cure system has shorter cure time at all blend ratios of NR and EVA compared with the DCP cure system. Moreover, the cure times of the blends having the mixed cure system were more similar to those of the blends containing .the sulphur system, especially at higher proportions of NR in the blends.

III.B.2 Physical properties

III.B.2.1 Tensile strength, modulus and elongation

The changes in tensile strength, 300% modulus and elongation at break with increase in EVA content in the blend and the effect of the three different cure systems on these properties are shown

in Figures III.B.3, III.B.4 and III.B.5, respectively. Tensile strength of those blends which contained sulphur and mixed cure systems was maximum when the proportion of NR in the blend was in the range of 70 to 80 per cent, whereas the tensile strength of the DCP cured blends increased steadily with increase in EVA content in the blend. When the proportion of the minor component in the blend is in the range of 20 to 30 per cent, it remains as ·dispersed particles and the bulk of the curative gets dispersed in the continuous phase. In the present case, this is more pronounced because sulphur is highly reactive with NR and not at all effective in curing EVA. This will facilitate migration of sulphur which is dispersed in the EVA phase to the NR phase during vulcanisation. Thus a higher extent of crosslinking of the NR phase of the blends B to D may be the reason for the observed higher tensile values of these blends in the case of sulphur and mixed cure systems.

At higher proportions of NR in the blend, the tensile strength values were in the order: sulphur cure $>$ mixed cure$>$ DCP cure. This observation can be explained based on the type of crosslinks normally obtained when such systems are used. In sulphur cure with conventional dosage, the crosslinks formed· are mainly polysulphidic in nature whereas, DCP cure gives carbon-carbon type crosslinks. The more flexible polysulphidic linkages facilitate higher extensions and higher tensile strength during stretching by reforming the ruptured crosslinks in preferred configurations whereas the less

flexible C-C type linkages provide only lower tensile strength[102]. In the case of mixed cure system there is a possibility that both the types of crosslinks are formed and the blends attain a higher crosslink density compared to the other cure systems. When mixed crosslinks are present, the tensile strength will be lower because of the unequal distribution of load during stretching[103]. This explains the lower tensile strength of the blends having mixed cure system compared with that of the sulphur cured blends. The higher flexibility of the polysulphidic linkages is also evident from the higher elongation at break of the blends cured with sulphur and mixed systems compared with those containing DCP (Figure III.B.5).

In the case of blends such as those of NR and EVA, crosslink density measurement by the normal swelling method is very difficult because of the wide difference in solubilities and polymer-solvent interaction parameters of the components. However, indirect evidence of a higher crosslink density can be obtained from the modulus values. Figure III.B.4 shows higher modulus values for those blends vulcanised with the mixed cure system compared with those of the sulphur and DCP cured blends at higher proportions of NR. This observation is further supported by the higher rebound resilience values of the blends having mixed cure system (Figure III.B.6) compared with those of the blends having the other two cure systems. For blends having a higher proportion of EVA also, the mixed cure system gave higher tensile strength than DCP and comparable modulus and resilience values.

III.B.2.2 Hardness

Hardness of the blends having different cure systems is shown in Figure III.B.7. Hardness increased with increase in the proportion of EVA in the blend. The change in hardness is more sharp in blends E and F compared with the other blends. This is because in these blends EVA also tends to form a continuous phase since its melt viscosity is lower than that of NR. In hardness measurement, the deformation involved is only at the surface and EVA can form an outer layer during processing. This is the reason for the more or less similar hardness of the blends from F to J. The mixed cure system gave higher hardness in the case of the blends having higher proportions of NR because of higher extent of crosslinking.

III.B.2.3 Compression set

Compression set of the blends is found to increase as the proportion of EVA in the blend increased (Figure III.B.8) which is due to the thermoplastic nature of EVA. For blends A to G the sulphur cure system caused higher set compared with the other two, because of the predominance of polysulphidic crosslinks and also due to the presence of the uncrosslinked EVA phase. It is seen that at the level of 40 per cent EVA in the blend, it also forms a continuous phase because of its lower melt viscosity. Between mixed and DCP cured blends, a change in the compression set pattern was observed at 60:40 NR:EVA (blend E). The mixed cure system which

caused higher compression set for blends A to E, showed lower set for blends G to J compared with the DCP cured blends. Blends A_3 to E_3 contained polysulphidic as well as carbon-carbon type cross-links and hence showed higher set values compared with blends A_2 to E_2 which contained only C-C crosslinks. In blends G to J, NR remained as the dispersed phase. It is possible that the continuous EVA phase of the blends G_3 to J_3 attained higher levels of crosslinking than blends G_2 to J_2 as it is well known that in peroxide vulcanisation of EPDM and EVA, sulphur can activate the reaction to produce higher extents of crosslinking[104]. The dispersed NR phase also can have a higher extent of crosslinking due to higher solubility of sulphur in this rubber.

III.B.2.4 Tear and abrasion resistance

Tear resistance of the blends followed similar trend as that of tensile strength (Figure III.B.9). As the proportion of EVA increased, the tear resistance also increased for the blends with DCP and mixed cure systems. The mixed cure system showed better tear strength compared with DCP cure system at almost all blend ratios. In the case of abrasion resistance also, as the proportion of EVA increased, the blends showed better resistance to abrasion (Figure III.B.10). The behaviour of the mixed cure system was different in blends having higher proportions of NR and EVA. When the proportion of NR was higher (blends A to D) this system caused

better resistance to abrasion than the DCP cure system. However this trend was reversed in blends E to J, in which the DCP cure system gave better abrasion resistance. A similar trend was seen in compression set which was already explained on the basis of the type of crosslinks and extent of crosslinking attained by using the mixed cure system.

Table II.1. Activation energy, rate constant and cure time of NR-EVA blends.

Blend number	Blend ratio NR:EVA	Activation energy, E (kcal mole^{-1})			Reaction rate constant k			Cure time, t_{90} at 160°C (min)		
		Sulphur cure	DCP cure	Mixed cure	Sulphur cure	DCP cure	Mixed cure	Sulphur cure	DCP cure	Mixed cure
A	100 : 0	15.68	19.44	19.44	0.454	0.117	0.191	7.5	22.5	8.0
B	90 : 10	15.25	20.59	19.44	0.454	0.108	0.207	8.0	24.5	8.5
C	80 : 20	15.23	20.50	20.02	0.454	0.108	0.196	8.5	22.5	10.0
D	70 : 30	15.44	20.31	0.36	0.413	0.107	0.163	9.5	21.5	11.0
E	60 : 40	15.78	21.73	21.34	0.399	0.107	0.140	10.5	22.5	14.5
F	50 : 50	16.01	23.79	21.23	0.374	0.102	0.139	12.5	22.5	16.5
G	40 : 60	16.83	24.39	21.59	0.359	0.105	0.137	13.0	23.0	17.0
H	30 : 70	16.73	24.60	22.08	0.357	0.104	0.130	13.5	22.5	16.5
I	20 : 80	-	24.11	22.28	-	0.100	0.129	-	23.5	17.0
J	0 : 100	-	24.25	22.33	-	0.100	0.126	-	27.5	21.5
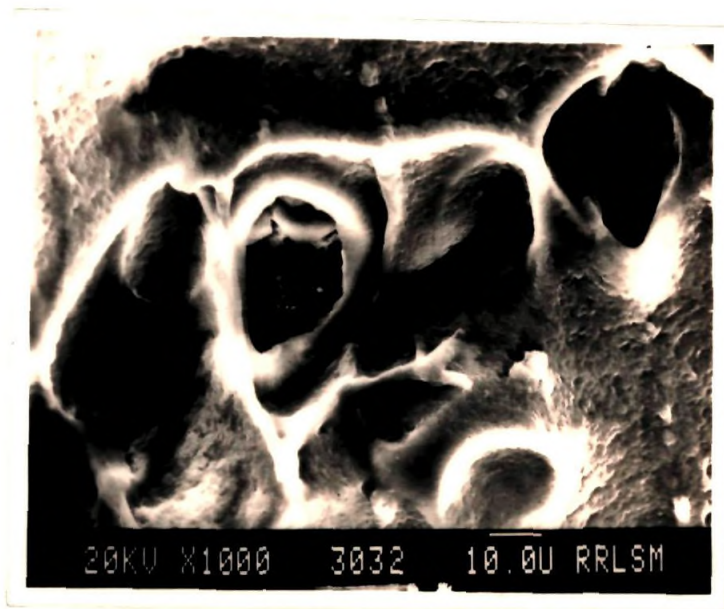
Figure III.A.1
SEM Photomicrograph of blend G,
NR remained as dispersed phase.
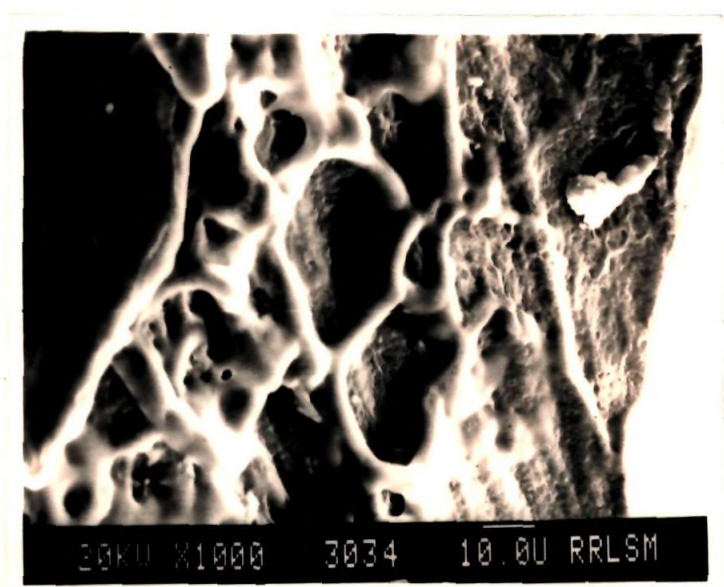
Figure III.A.2
SEM Photomicrograph of blend F,
both phases continuous
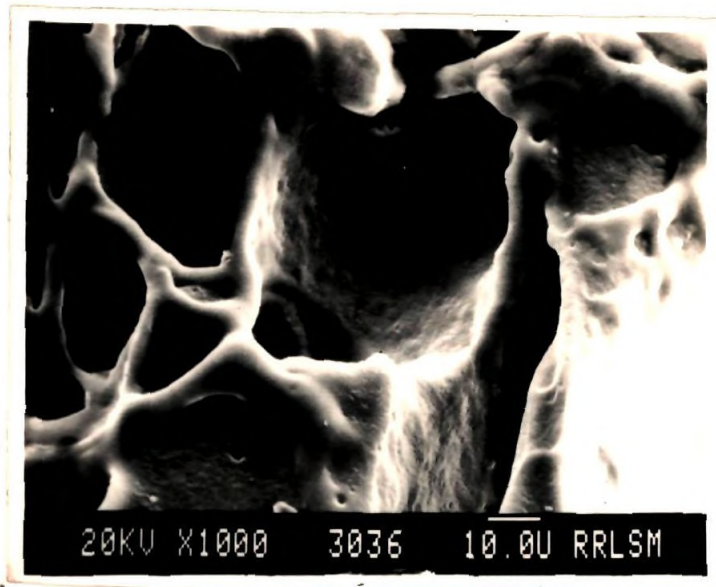
Figure III.A.3
SEM Photomicrograph of blend E,
both phases continuous.
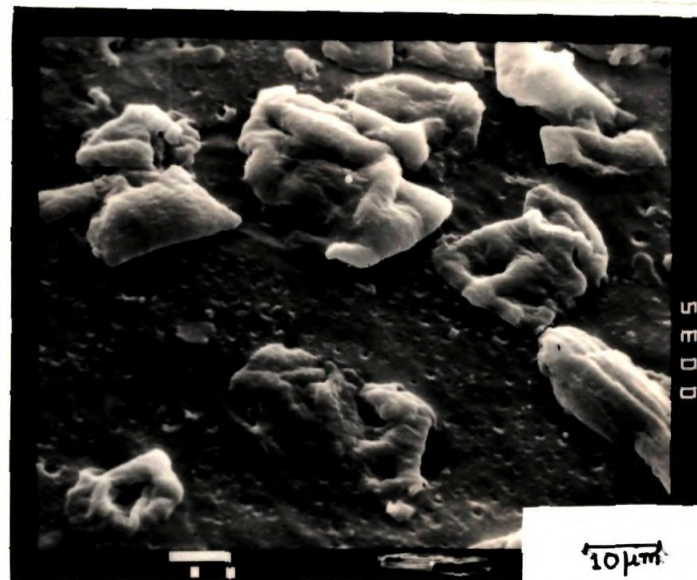
Figure III.A.4
SEM Photomicrograph of blend D, particles
of EVA resting on the extracted surface.
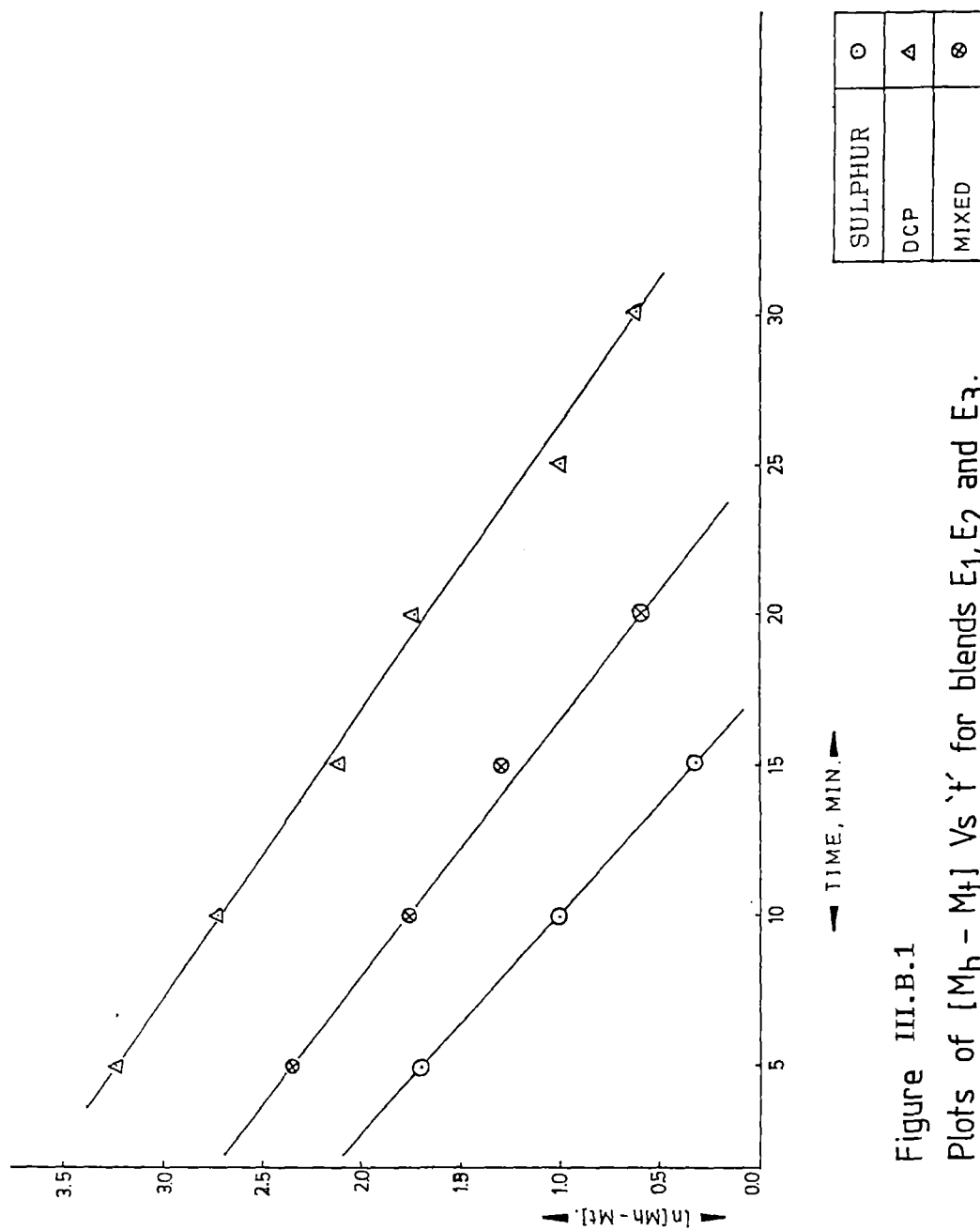
Figure III.B.1

Plots of $[M_h - M_t]$ Vs 't' for blends E_1, E_2 and E_3.
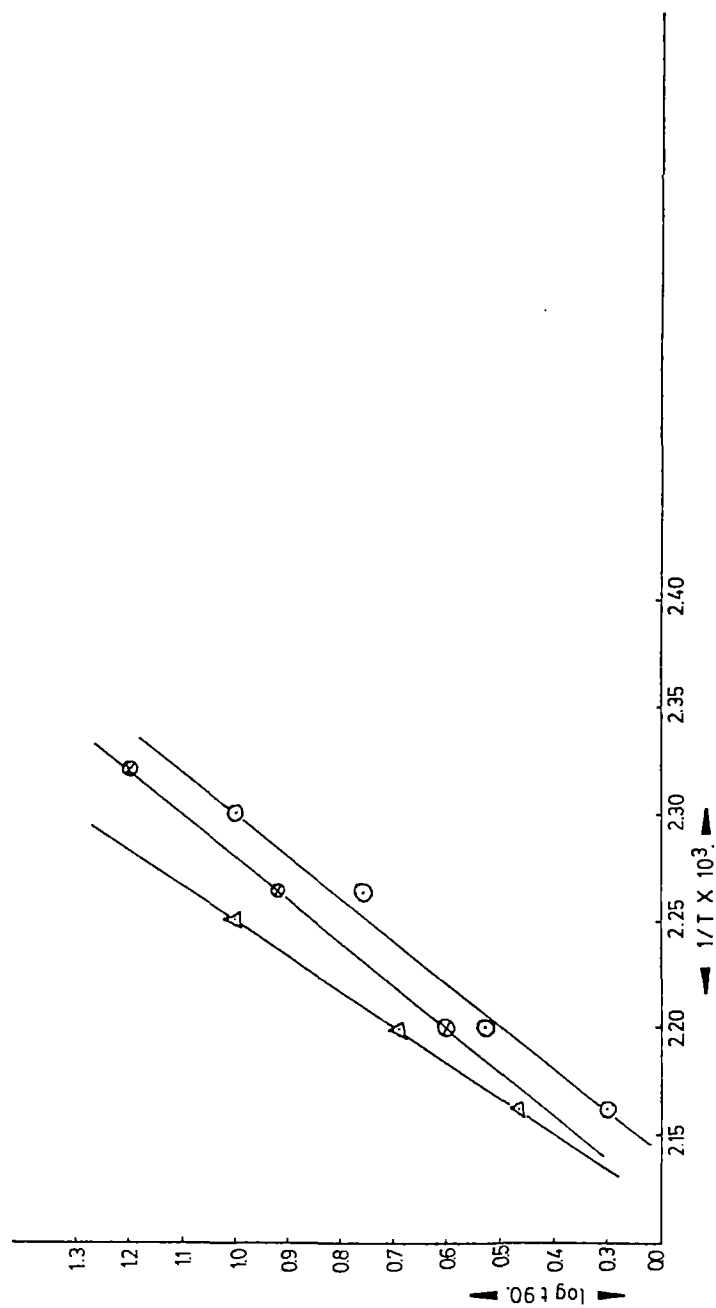
SULPHUR	⊙
DCP	△
MIXED	⊗

Figure III.B.2
Arrhenius plots for blends E_1, E_2, and E_3.
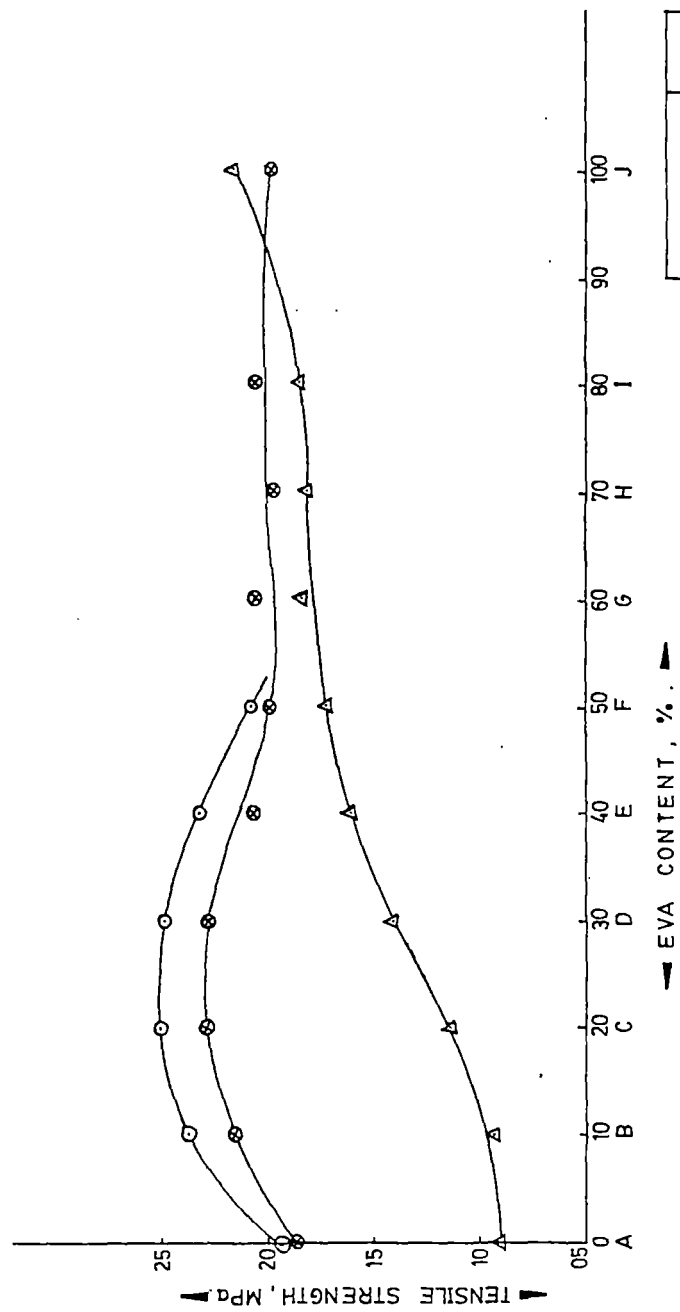
Figure III.B.3
Effect of blend ratio and cure system on tensile strength.
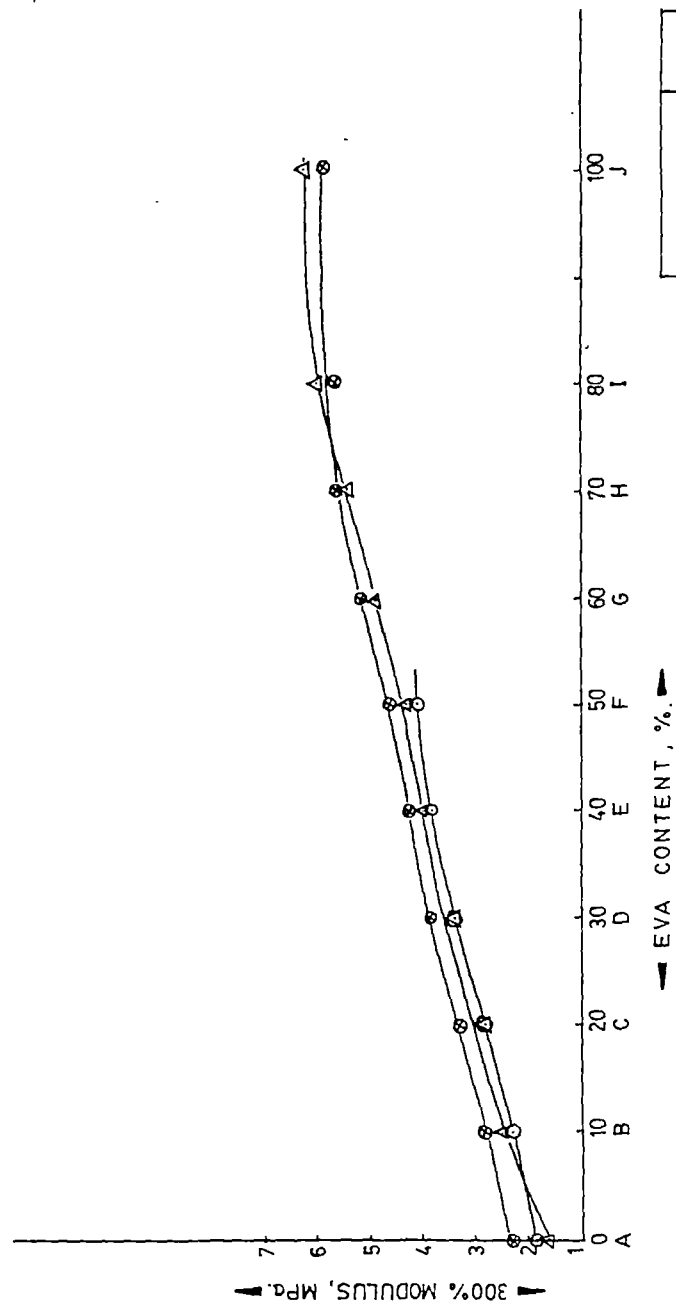
Figure III.B.4
Effect of blend ratio and cure system on 300% modulus.
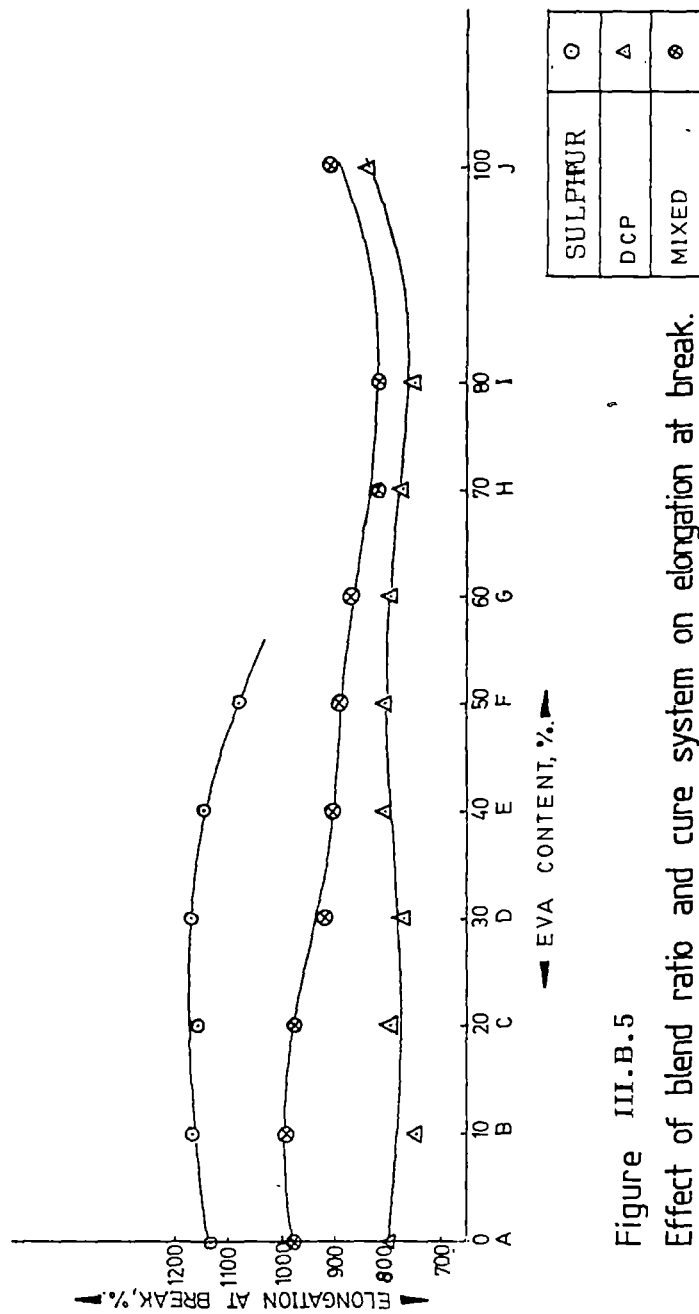
Figure III.B.5
Effect of blend ratio and cure system on elongation at break.
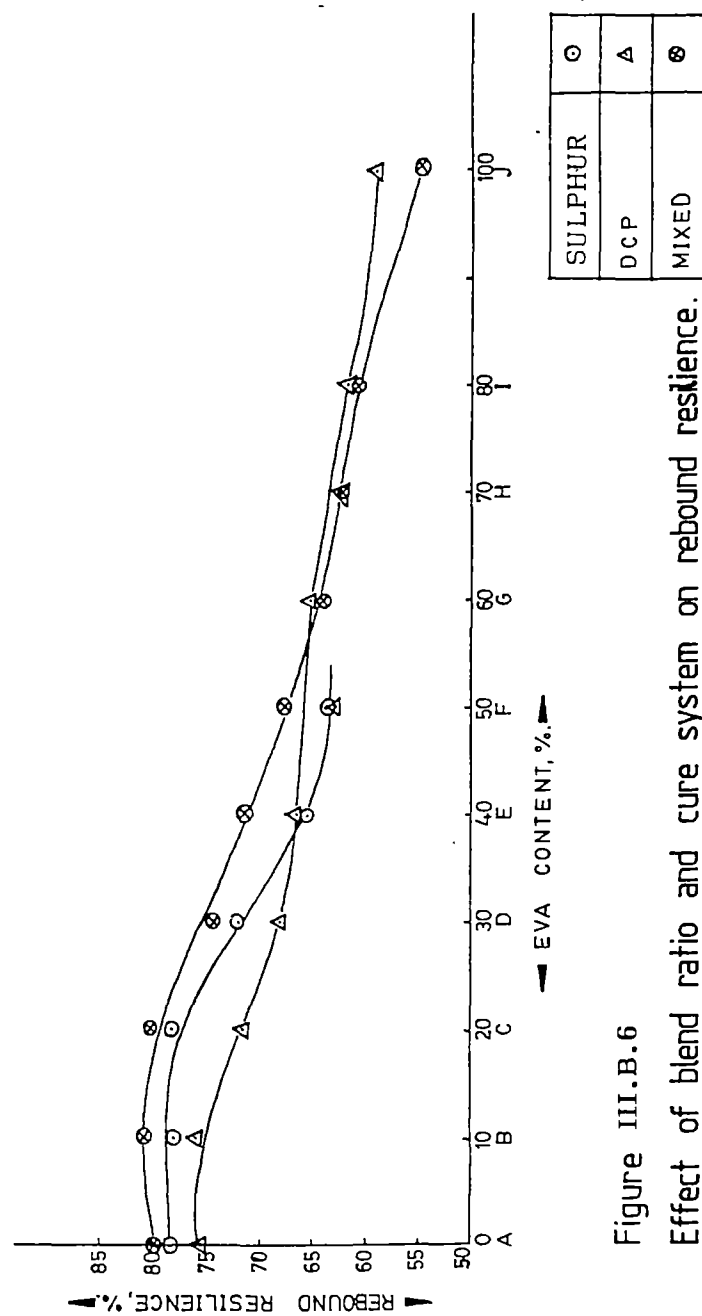
Figure III.B.6

Effect of blend ratio and cure system on rebound resilience.
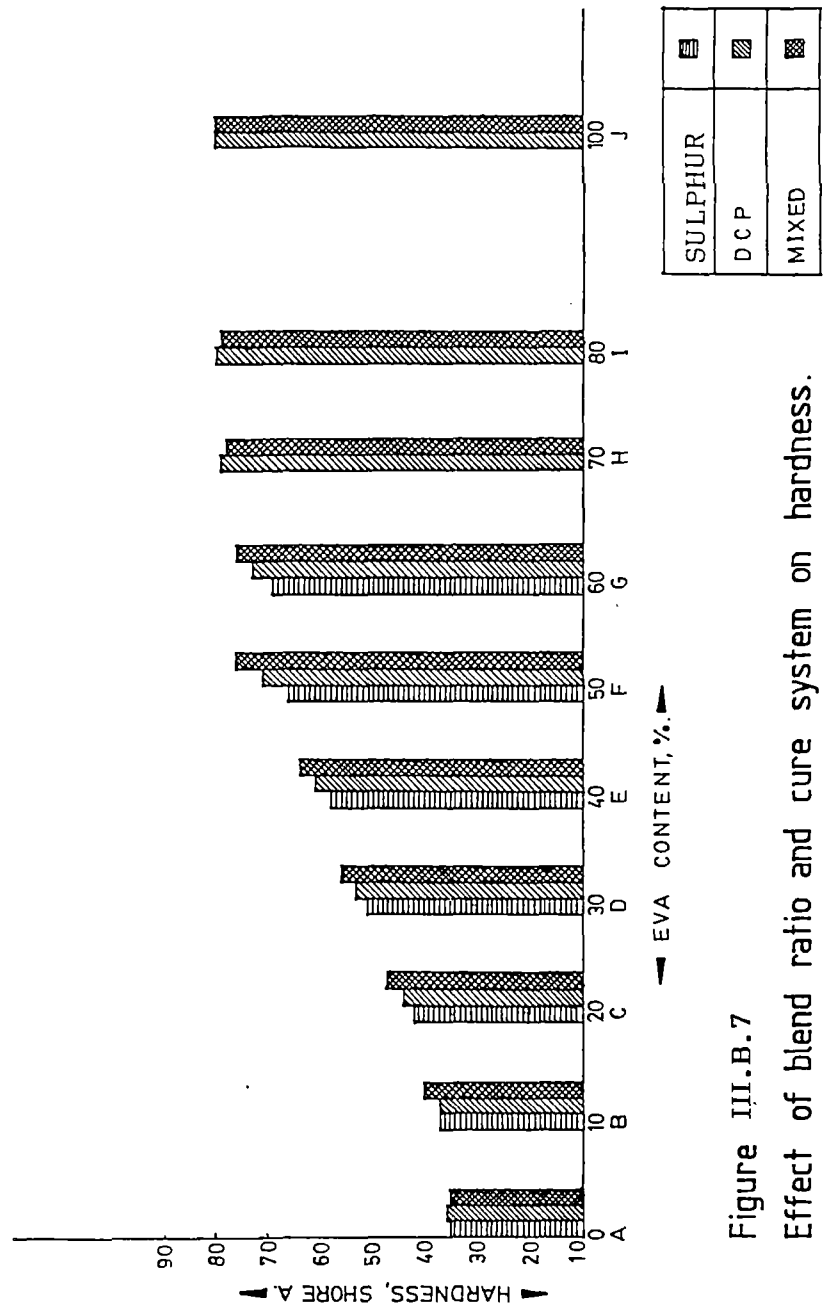
Figure III.B.7

Effect of blend ratio and cure system on hardness.
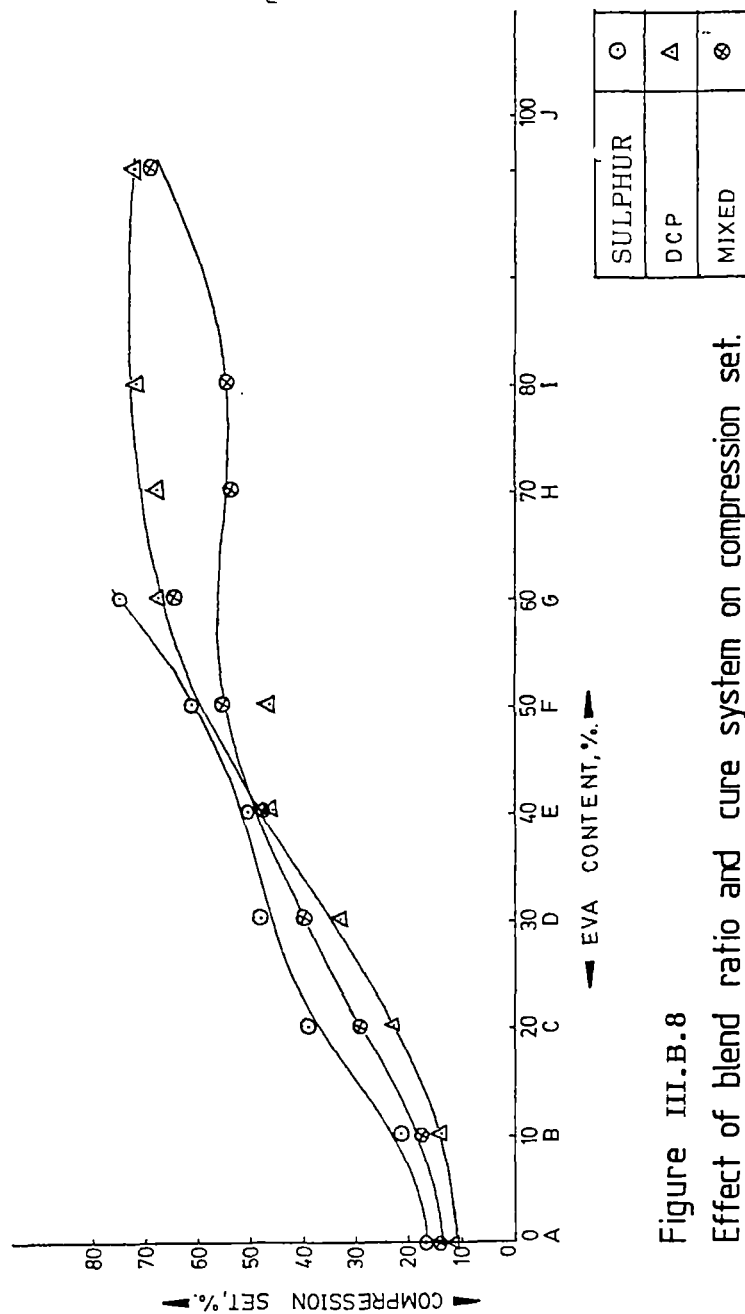
Figure III.B.8
Effect of blend ratio and cure system on compression set.
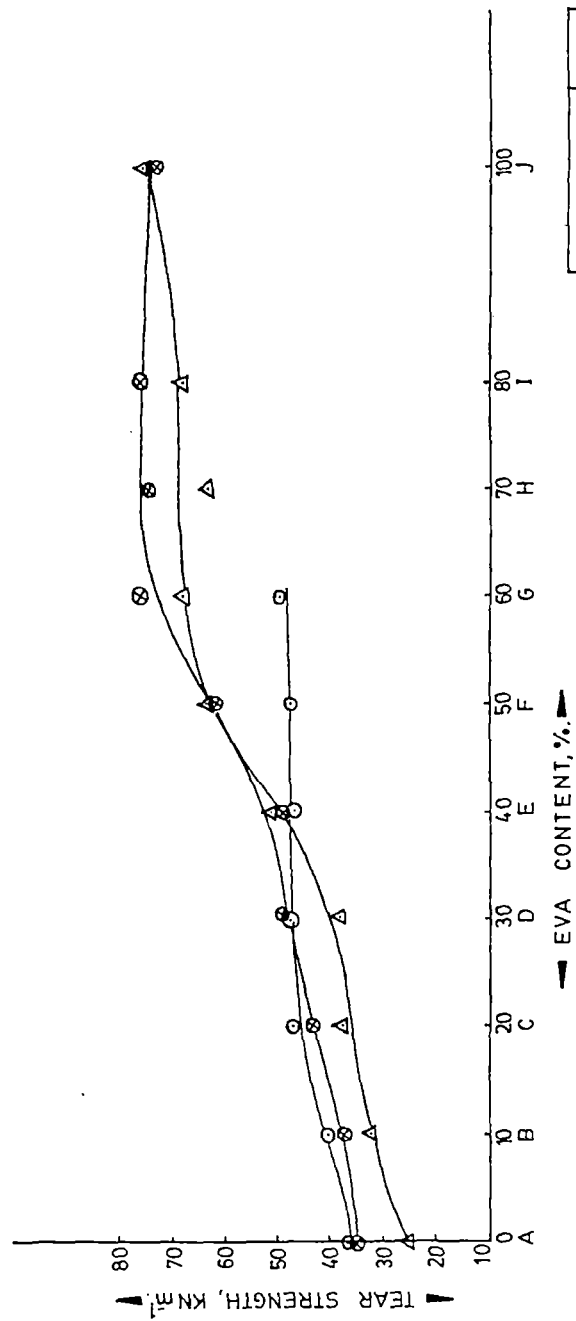
Figure III.B.9
Effect of blend ratio and cure system on tear strength.
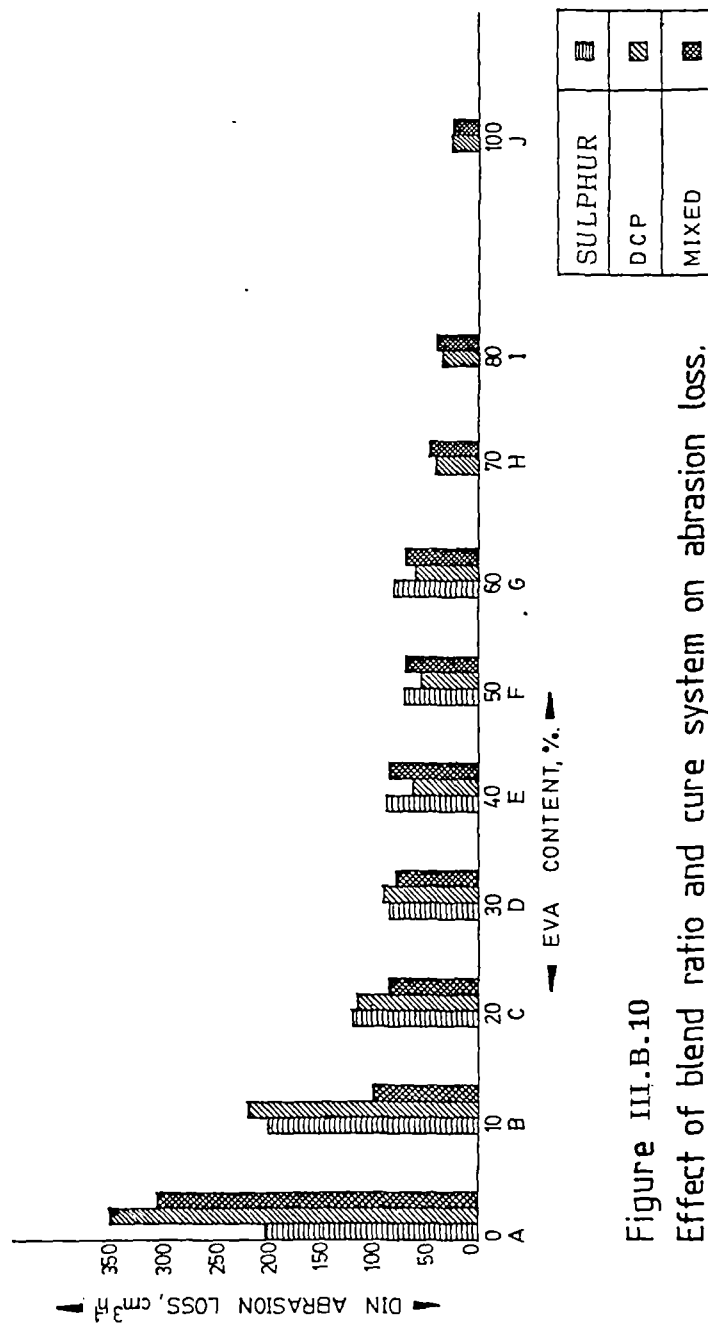
Figure III.B.10

Effect of blend ratio and cure system on abrasion loss.

CHAPTER IV – MISCIBILITY, CRYSTALLIZATION AND DYNAMIC MECHANICAL BEHAVIOUR OF NR-EVA BLENDS.

The results of the above study have been communicated for publication in POLYMER.

The basic issue confronting the designer of polymer blends is to guarantee efficient stress transfer between the components of a multi-component system. Only in this way the physical properties of the components can be efficiently utilised to produce blends having the desired properties. One approach is to find blend systems which form miscible amorphous phases. In polymer blends of this type, the various components have the thermodynamic ability to be mixed at the molecular level. Since these systems form only miscible amorphous phase, interphase stress transfer is not an issue and the physical properties of miscible blends approach and frequently exceed those expected for a random copolymer having the same chemical constituents. In recent years a large number of immiscible polymer blends has been reported. Since the physical and chemical interactions across the phase boundaries are weak, immsicible blends exhibit poor mechanical properties. This problem can be alleviated by the addition of copolymers or by the introduction of interfacial crosslinks. Several studies have been reported in this direction[105] Miscibility of polymer blends can be analysed by Differential Scanning Calorimeter or Dynamic Mechanical Thermal Analyser. Addition of an amorphous component into a crystalline polymer usually influences the crystallinity of the latter. This can be understood from DSC and X-ray analysis.

In this chapter using different techniques such as X-ray, differential scanning calorimetry (DSC) and dynamic mechanical

thermal analyser (DMTA), the crystallinity, miscibility and dynamic mechanical properties of NR-EVA blends with special reference to effects of blend ratio and crosslinking systems were evaluated. The details of the experimental procedures adopted for studying X-ray, DSC and DMTA are given in Chapter II.

IV.1 THERMAL PROPERTIES

The thermal properties of NR, EVA and crosslinked and un-crosslinked blends of these two polymers were analysed by using DSC. The melting temperature (T_m), fractional crystallinity (X_c), heat of fusion (ΔH) and glass transition temperature (T_g) of the blends are reported in Table IV.1.

DSC results of the crosslinked and uncrosslinked blends are given in Figures VI.1 and IV.2, respectively. The peak point temperature of the thermogram was taken as the melting point. It is interesting to note (Table IV.1) that in the case of uncrosslinked and sulphur crosslinked blends T_m is almost independent of the composition. However, a slight decrease in melting temperature is observed in the case of peroxide and mixed cured blends.

The area of the melting edotherm is calculated and reported as the heat of fusion(ΔH). The fractional crystallinity of EVA in the blends is calculated from ΔH values based on the reported crystallinity value of EVA containing 18 per cent vinyl acetate

content[85]. It is seen that the fractional crystallinity, 'X$_c$' and heat of fusion values decreased with increase in NR content, under similar conditions of crystallization The crystallinity of EVA was found to be 32 per cent. With gradual incorporation of NR (30 parts, 50 parts and 70 parts), it comes down to 29.0 per cent for 30:70 NR:EVA, 13.3 per cent for 50:50 and 11.6 per cent for 70:30 NR:EVA blends. Martuscelli et al[106] have shown that crystallinity is affected by blend composition and crystallization conditions such as temperature, pressure, orientation, molecular weight and diluent. The crystallization of PE segments in EVA is controlled by the segmental diffusion rate of other polymeric chains. The separation is enhanced as the NR content is increased. Incomplete crystallization thus leads to decrease in ΔH and hence crystallinity.

The glass transition temperatures (T_gs) as obtained from the DSC are reported in Table IV.1 for crosslinked and uncrosslinked NR-EVA blends. The T_g of pure NR and EVA is found to be-65.3°C and -27.0°C, respectively. In the case of uncrosslinked NR-EVA blends, the glass transition temperature of NR was found to be -65.0°C. It is interesting to note that T_g values of NR phase remained almost constant with increasing proportion of EVA. The T_g of EVA phase could not be detected in the blends using DSC. However, DMTA analysis as discussed later, could detect the T_g of EVA. It seems that the T_gs of the two phases in the uncrosslinked blends do not undergo substantial shift. This observation, coupled with almost

constant T_m with the increase in NR content indicated that the blends are immiscible.

It is interesting to note that in the case of crosslinked systems depending on the type of crosslinking systems used (sulphur, peroxide or mixed), the T_g of NR phase undergoes substantial shift from its normal position to high temperatures (Table IV.1). Generally introduction of crosslinks increases the T_g value due to the restriction on the segmental motion of the polymer by crosslinks. When sulphur is used as the crosslinking system the NR phase is preferentially crosslinked. DCP crosslinks both the phases. In mixed system, sulphur crosslinks the NR phase and DCP crosslinks both the phases. In the case of 70:30 NR:EVA blend, the T_g of NR phase in the blend for the sulphur, peroxide and mixed system are -58.0, -63.8 and -57.0°C, respectively. The T_g of natural rubber phase in the uncrosslinked 70:30 NR:EVA blend is -66.3°C. Therefore it can be concluded that increase in T_g of NR phase with extent of crosslinking is maximum when a mixed cure system is used as the crosslinking agent. A similar behaviour was observed for 50:50 and 30:70 NR:EVA blends. Since the resolution of DSC was limited to 15 nm, the T_g corresponding to the EVA phase could not be detected.

IV.2 X-RAY DIFFRACTION ANALYSIS

Figures IV.3 and IV.4 depict the X-ray diffraction pattern of crosslinked and uncrosslinked blends. The results of X-ray

analysis of the samples are given in Table IV.2. From the table it can be seen that the degree of crystallinity, X_c of EVA- is 36.7 per cent. This is higher than that obtained by DSC measurements. The value of X_c depends very much on the method of preparation of the sample and the technique of measurement[107]. The decrease in crystallinity caused by   natural rubber is due to the addition of an amorphous component which migrates into the crystalline phase of pure EVA, reducing its crystalline domains. Introduction of crosslinks further reduced the crystallinity of the EVA. This is due to the fact that crosslinking retards the regular arrangement of crystalline region within the samples. The 'd' values are reported in Table IV.2. With the addition of rubber there was a tendency for the 'd' value to increase in all systems both in crosslinked and uncrosslinked blends. This indicates migration of NR phase into the interchain space of EVA. Similar observations have been reported in the case of NR-PE blends by Roychoudhury et al[108].

IV.3 DYNAMIC MECHANICAL PROPERTIES

The dynamic mechanical behaviour of crosslinked and uncross-linked systems is shown in Figures IV.5 to IV.16. The glass transition temperature was selected at the peak position of tan δ and E", when plotted as a function of temperature. The T_g values of all the systems are given in Table IV.3.

The tan δ values of uncrosslinked blends as a function of temperature are given in Figure IV.5. It is seen that pure NR exhibits transition at -46°C. For pure EVA the transition is detected at -10°C. All the blends exhibit two transitions corresponding to NR and EVA phases, which indicated the incompatibility of the system. As compared to DSC results, the DMA thermograms exhibit transition at higher temperatures. This shows the different nature of responses of the molecular segments of the sample towards DMA and DSC analysis conditions. It can be seen that the tan δ_{max} due to NR phase decreased as the EVA content increased and the decrease is much sharper when the EVA content is 50 per cent or more.

As expected the loss modulus (Figure IV.6) sharply increased in the transition zone until they attained maxima and then fell off with the rise in temperature. The T_g values obtained from the E" vs temperature plot are always higher that those obtained from tan δ_{max} (Table IV.3). The sharp loss peaks indicated that the system is incompatible. Figure IV.7 shows the elastic modulus (E') of various blends over a wide range of temperatures. The curves for all the compositions have three distinct regions: a glassy region, a transition region (leathery region), and a rubbery region. Since the experiment was not performed above 20°C, the high temperature viscous region is not obtained. It is seen that the storage modulus decreased with the increase of temperature due to the decrease in

stiffness of the sample. The decrease is sharp in the case of high NR blends.

The dynamic mechanical properties of crosslinked systems are shown in Figures IV.8 to IV.16. The important properties are listed in Table IV.4. It is seen that as compared to the uncrosslinked blends, the T_g values of NR phase increase sharply in the case of sulphur and mixed crosslinked systems. For example, the T_g value of uncrosslinked NR is -46.3°C. The corresponding values for sulphur, peroxide and mixed cured systems are -42.0, -46.0 and -39.8°C, respectively. Similarly for 70:30 NR:EVA blend the T_g values of NR phase in the uncrosslinked, sulphur, peroxide and mixed systems are -46.3, -42.3, -46.0 and -37.5°C, respectively. This suggests that the degree of crosslinking of NR phase is maximum in the case of mixed systems. However, the T_g value of EVA does not show substantial shift with respect to crosslinking. This further suggests that in NR-EVA blends the extent of crosslinking of the NR phase is substantially higher than that of the EVA phase. This is associated with the faster curing nature of NR as a result of the high level of unsaturation in the isoprene units.

In some recent studies on similar systems it was interpreted that the shift in T_g values is due to interphase crosslinking which resulted in some type of compatibilisation[109]. However, in the case of NR-EVA system all the crosslinked blends showed two transitions

corresponding to EVA and NR phases. Therefore the crosslinked systems are incompatible. However, the observed shift in the T_g value of NR phase as seen from DSC and DMTA studies may be associated with the predominant crosslinking of that phase and is not due to the compatibilising action.

The $\tan \delta_{max}$ values of both NR and EVA phases increased with crosslinking (Figures IV.8, IV.11, IV.14). Introduction of crosslinks also increases the storage modulus of the blends (Figures IV.10, IV.12, IV.16. The activation of energy of NR transition has been calculated from a plot of reciprocal of NR trasition temperature as a function of frequency. It is seen that all the data points lie on a straight line. The activation energy of transition of the NR phase is given in Table IV.3. It can be seen that in most cases except for the mixed cure system, the activation energy decreased with the increase of EVA content in the blend.

Table IV.1. Thermal properties of NR-EVA blends.

Properties	Uncrosslinked blends					Crosslinked blends							
	A	D	F	H	J	D_1	F_1	D_2	F_2	H_2	D_3	F_3	H_3
Heat of fusion ΔH (cal/g)	--	1.8	3.7	4.8	5.2	1.9	3.6	1.9	4.6	3.9	1.9	4.7	4.3
Peak temperature T_m (0°C)	--	85.3	84.9	83.9	86.7	85.3	85.0	81.0	81.5	79.4	81.4	81.6	82.0
Onset of T_g	-67.4	-71.2	-60.3	-70.2	-35.7	-69.1	-67.9	-65.7	-65.4	-65.0	-64.4	-65.5	-66.0
Glass transition temperature (T_g') NR phase	-65.3	-66.3	-66.9	-66.5	--	-58.0	-54.6	-63.8	-62.7	-63.0	-57.1	-53.4	-43.8
Glass transition temperature (T_g') EVA phase	--	--	--	--	-27.0	--	--	--	--	--	--	--	--
Per cent crystallinity (%)	--	11.2	23.3	29.0	32.1	11.6	22.2	11.5	28.4	24.1	11.7	29.0	26.6

The subscripts 1, 2 and 3 stands for sulphur, peroxide and mixed cure systems, respectively.

Table IV.2. X-ray study.

Sample reference	Crystallinity, X_c (%)	d-value (A°)
UNCROSSLINKED		
Sample D	10.3	4.164
		3.799
		2.499
Sample F	24.6	4.164
		3.796
		2.493
Sample H	26.5	4.164
		3.786
		2.483
Sample J	36.7	4.164
		3.776
		2.473

Table IV.2 contd......

Sample reference	Crystallinity, X_c (%)	d-value (A°)
CROSSLINKED		
Sample D_1	7.6	4.165 3.800 2.494
Sample F_1	20.1	4.164 3.797 2.493
Sample D_2	7.6	4.164 3.799 2.495
Sample F_2	20.4	4.165 3.798 2.493
Sample H_2	22.6	4.165 3.777 2.473
Sample D_3	7.7	4.166 3.800 2.495
Sample F_3	20.4	4.164 3.799 2.495
Sample H_3	22.1	4.165 3.776 2.473

The subscripts 1, 2, 3 stand for sulphur, peroxide and mixed cure systems.

Table IV.3. Dynamic mechanical properties.

Sample	T_g (NR phase)	T_g (EVA phase)	Tan δ_1 max (NR phase)	E (kJ/mol) NR transition	Tan δ_2 max (EVA phase)	E" (Peak temperature, NR transition) °C	E" (Peak temperature, EVA transition) °C
Sample A (0:100)	-46.3	--	--	211.12	--	-55.0	--
Sample D (70:30)	-46.3	--	0.856	205.50	--	-51.0	--
Sample F (50:50)	-50.0	-10.9	0.400	178.45	0.200	-51.0	-20.4
Sample H (30:70)	-51.7	-10.1	0.165	191.29	0.200	-51.0	-20.4
Sample J (100:0)	--	-10.1	--	--	0.114	--	-20.0
Sample A_1	-42.0	--	2.200	204.62	--	-51.1	--
Sample D_1	-42.3	--	1.020	170.89	--	-48.0	--
Sample F_1	-43.6	-5.0	0.580	161.46	0.280	-45.0	-20.0
Sample A_2	-45.0	--	2.200	209.84	--	-53.1	--
Sample D_2	-46.0	--	1.040	218.23	--	-52.6	--
Sample F_2	-48.0	-10.0	0.440	176.05	0.224	-50.0	-20.0
Sample H_2	-47.5	-8.0	0.224	216.35	0.400	-46.3	-20.0
Sample J_2	--	-10.0	--	--	0.251	--	-20.0
Sample A_3	-39.8	--	2.100	192.73	--	-48.7	--
Sample D_3	-37.5	--	0.184	186.57	--	-42.6	--
Sample F_3	-36.0	-10.0	0.475	228.01	0.304	-41.0	-20.0
Sample H_3	-37.0	-10.0	0.240	237.65	0.264	-40.0	-20.0
Sample J_3	--	-10.0	--	--	0.250	--	-29.1

The subscripts 1, 2 and 3 stand for sulphur, peroxide and mixed systems.
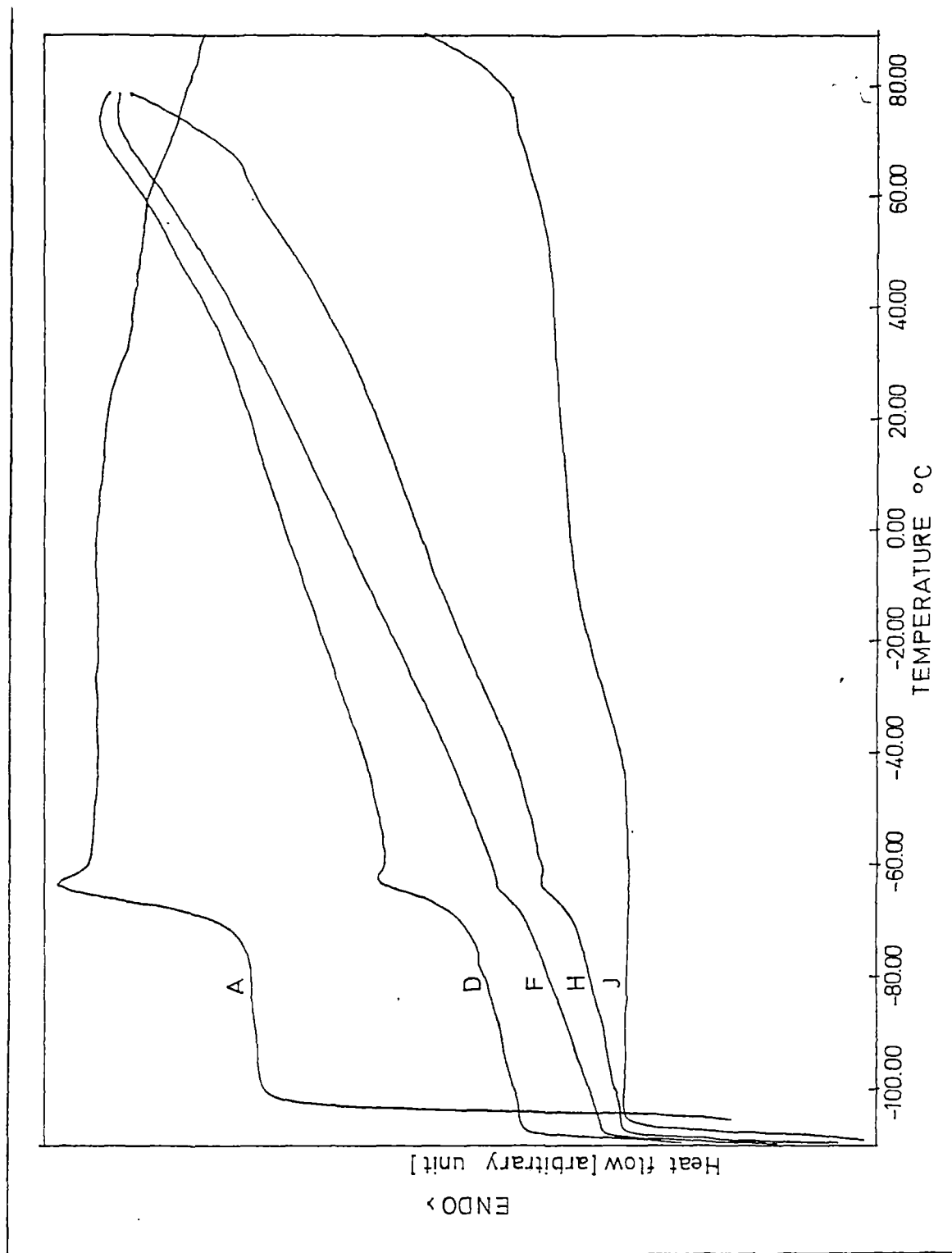
Figure IV.1
DSC thermograms of uncrosslinked NR-EVA blends.
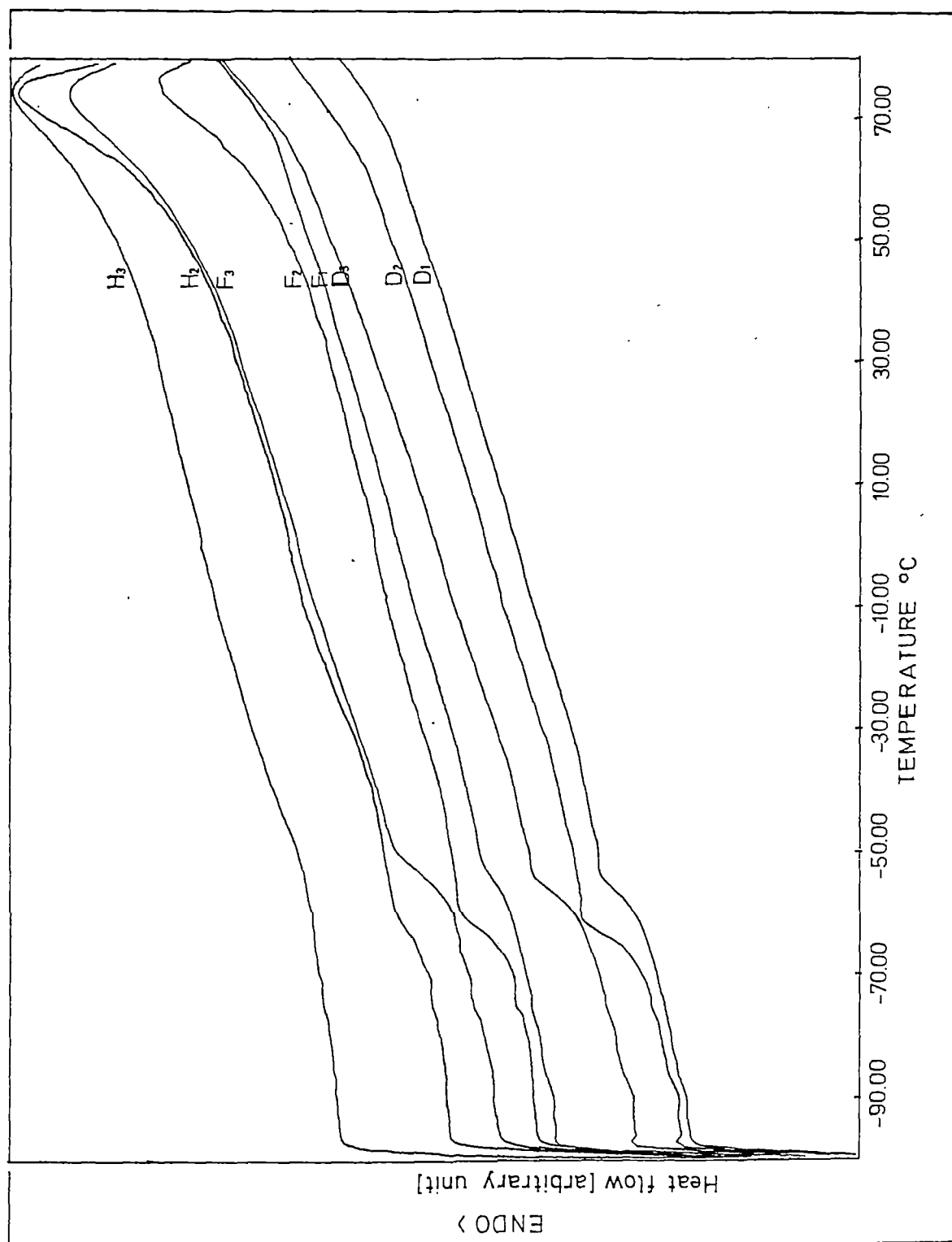
Figure IV.2
DSC thermograms of crosslinked NR-EVA blends
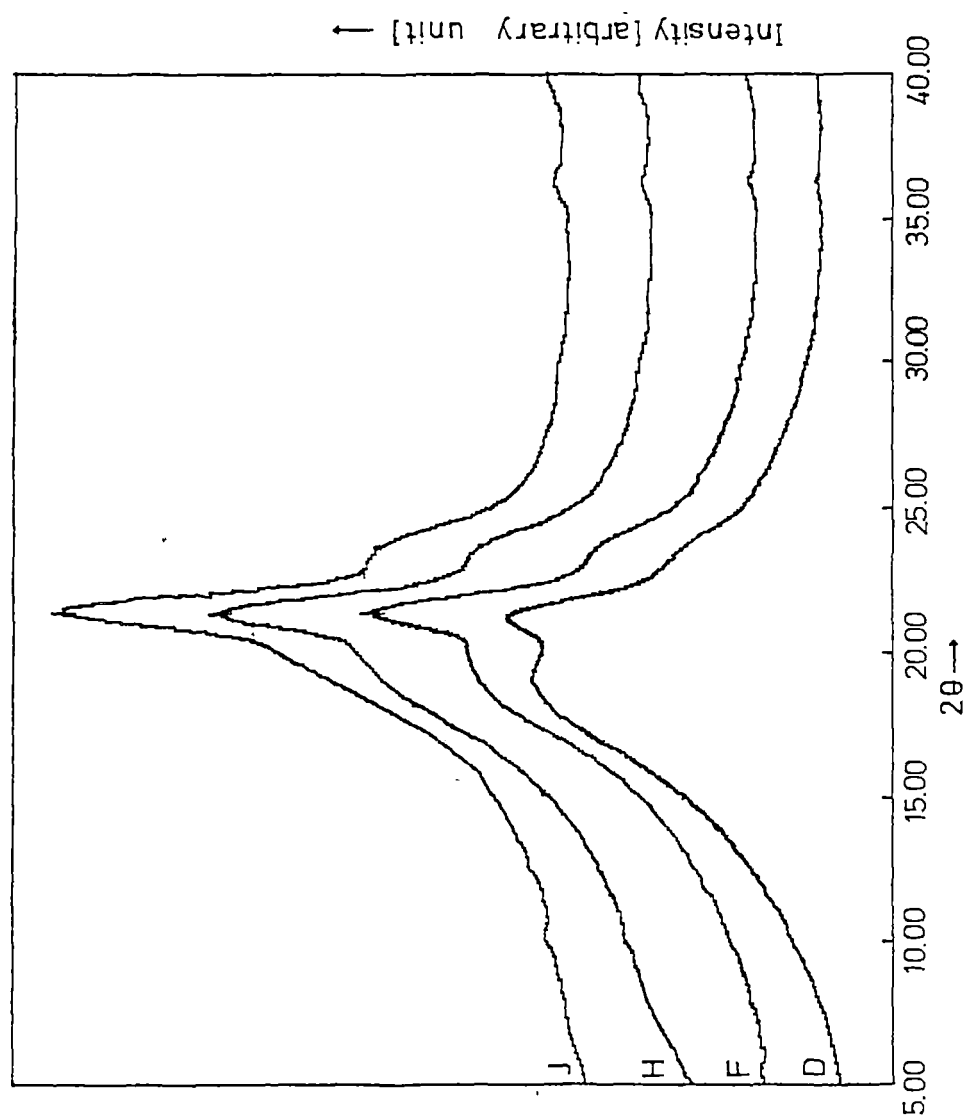
Figure IV.3
X-ray diffraction pattern of uncrosslinked NR-EVA blends.
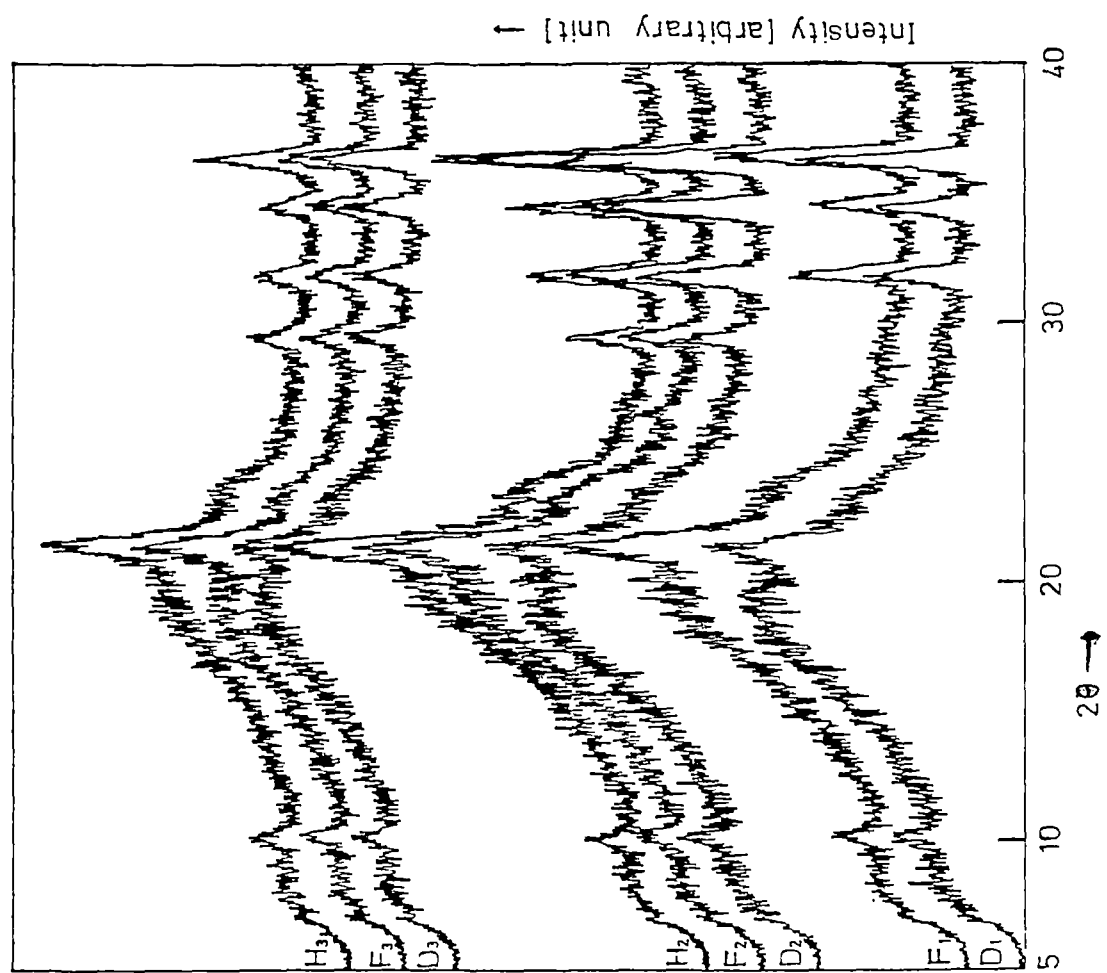
Figure IV.4
X-ray diffraction pattern of crosslinked NR–EVA blends.
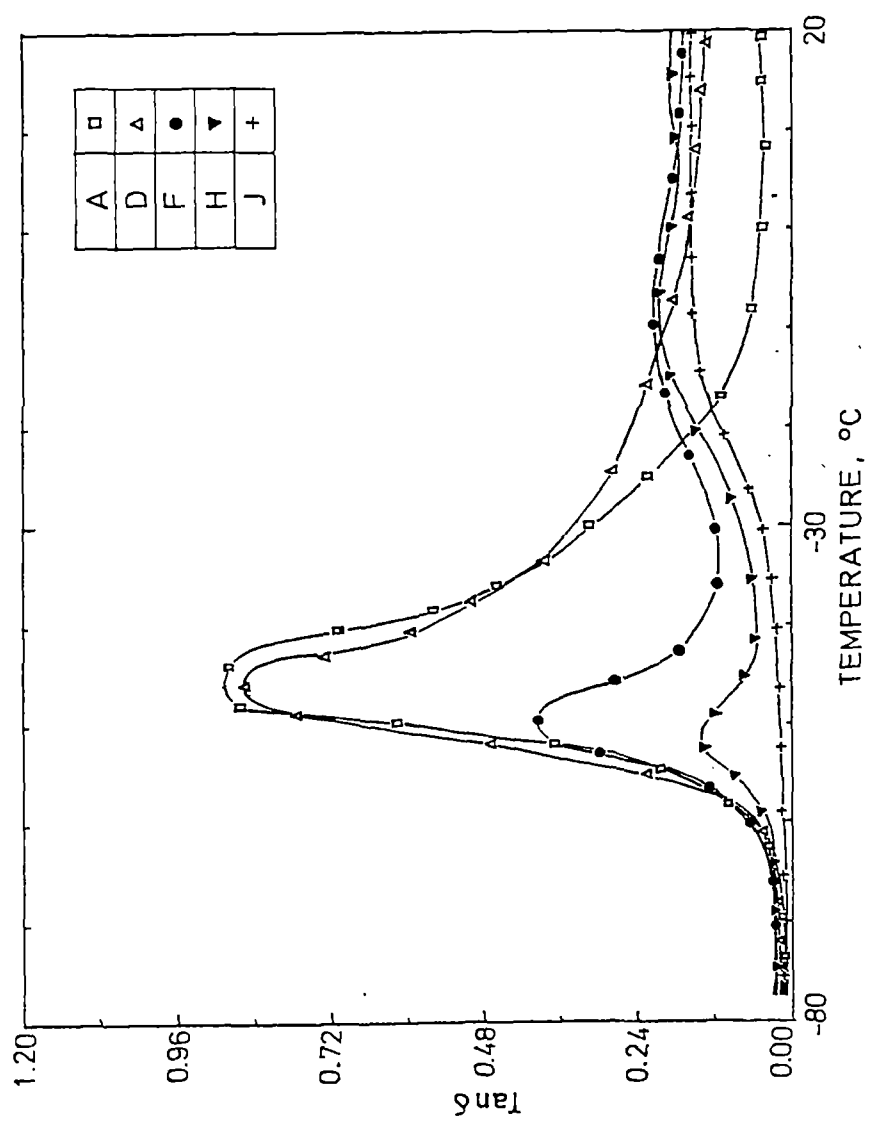
Figure IV.5
Effect of temperature on less tangent of uncrosslinked NR-EVA blends.
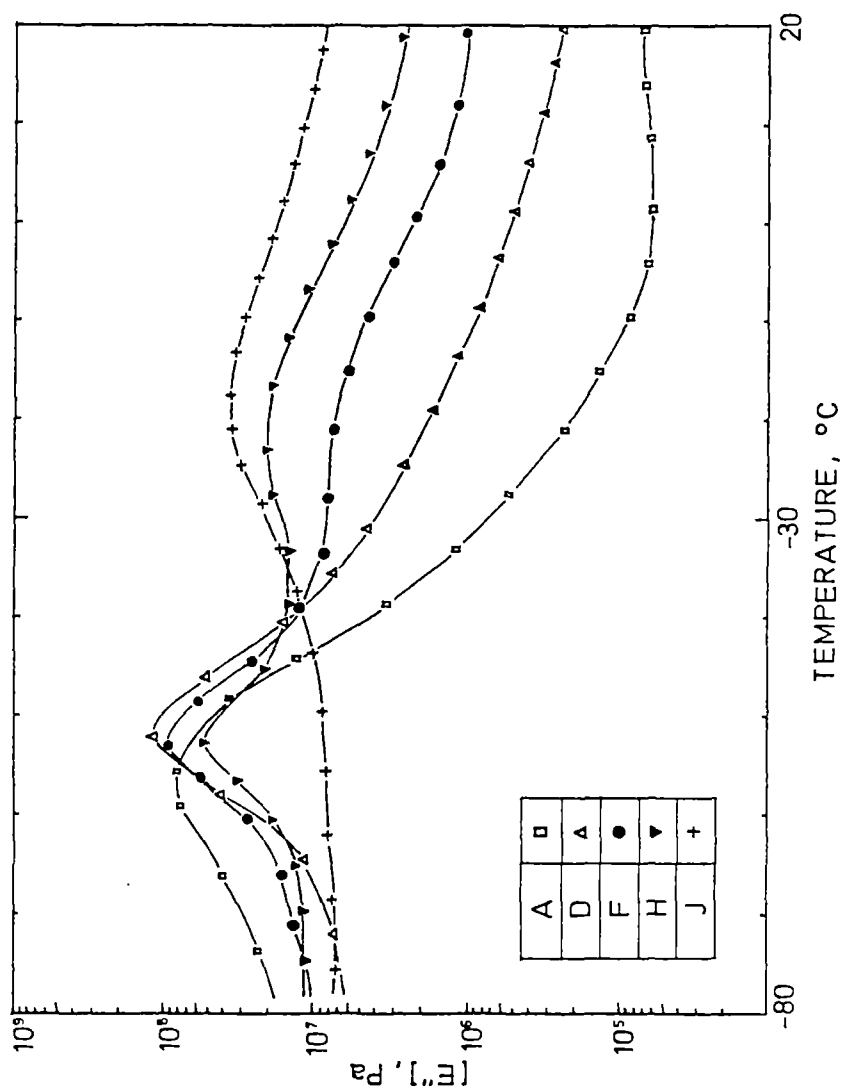
Figure IV.6
Effect of temperature on loss modulus of uncrosslinked NR-EVA blends.
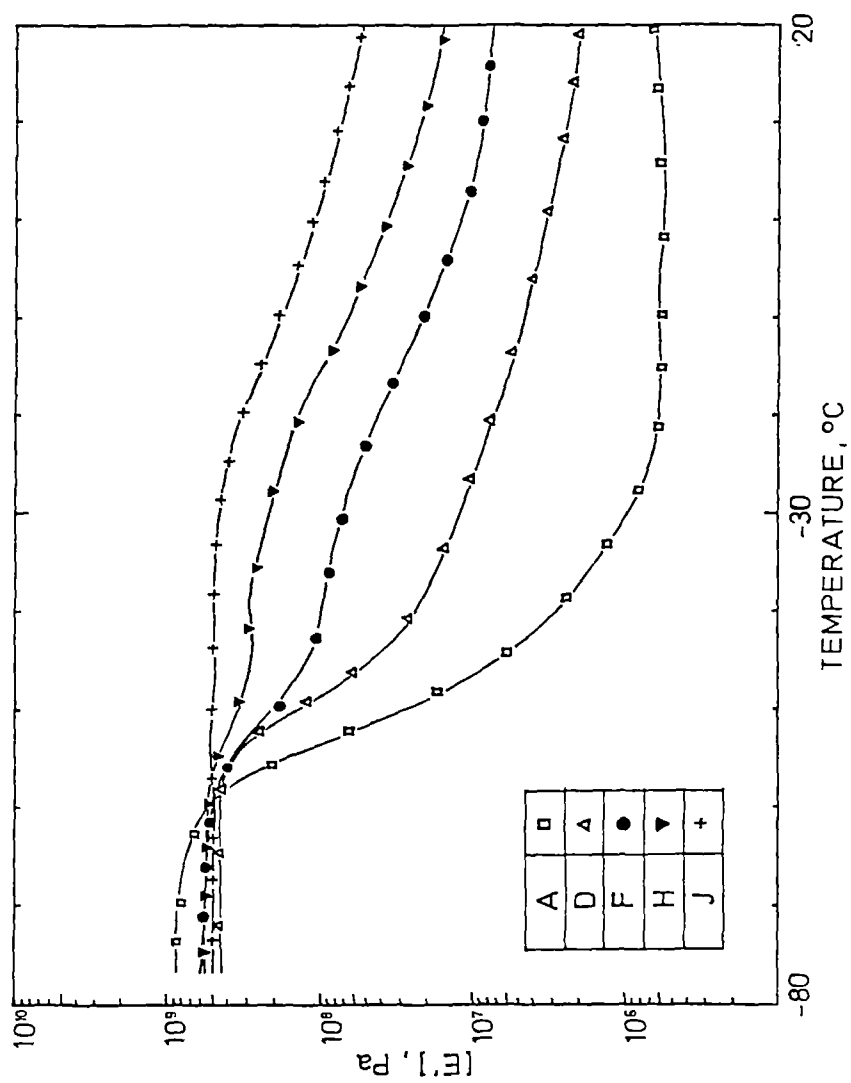
Figure IV.7
Effect of temperature on storage modulus of uncrosslinked NR-EVA blends.
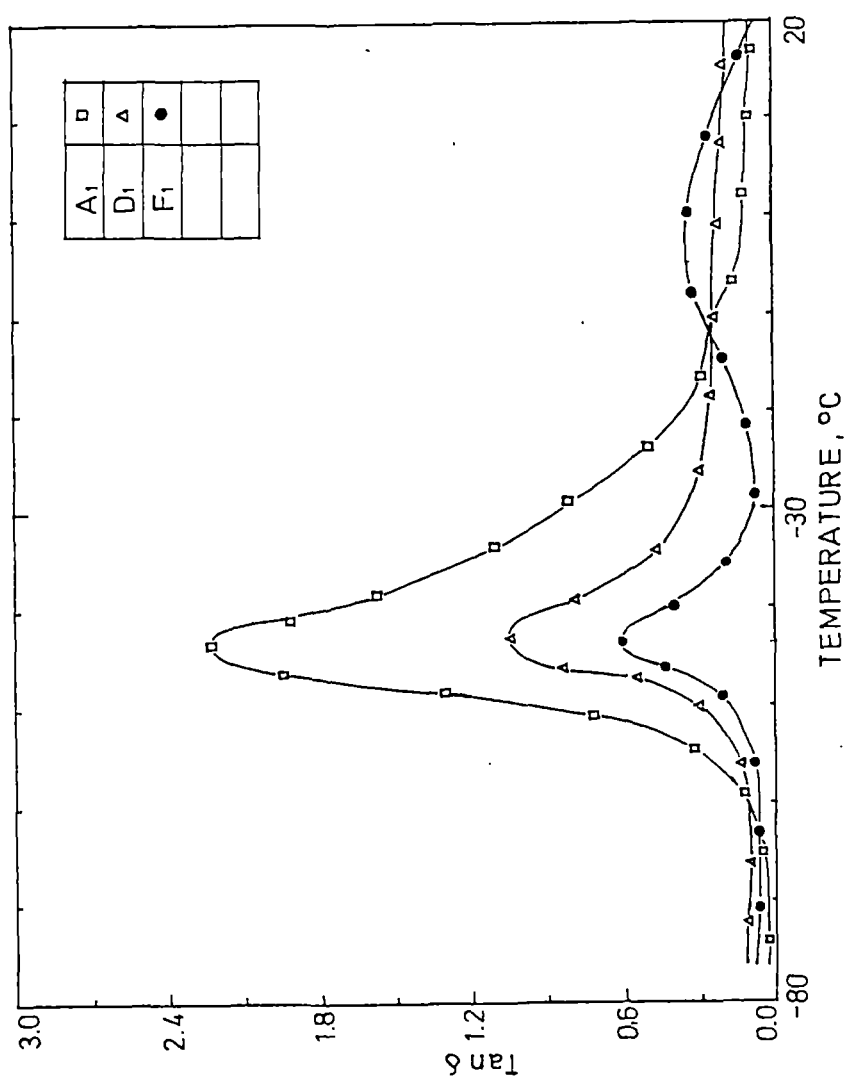
Figure IV.8
Effect of temperature on loss tangent of sulphur cured NR–EVA blends.
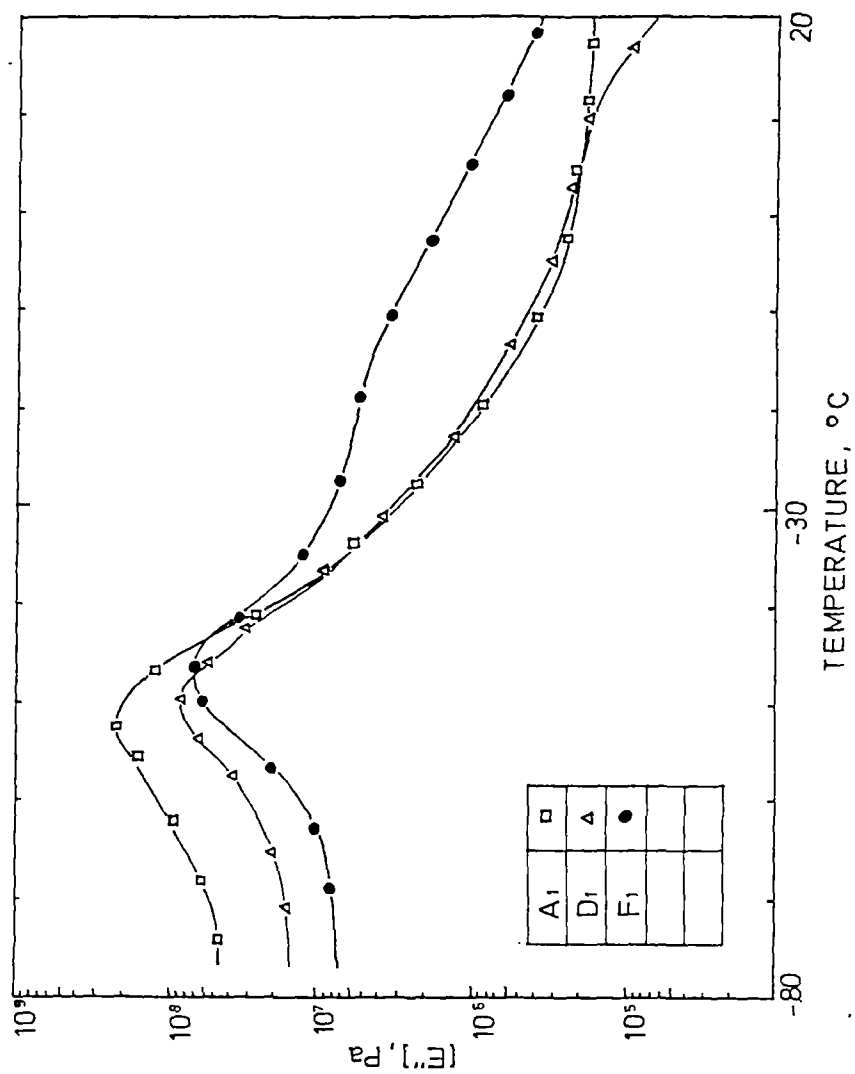
Figure IV.9
Effect of temperature on loss modulus of sulphur cured NR-EVA blends.
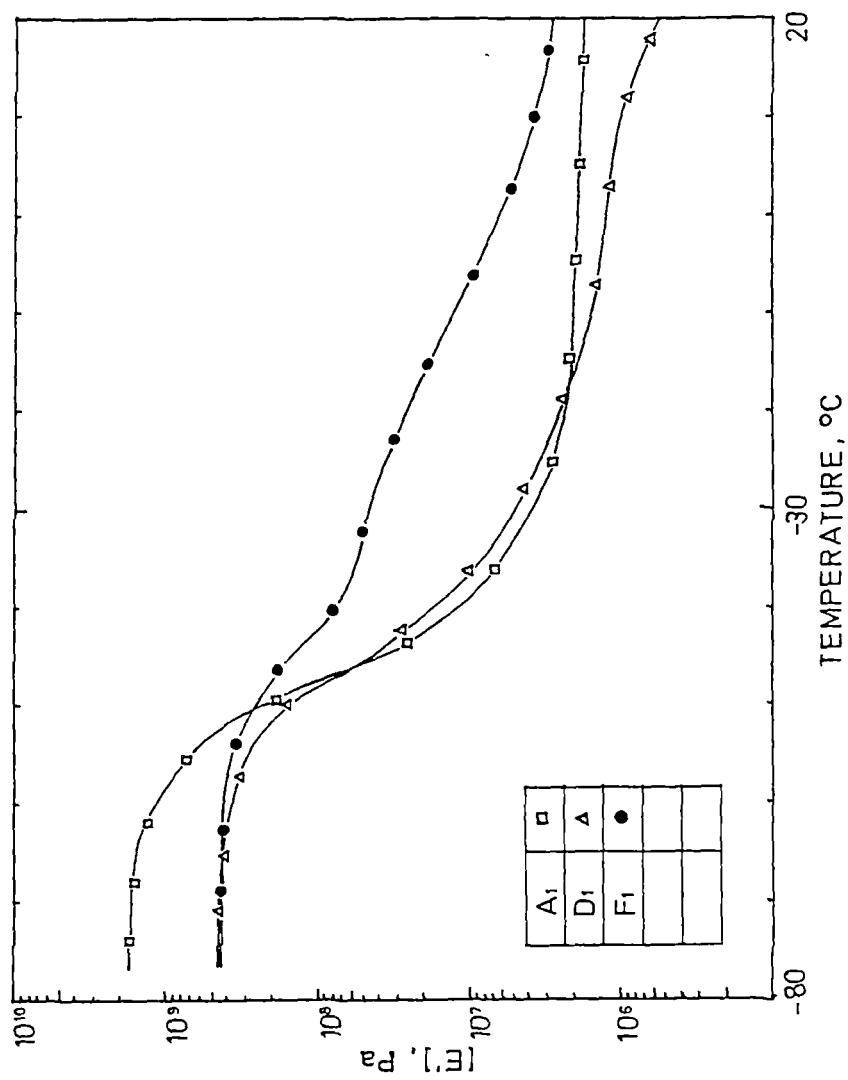
Figure IV.10
Effect of temperature on storage modulus of sulphur cured NR-EVA blends.
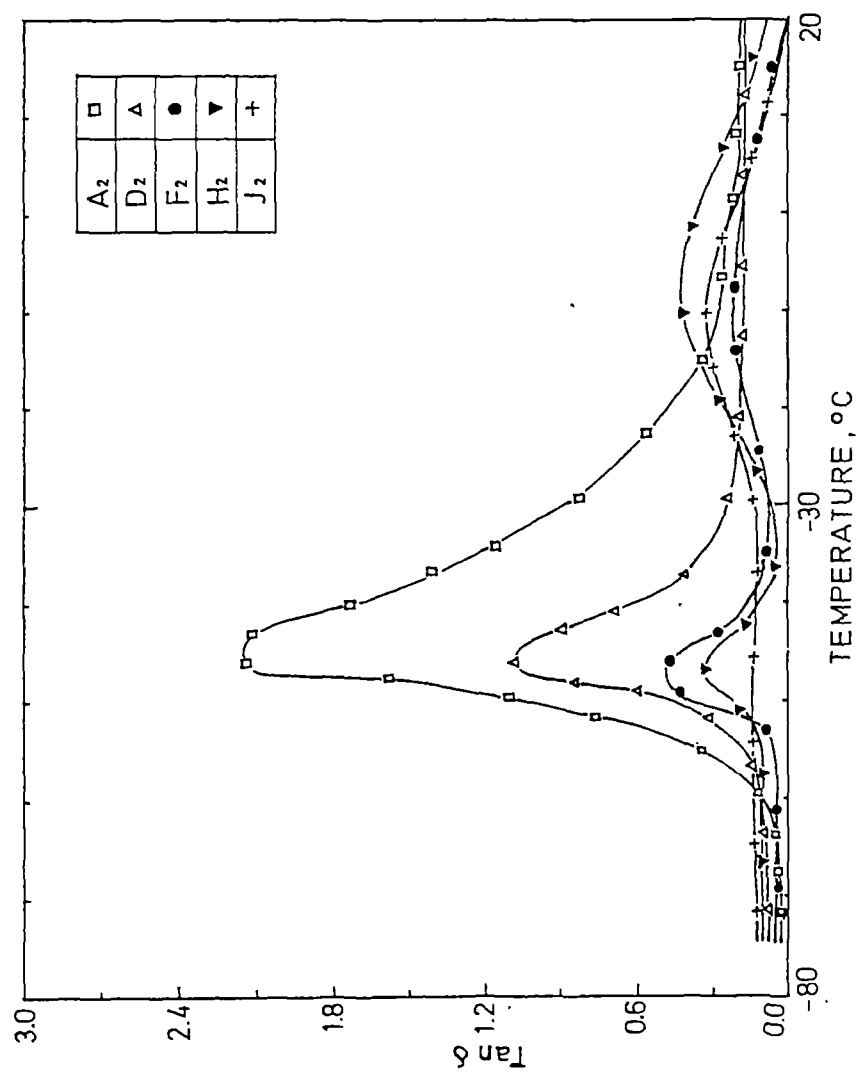
Figure IV.11   Effect of temperature on loss tangent of peroxide cured NR-EVA blends.
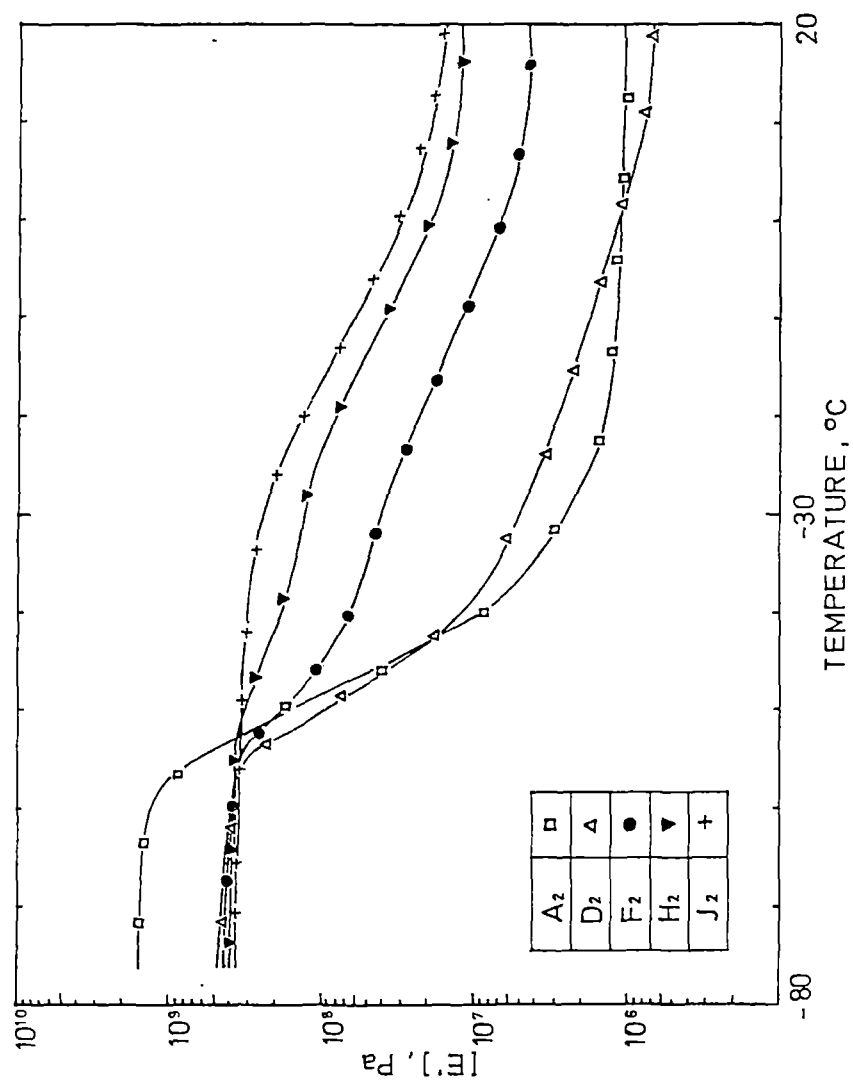
Figure IV.12
Effect of temperature on storage modulus of peroxide cured NR-EVA blends.
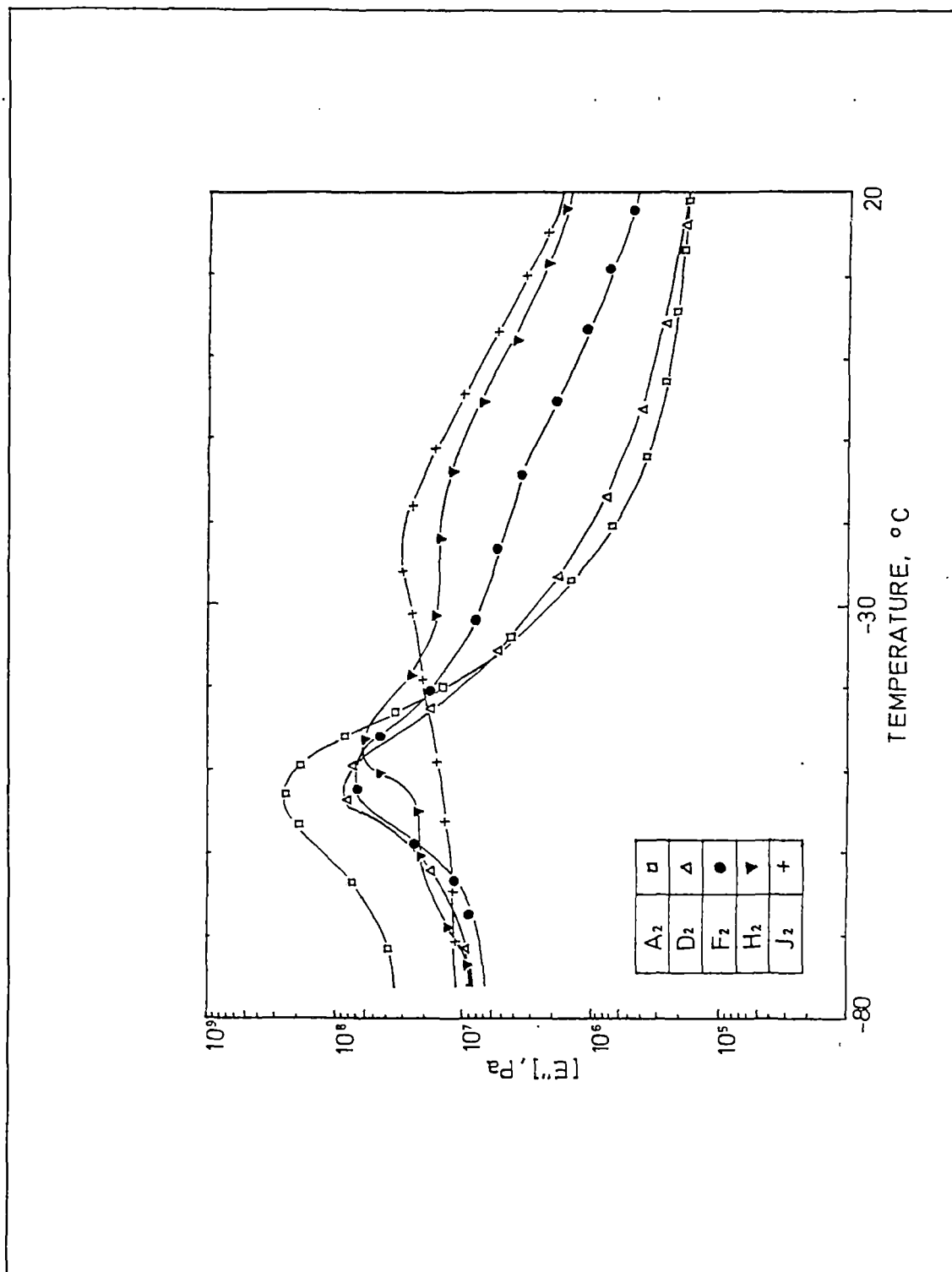
Figure IV.13
Effect of temperature on loss modulus of peroxide cured NR-EVA blends.
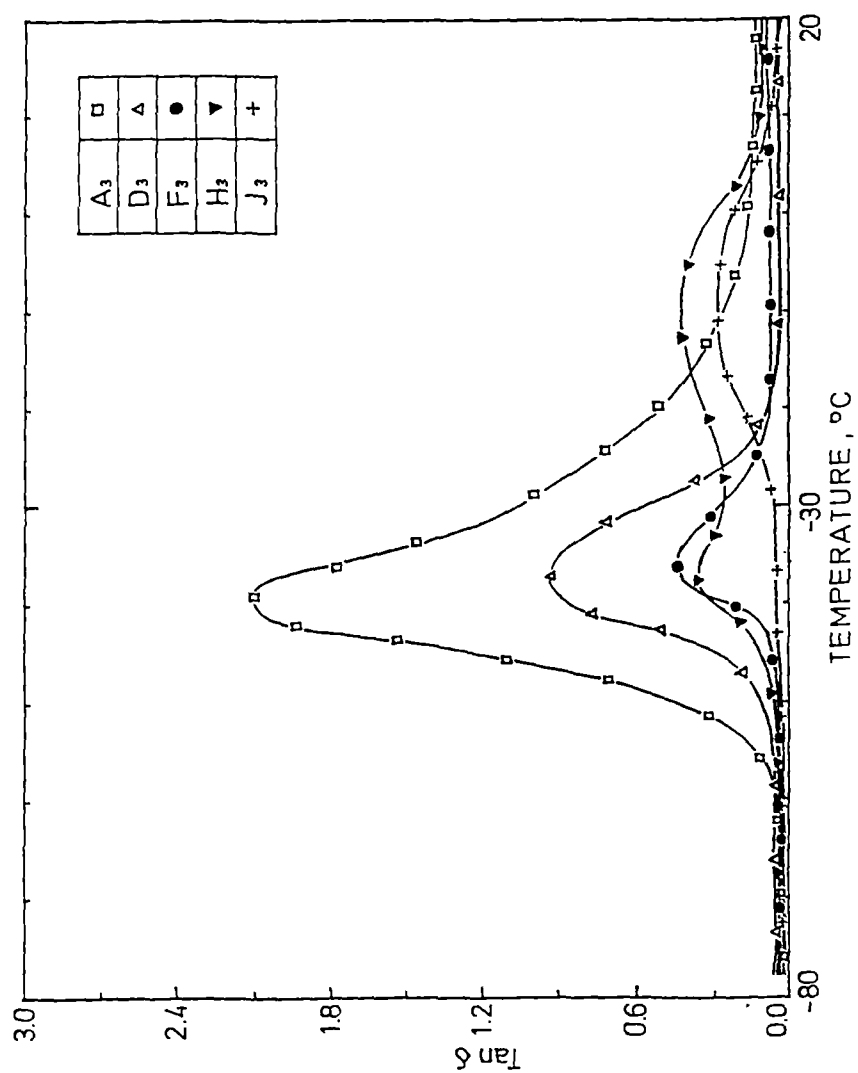
Figure IV.14
Effect of temperature on loss tangent of mixed cured NR-EVA blends.
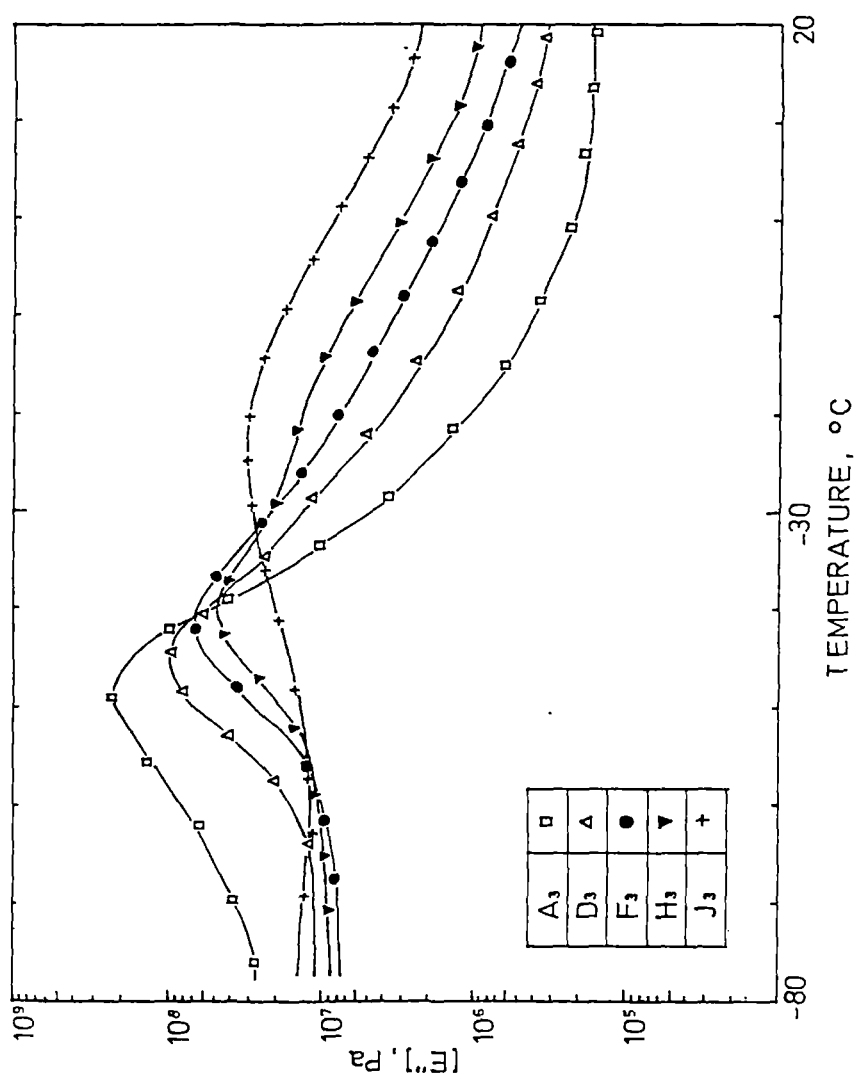
Figure IV.15
Effect of temperature on loss modulus of mixed cured NR-EVA blends.
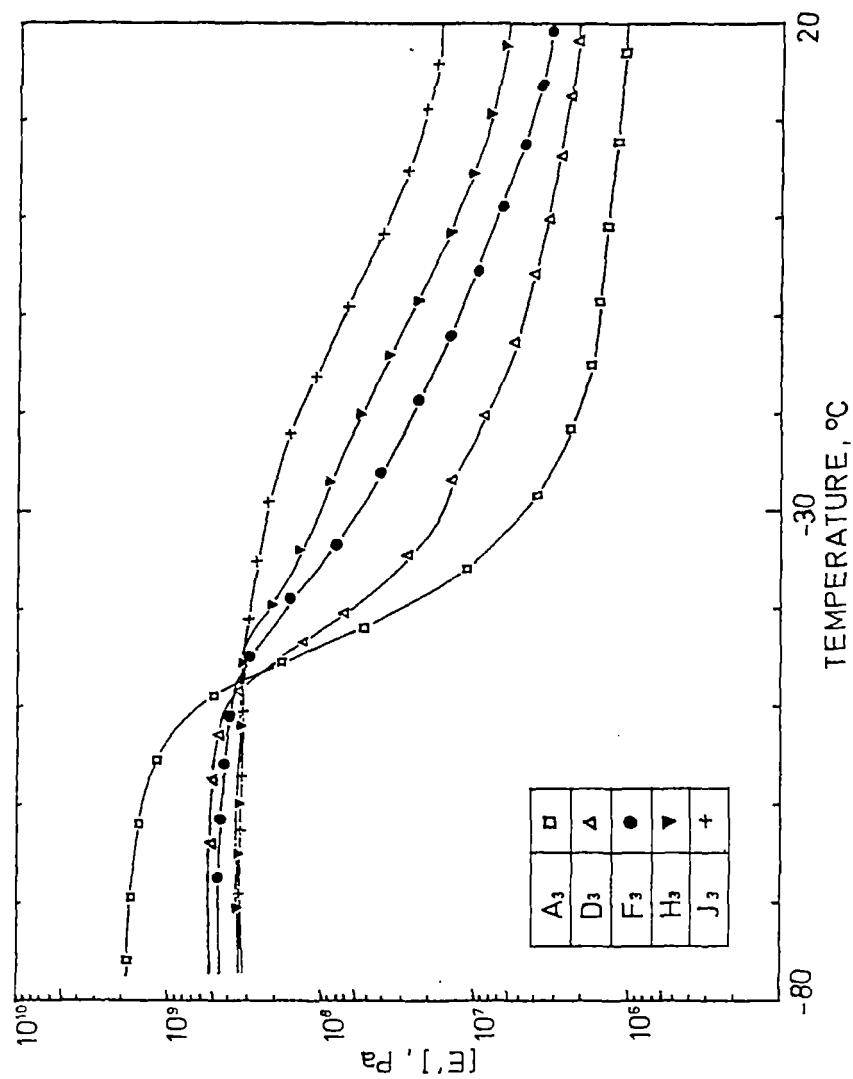
Figure IV.16
Effect of temperature on storage modulus of mixed cured NR–EVA blends.

CHAPTER V — MELT FLOW BEHAVIOUR AND EXTRUDATE MORPHOLOGY OF NR-EVA BLENDS.

Results of this chapter have been communicated for publication in

   (1) Polymer Engineering and Science

   (2) Journal of Materials Science Letters.

Melt flow studies of polymers are of paramount importance in optimising the processing conditions and in designing processing equipments such as extruders injection moulding machines and dies required for various products. Therefore the viscosity functions of a polymer ie., the shear viscosity as a function of shear rate or shear stress and temperature have become more and more important. A large number of indepth studies have been reported on the melt flow behaviour of elastomers and their blends[22,109a-118]. Several studies have also been reported on die swell, melt fracture and deformation of extrudates[23,109a,110].

The properties of polymer blends depend on their morphology. During the last few years, several studies have been reported on the morphology - property relationship of polymer blends . The existence of phenomena such as segregation and stratification during extrusion of the heterogeneous polymer blends has been established through morphological studies[22,111]. Since NR-EVA blends find applications in products such as cables, tubings and hoses, studies on the flow characteristics and the extrudate morphology of these blends become very important.

This chapter of the thesis presents the results of the studies on the melt flow behaviour and extrudate morphology of NR-EVA blends. The melt flow characteristics such as viscosity, flow behaviour index, melt elasticity and deformation of the extrudates

have been studied with special reference to the effects of blend ratio, crosslinking system, temperature and shear stress. The elastic parameters such as principal normal stress difference, recoverable shear strain and shear modulus were calculated. The extrudate morphology of the blends has been studied as a function of blend ratio and shear rates. The experimental techniques for assessing the rheological characteristics and extrudate morphology are given in Chapter II.

V.1 EFFECT OF BLEND RATIO AND SHEAR STRESS ON VISCOSITY

The effect of blend ratio and shear stress on the viscosity of uncrosslinked NR-EVA blends at 120°C is shown in Figures V.1a and V.1b. It can be seen that the viscosity of all the blends decreased with increase in shear stress, indicating pseudoplastic behaviour. The pseudoplastic behaviour is due to the fact that at zero shear the molecules are extensively entangled and randomly oriented. Under the application of shear, the molecules become oriented and get disentangled, as a result of which the viscosity decreases.

It is interesting to note that at low shear stress region (<3 x 10^5 Pa), when EVA content is less than 50 per cent (Figure V.1a), the viscosity of the blends is a non-additive function. NR exhibits slightly higher viscosity than EVA and the viscosity of the blends is higher than that of the components. This is clear

from Figure V.2 where the apparent viscosity of the blends at a low and ·high shear rate· is plotted as a function of the weight per cent of EVA. · It can be seen that this phenomenon is observed only at a lower shear region and also at lower proportions of the EVA phase where it formed the dispersed phase in the continuous NR matrix. The non-additive nature in the viscosity function of NR-EVA blends at the low shear stress region can be explained as follows.

At low shear stress region, there would be little deformation of the EVA domains and strong interactions among domains can be expected. Therefore, such a state of interaction can give rise to structural build up of EVA domains in the NR matrix. This can lead to a bulk viscosity greater than that of the constituent components. As the level of shear stress is increased, the structure breaks down and the chances of interactions between the domains are reduced. Some support for such a model can be drawn from the scanning electron micrograph (Figure V.3) of 20:80 EVA:NR blend, extruded at a low shear rate. The figure shows aggregates of EVA domains resting on the NR surface. It is also important to note that the increase in viscosity at low shear stress region is more pronounced at lower proportion of EVA in the blend (Figure V.2) where the domain size is minimum. This is due to the fact that smaller domains give rise to strong structure build up and as the proportion of EVA increases, the domain size increases and it tends to become a continuous phase. It is seen that when the EVA phase becomes fully

continuous, the anomaly disappears completely (Figure V.1b). This sort of positive deviation in the viscosity of polymer blends has been reported by many researchers[112,113].

V.2 EFFECT OF CROSSLINKING SYSTEM ON VISCOSITY

The viscosity of NR-EVA blends containing three vulcanising systems, namely sulphur, peroxide and a mixed one, at different shear stress is given in Figures V.4, V.5(a&b) and V.6(a&b), respectively. Since the experiment was conducted at 120°C, no cross-linking reaction is expected to take place during extrusion. Therefore, the flow behaviour of these compounds are similar to those of unvulcanised blends. However, slight variation is observed in certain cases due to the presence of compounding ingredients.

V.3 EFFECT OF PRECIPITATED SILICA ON VISCOSITY

The effect of precipitated silica (INSIL VN_3) on the viscosity of NR-EVA blends at three apparent shear rates is shown in Figure V.7. It is seen that the filled systems exhibit higher viscosity than the pure polymers at all shear rates. This is an expected trend in silica filled systems since it has good physico-chemical interaction with the polymers. The decrease in viscosity at high shear rates is due to the orientation of polymer chains in the direction of shear. In the presence of filler this alignment becomes more restricted. Therefore, the viscosity increases as filler loading increases.

V.4   EFFECT OF TEMPERATURE ON VISCOSITY

Figure V.8 illustrates the effect of temperature on the viscosity of NR-EVA blends at different shear rates. As expected the viscosity decreased with the increase of temperature for all the blends. However, at low shear rate region, the decrease in viscosity is more predominant than that at high shear rate. It is also noticed that temperature has only marginal effect on viscosity whereas the effect of shear rate on viscosity is substantial as seen from Figure V.8.

In order to further understand the influence of temperature on the viscosity of the blends, Arrhenius plots at a constant shear rate were made (Figure V.9). In this figure, the logarithm of viscosity is plotted as a function of reciprocal temperature. It can be noticed that the points for all the systems lie on straight lines. The activation energies of flow, calculated from the slopes of these lines are given in Table V.1. The activation energy of a material provides valuable information on the sensitivity of the material towards the change in temperature. The higher the activation energy, the more temperature sensitive the material will be. Such information is highly useful in selecting the processing temperature during the shaping process. It can be noticed from Table V.1 that EVA has the maximum value of activation energy and that it is unaffected by the addition of small quantities of NR where it remained as

domains. However, when the proportion of NR in the blend is more than 40 per cent, where it formed a continuous phase, the activation energy decreased sharply. Therefore, it can be concluded that the viscosity of EVA rich blends exhibits greater temperature dependence than those blends having a higher proportion of NR.

V.5   FLOW BEHAVIOUR INDEX (n')

The effect of temperature and blend ratio on the flow behaviour indices of the samples can be assessed from the data given in Table V.2. The extent of non-Newtonian behaviour of polymeric materials can be understood from n' values. Pseudoplastic materials are characterised by n' below 1. Therefore a high value of n' shows a low pseudoplastic nature of the material. The results indicate that as the proportion of EVA in the blend is increased, n' values are increased. It can also be noted that in all cases, n' values increased with the increase of temperature and this effect is pre-dominant in the case of pure EVA and high EVA blends. Therefore, it can be concluded that pseudoplastic nature of NR-EVA blends decreased with temperature and that the high EVA blends are less pseudoplastic than low EVA blends.

The effect of addition of filler on the n' value is given in Table V.3. The results show that in all cases,   increase of filler loading decreased the n' values. However, the decrease is pronounced in the case of high EVA blends. This is due to the fact that silica has more affinity towards the EVA phase.

V.6 MELT ELASTICITY

Properties such as extrudate swell, principal normal stress difference ($\tau_{11} - \tau_{22}$), recoverable shear strain (S_R) and elastic shear modulus (G) characterise the elasticity of polymer melts.

The principal normal stress difference ($\tau_{11} - \tau_{22}$) was calculated from the extrudate swell values and shear stress according to Tanner's equation[114].

$$\tau_{11} - \tau_{22} = 2\tau_w \left[2 \left(d_e/d_c \right) - 2 \right]^{1/2}$$

Recoverable shear strain (S_R) and the apparent shear modulus (G) were calculated from the following equations:

$$S_R = \left(\tau_{11} - \tau_{22} \right) / 2\tau_w$$

$$G = \tau_w / S_R$$

V.6.1 Extrudate swell

As molten polymer flows through the capillary, orientation of polymer chains occurs due to shear. When the melt emerges from the die, polymer molecules tend to recoil leading to the phenomenon of die swell or extrudate swell. This is a relaxation imposed in the capillary. Factors such as chain branching, stress relaxation,

crosslinking, presence of fillers and plasticizers etc. control the elastic recovery. Table V.4 shows the die swell values of uncross-linked NR-EVA blends extruded at 120°C at two shear rates. It can be noticed that EVA shows the lowest die swell due to its low elastic recovery and the addition of NR increases the die swell of the blend. It can also be noted that for a given blend, die swell increased with shear rate. This is due to the fact that at high shear rates, the residence time of the material in the capillary decreases and hence more elastic energy is stored by the polymer. This results in an increase in die swell[6,115]. The die swell values of silica filled blends containing mixed cure system, extruded at 120°C at an apparent shear rate of 3330 s^{-1} are given in Table V.5. It is seen that, in general, die swell decreased with filler loading. Silica filler increases the rigidity and stiffness of the polymer chain. This results in low mobility of the polymer chains under the influence of applied shear stress. Hence the elastic recovery and consequently die swell decrease with the increase of filler loading.

V.6.2 Deformation of extrudates

Figure V.10 shows the photograph of the blends extruded at two different shear rates. At low shear rate most of the extrudates have smooth surfaces. However, at high shear rates, extrudate surfaces exhibit different extent of distortion. These extrudates have rough surfaces and are of non-uniform diameter.

This is associated with melt fracture which occurs at high shear forces where the shear stress exceeds the strength of the melt. The effect of silica filler on the deformation of the crosslinkable extrudate can be understood from Figure V.11. It is seen that the addition of silica decreased the deformation of the extrudates.

V.6.3 Principal normal stress difference $(\tau_{11} - \tau_{22})$

Table V.6 shows the principal normal stress difference of uncrosslinked blends extruded at low and high shear rates. The temperature of extrusion was 120°C. EVA showed the lowest value of principal normal stress difference. Addition of NR increased the normal stress difference of EVA. The principal normal stress difference increased with the increase of shear rates. The higher value of $\tau_{11} - \tau_{22}$ implies higher elasticity of the blends. This is reflected in higher die swell values also.

V.6.4 Recoverable elastic shear stress (S_R)

It has been reported[115] that when the stored elastic strain energy of a polymer melt exceeds a critical value, the excess amount may be converted into surface free energy yielding distortion to the extrudate. Table V.6 shows the S_R values of the blends at two different shear rates. It is seen that S_R increases with the increase of shear rates. This is related to the extent of extrudate distortion of the blends (Figure V.10). At low and high shear rates, the S_R

values of the blends increase with the increase of NR content.

V.6.5 Elastic shear modulus (G)

The elastic shear modulus of the blends as shown in Table V.6 indicated that the melt elasticity of EVA is increased by the addition of NR. The elastic shear modulus increased with the increase of shear rate, especially in the case of blends containing a higher proportion of EVA.

V.7 EXTRUDATE MORPHOLOGY

The factors such as component ratio, their melt viscosity, rate of shear during melt mixing and presence of other ingredients such as lubricants, extenders, plasticizers, fillers etc. control the final morphology of the polymer blends. Danesi and Porter[22] have reported that for the same processing history, the composition of the blend and the melt viscosity difference determine the morphology. Figure V.12a gives the core region of the extrudate of 80:20 EVA:NR blend extruded at a shear rate of 330 s^{-1}. The holes in the surface correspond to the NR phase which had been extracted by benzene. It is quite evident that the NR phase exists as domains in the continuous EVA matrix. The average domain size measured from the photograph was 14.5 μm. The dispersed nature of the NR phase is associated with its lower proportion and slightly higher viscosity than EVA. Figure V.12b shows the morphology of the core region

of the same composition (80:20 EVA:NR) extruded at a shear rate of 3330 s^{-1}. It is interesting to note that the particle size has been considerably reduced at a high shear rate. The measured particle size was 7.8 µm. Figure V.12c shows a clear demarcation between periphery of the extrudate which is occupied mostly by EVA phase and the centre by NR phase.

Figures V.13 and V.14 show the morphology of the blends of 30:70 and 40:60 NR:EVA, respectively, extruded at a shear rate of 330 s^{-1}. In these blends also, it can be seen that NR phase is dispersed as domains at the core of the extrudate which is surrounded by an EVA sheath. The size of the NR domain is considerably higher. A further increase in the proportion of NR to 50 per cent makes the two phases co-continuous. This is seen from the photomicrograph of core region of 50:50 NR:EVA blend extruded at a shear rate of 330 s^{-1} (Figure V.15). A clear phase inversion can be seen from the morphology of 70:30 NR:EVA extruded at a shear rate of 330 s^{-1} (Figure V.16). It is interesting to note that the aggregates of EVA domains having size of 24 µm are resting on the NR surface. From the above observations it can be concluded that the morphology of NR-EVA blends exhibits a two phase structure in which the minor component is dispersed as domains in the continuous phase of the major component. However, at 50:50 composition both the components exist as continuous phases.

The stratification (division into periphery and core) of the extrudate may be associated with the migration of the low viscosity EVA phase towards the periphery of the extrudates and the resulting encapsulation of the high viscosity NR phase. The stratification phenomenon has been reported in the case of binary polymer blends by many researchers. These include the studies of Yu and Han[116], Southern and Ballman[117], Danesi and Porter[22] and Thomas et al.[118]. All these authors concluded that the differences in shear viscosity between the components lead to interphase distortion, with the lower viscosity component encapsulating the high viscosity component.

The decrease in domain size with the increase of shear rate is associated with particle break down. During extrusion, the dispersed domains are elongated at the entrance of the capillary under the action of shear force. At sufficiently high shear forces, the elongated domains are broken down into small particles. However, under low shear forces, the elongated domains retain their morphology and are not broken down into smaller sizes.

Finally, the increase of NR domain size with increasing concentration of NR phase is associated with recombination and coalescence of the dispersed domains. The occurrence of coalescence at high concentration of one of the components in a binary blend has been reported. Thomas et al.[118] have reported similar phenomenon in the case of hytrel-PVC blends.

Table V.1.   Activation energy.

Sample No.	Blend ratio (NR:EVA)	$E \times 10^{-3}$ (kcal/mol)
B	90:10	0.4145
C	80:20	0.4606
D	70:30	0.5066
E	60:40	0.5066
F	50:50	0.6440
G	40:60	0.8751
H	30:70	0.9212
I	20:80	0.9212
J	0:100	0.9212

Table V.2. Flow behaviour index (n')

Sample No.	120°C	170°C	180°C	190°C	200°C
A	0.165	0.195	0.220	0.220	0.237
B	0.171	0.208	0.221	0.230	0.244
C	0.183	0.208	0.238	0.261	0.354
D	0.188	0.218	0.240	0.270	0.360
E	0.194	0.239	0.248	0.275	0.376
F	0.223	0.245	0.270	0.280	0.382
G	0.233	0.309	0.303	0.314	0.398
H	0.245	0.327	0.362	0.358	0.437
I	0.296	0.358	0.360	0.415	0.439
J	0.289	0.371	0.436	0.452	0.484

Table V.3.   Effect of silica on flow behaviour index of
            NR-EVA blends.

Sample No.	Silica loading, phr			
	0	15	30	45
A	0.166	0.155	0.142	0.131
C	0.198	0.192	0.175	0.168
E	0.239	0.211	0.174	0.164
F	0.249	0.239	0.194	0.144
G	0.282	0.271	0.260	0.149
I	0.318	0.308	0.279	0.143
J	0.344	0.312	0.281	0.152

Table V.4.   Extrudate swell of uncrosslinked NR-EVA blends, at 120°C.

Sample No.	Apparent shear rate, s^{-1}	
	3330	330
A	1.46	1.19
B	1.61	1.43
C	1.46	1.35
D	1.40	1.26
E	1.36	1.26
F	1.26	1.25
G	1.26	1.24
H	1.25	1.23
I	1.24	1.23
J	1.08	1.03

Table V.5. Effect of silica on die-swell values of crosslinkable (mixed) NR-EVA blends extrudated at 3330 s^{-1}.

Sample No.	Silica loading, phr			
	0	15	30	45
A$_3$S	1.07	1.07	1.06	1.05
C$_3$S	1.07	1.07	1.05	1.04
E$_3$S	1.06	1.06	1.00	1.00
F$_3$S	1.35	1.22	1.12	1.01
G$_e$S	1.35	1.12	1.12	1.01
I$_3$S	1.35	1.12	1.11	1.01
J$_3$S	1.08	1.07	1.06	1.01

Table V.6. Melt elasticity of NR-EVA blends extruded at 120°C.

Sample No.	Shear rate 330 s^{-1}			Shear rate 3330 s^{-1}		
	$\tau_{11}-\tau_{22}$, Nm^{-2}	G Nm^{-2}	S_R	$\tau_{11}-\tau_{22}$ Nm^2	G Nm^{-2}	S_R
B	23.98×10^5	0.80×10^5	3.86	49.00×10^5	0.82×10^5	5.44
C	18.47×10^5	0.94×10^5	3.13	38.82×10^5	1.12×10^5	4.16
D	14.06×10^5	1.17×10^5	2.44	38.84×10^5	1.12×10^5	4.16
E	13.66×10^5	1.14×10^5	2.44	29.33×10^5	1.38×10^5	3.25
F	12.68×10^5	1.15×10^5	2.33	22.78×10^5	1.86×10^5	2.47
G	12.41×10^5	1.18×10^5	2.28	22.83×10^5	1.85×10^5	2.48
H	12.02×10^5	1.22×10^5	2.21	21.88×10^5	2.04×10^5	2.32
I	12.01×10^5	1.22×10^5	2.21	21.98×10^5	2.14×10^5	2.23
J	3.35×10^5	4.38×10^5	0.62	5.15×10^5	8.99×10^5	0.53

Figure V.1a
Viscosity-shear stress plots of uncrosslinked NR-EVA blends
at 120°C.
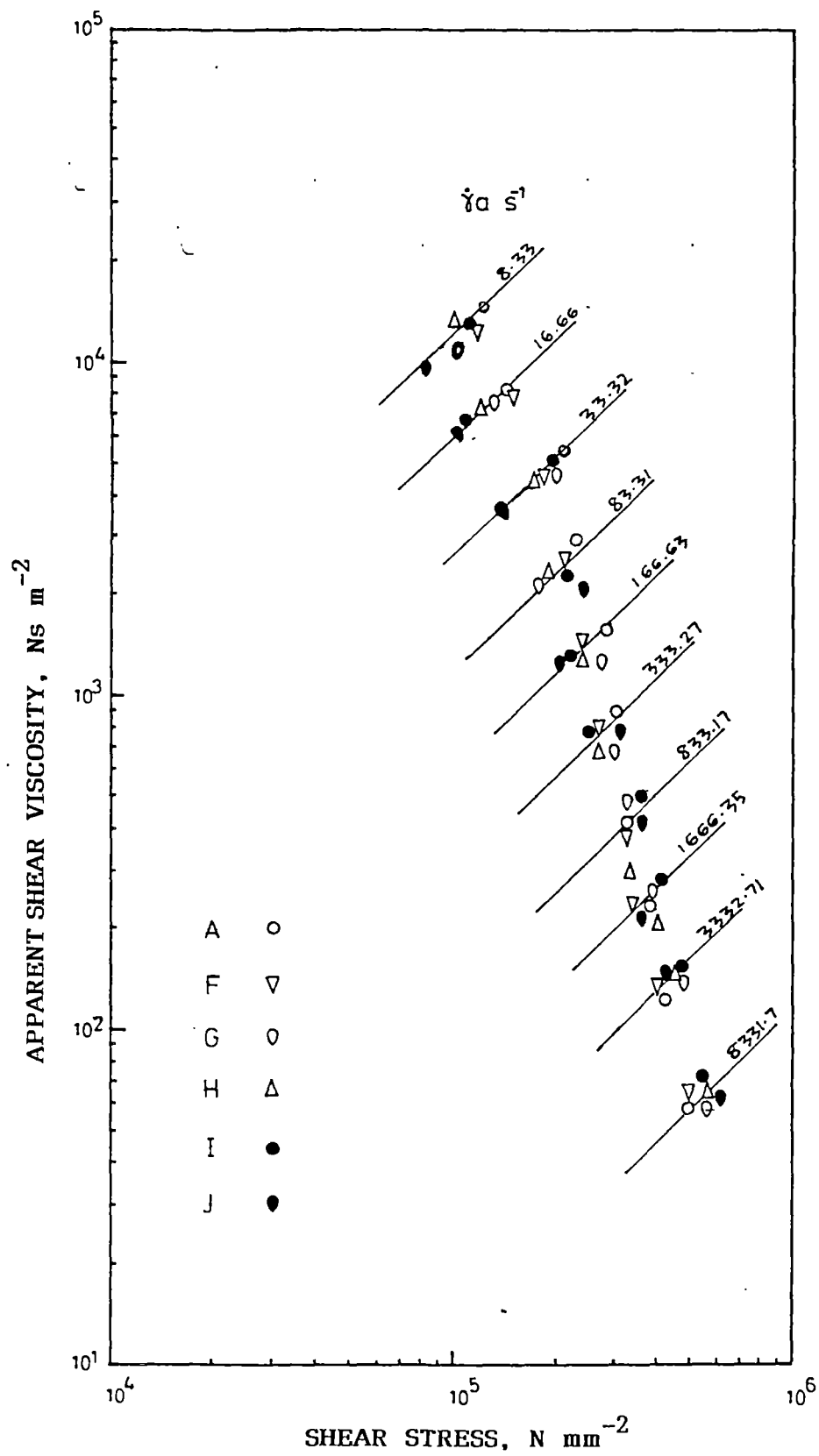
Figure V.1b
Viscosity-shear stress plots of uncrosslinked
NR-EVA blends at 120°C.
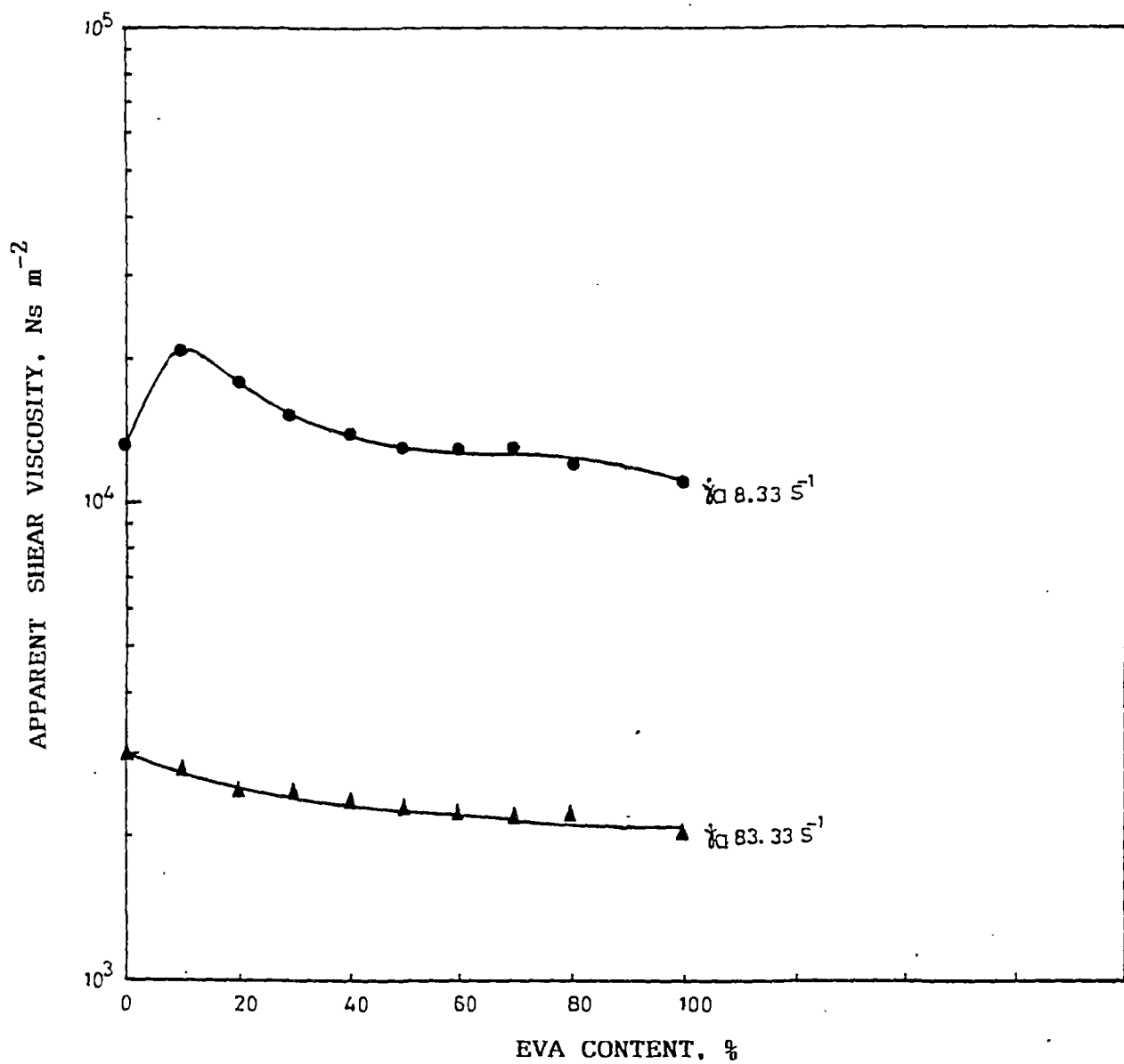
Figure V.2
A plot of viscosity vs EVA content at low and high shear rates, at 120°C.
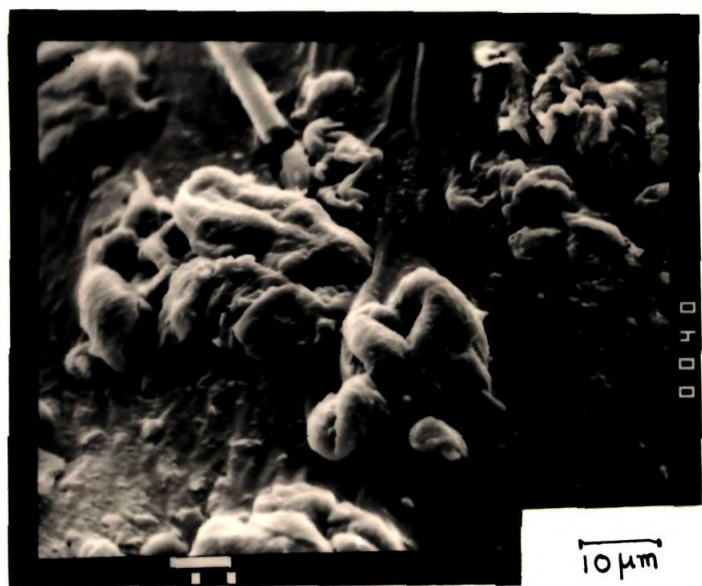
Figure V.3
SEM Photomicrograph of blend C, aggregates
of EVA domains resting on NR surface.
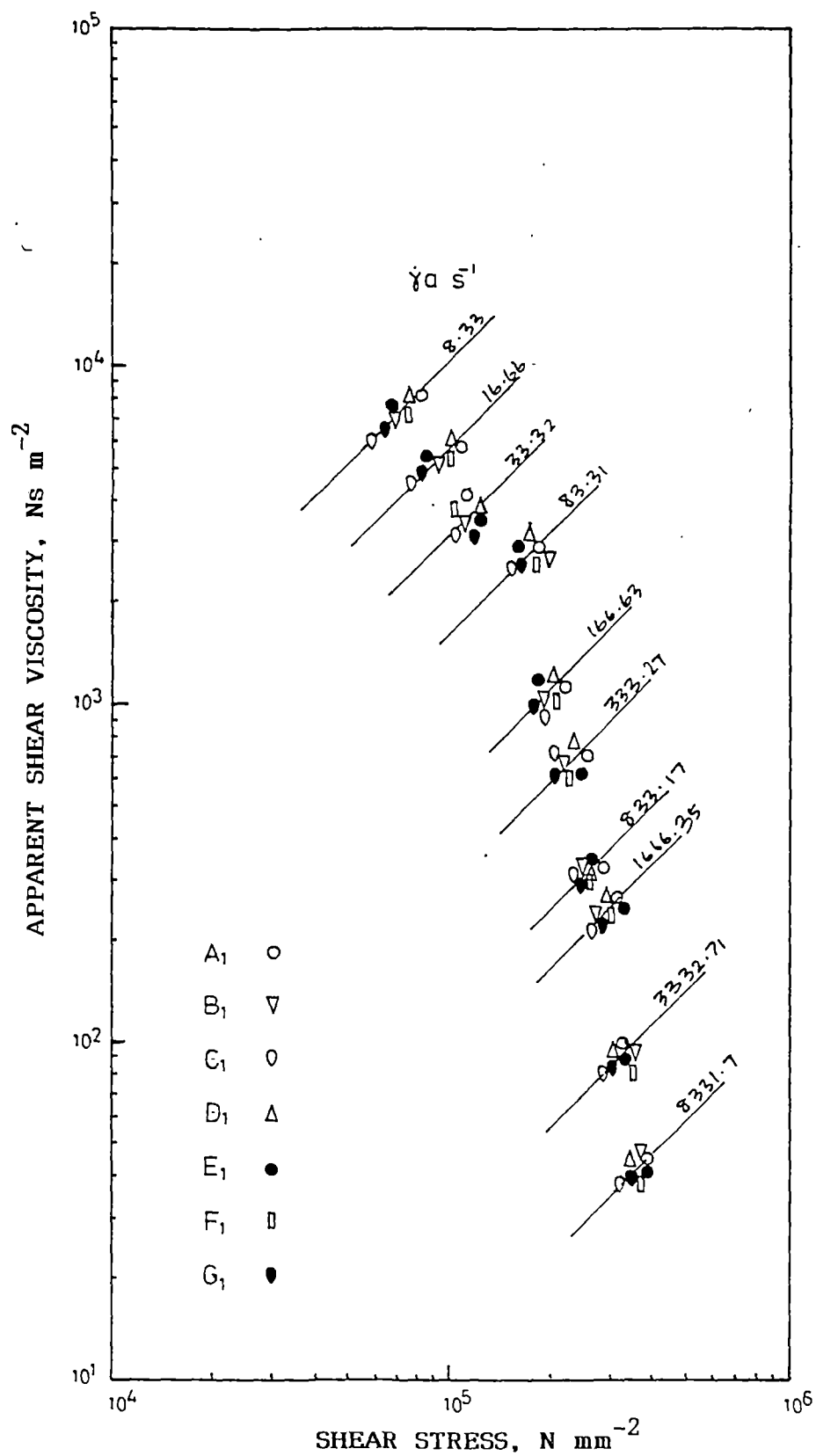
Figure V.4
Viscosity-shear stress plots of NR-EVA blends containing
sulphur cure system, at 120°C.

APPARENT SHEAR VISCOSITY, Ns m^{-2}

10^5

$\dot{\gamma}_a$ s^{-1}

10^4

8.33

16.66

33.32

83.31

10^3

166.63

333.27

833.17

A$_2$ O

B$_2$ ∇

C$_2$ O

D$_2$ $\triangle$

E$_2$ ●

J$_2$ ●

10^2

166.35

333.71

833.7

10^1

10^4 10^5 10^6
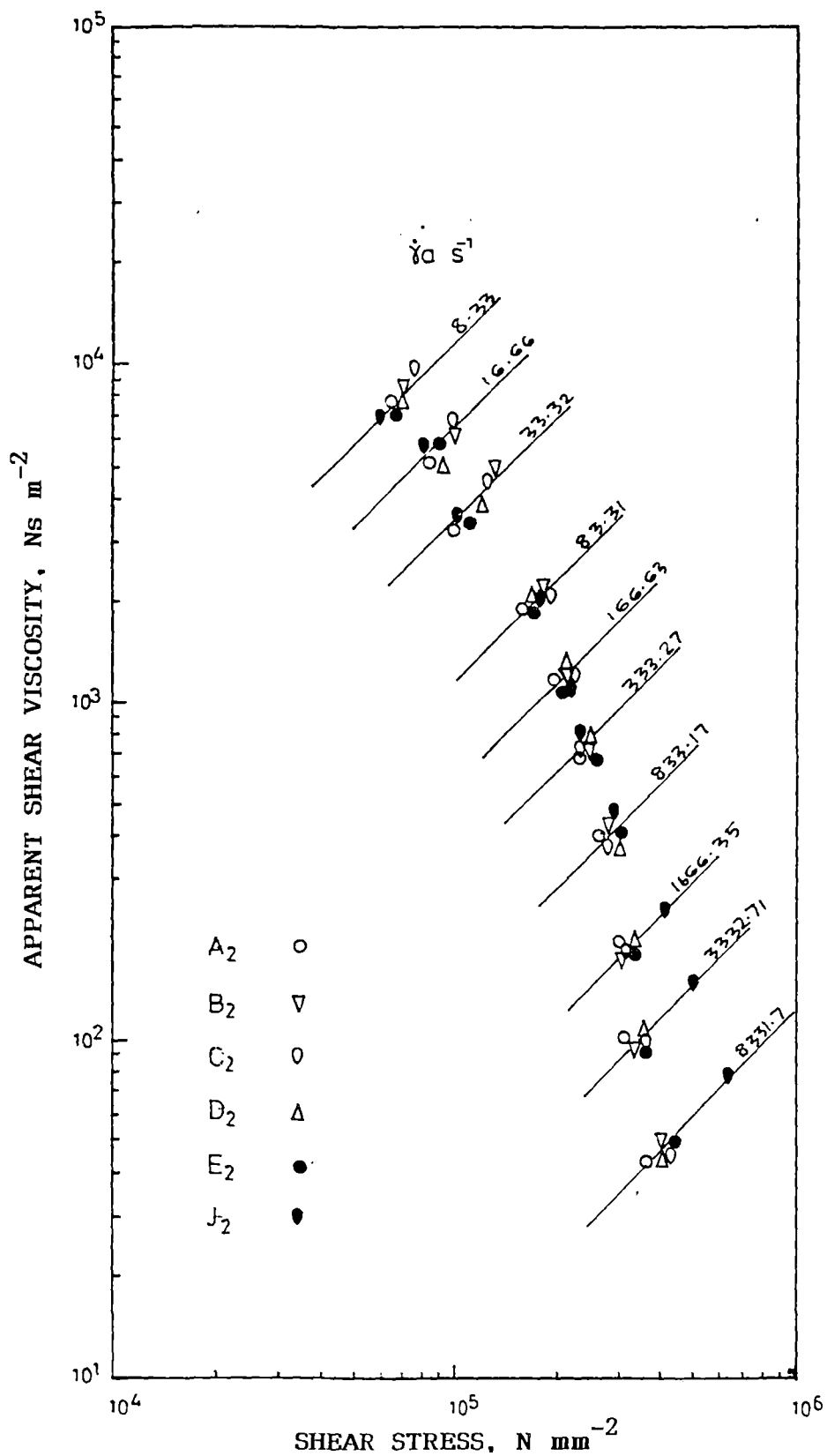
SHEAR STRESS, N mm^{-2}

Figure V.5a
Viscosity-shear stress plots of NR-EVA blends containing
peroxide cure system, at 120°C.
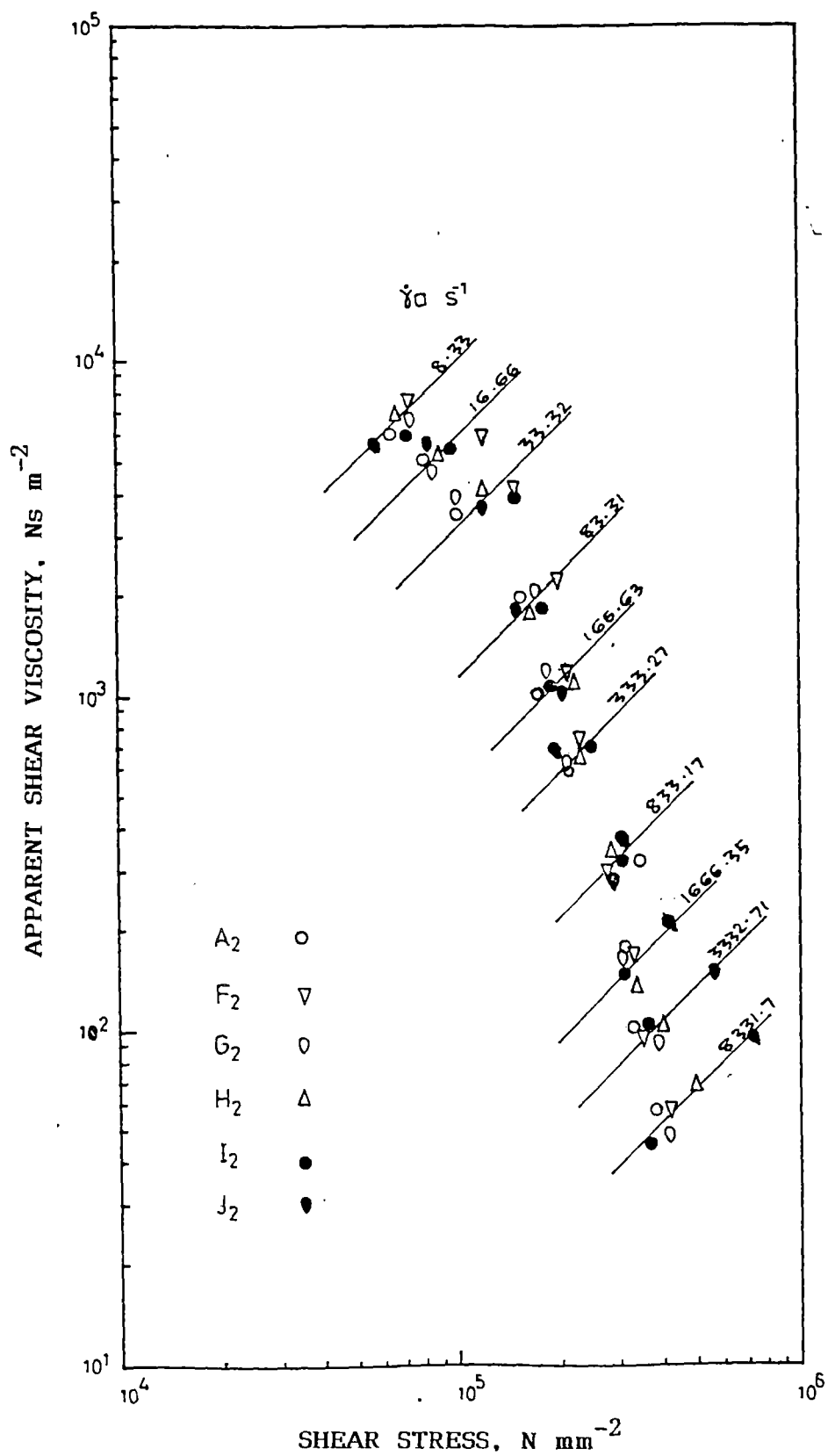
Figure V.5b
Viscosity-shear stress plots of NR-EVA blends containing peroxide cure system, at 120°C.
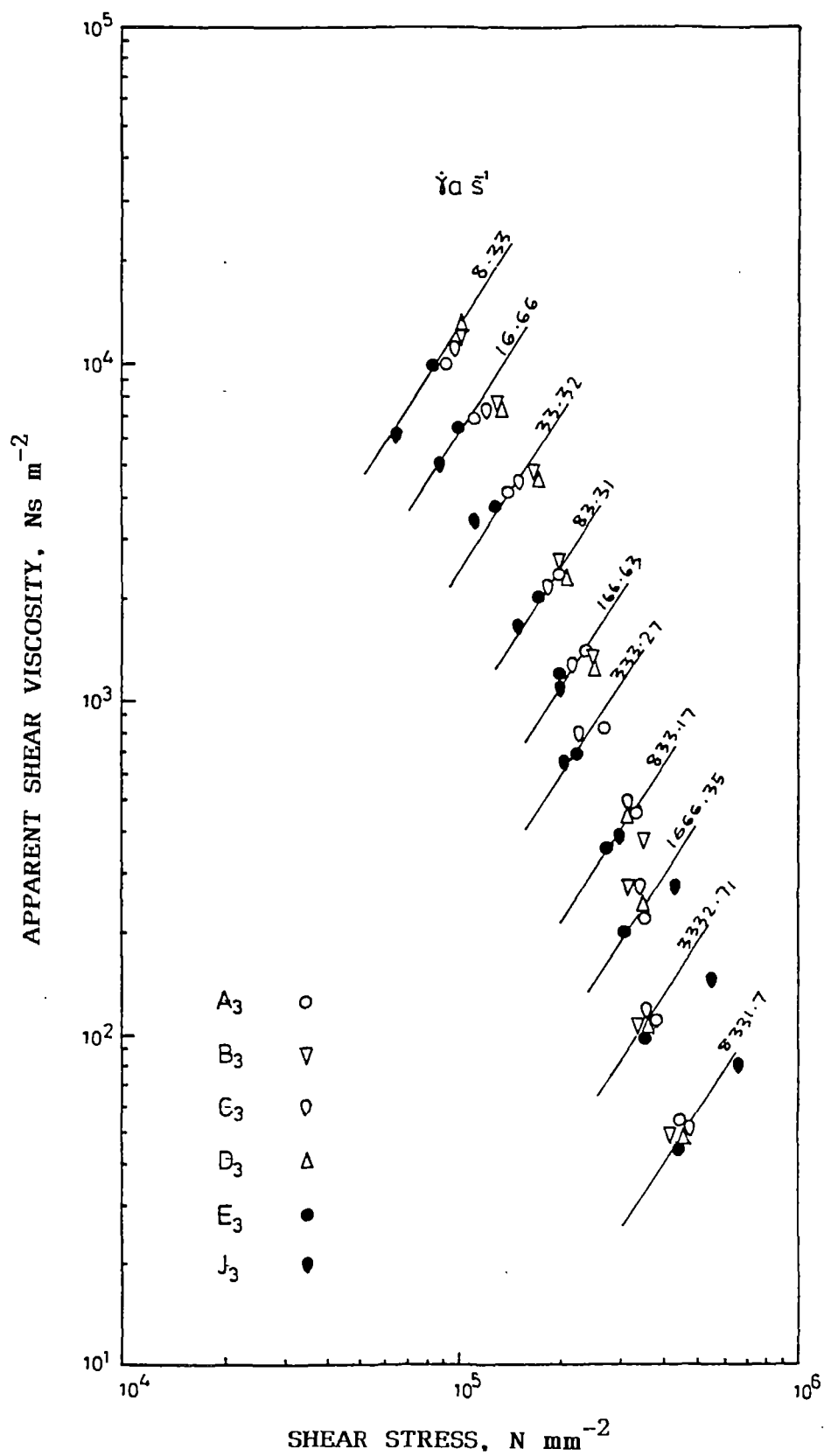
Figure V.6a
Viscosity-shear stress plots of NR-EVA blends containing
mixed cure system, at 120°C.
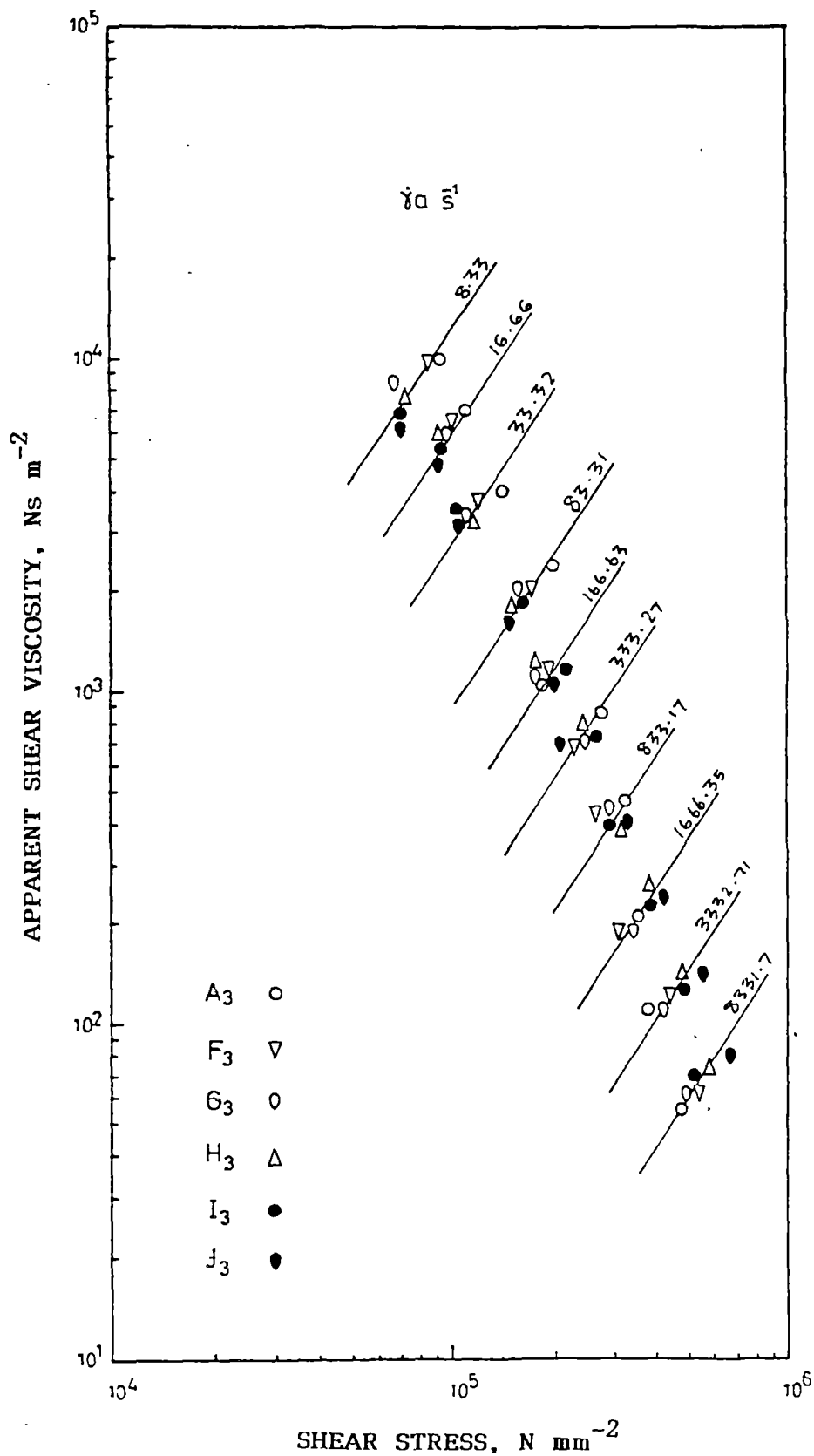
Figure V.6b
Viscosity-shear stress plots of NR-EVA blends containing
mixed cure system, at 120°C.
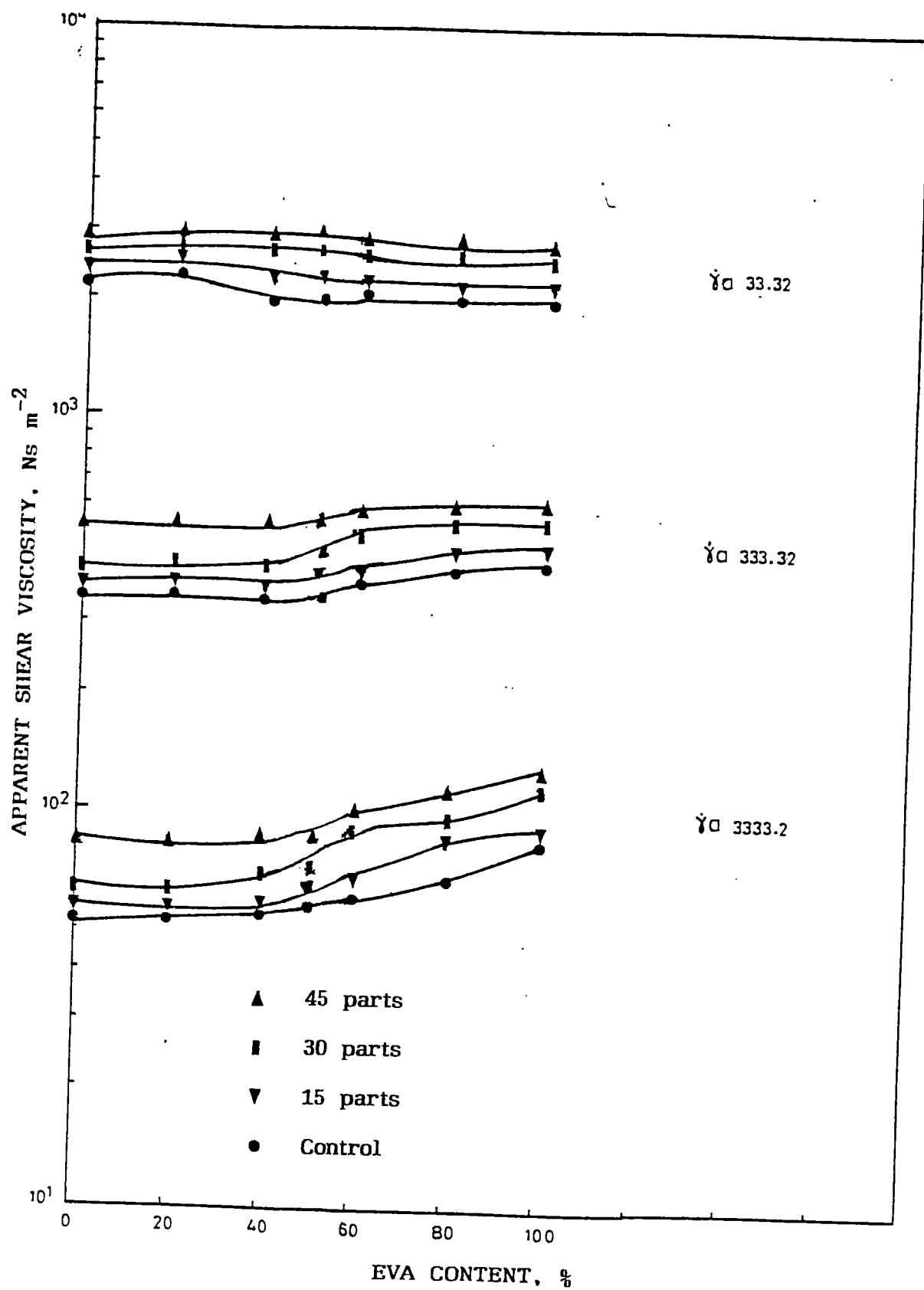
Figure V.7
Effect of EVA content and shear rate on apparent shear viscosity
of NR-EVA blends having different silica content.
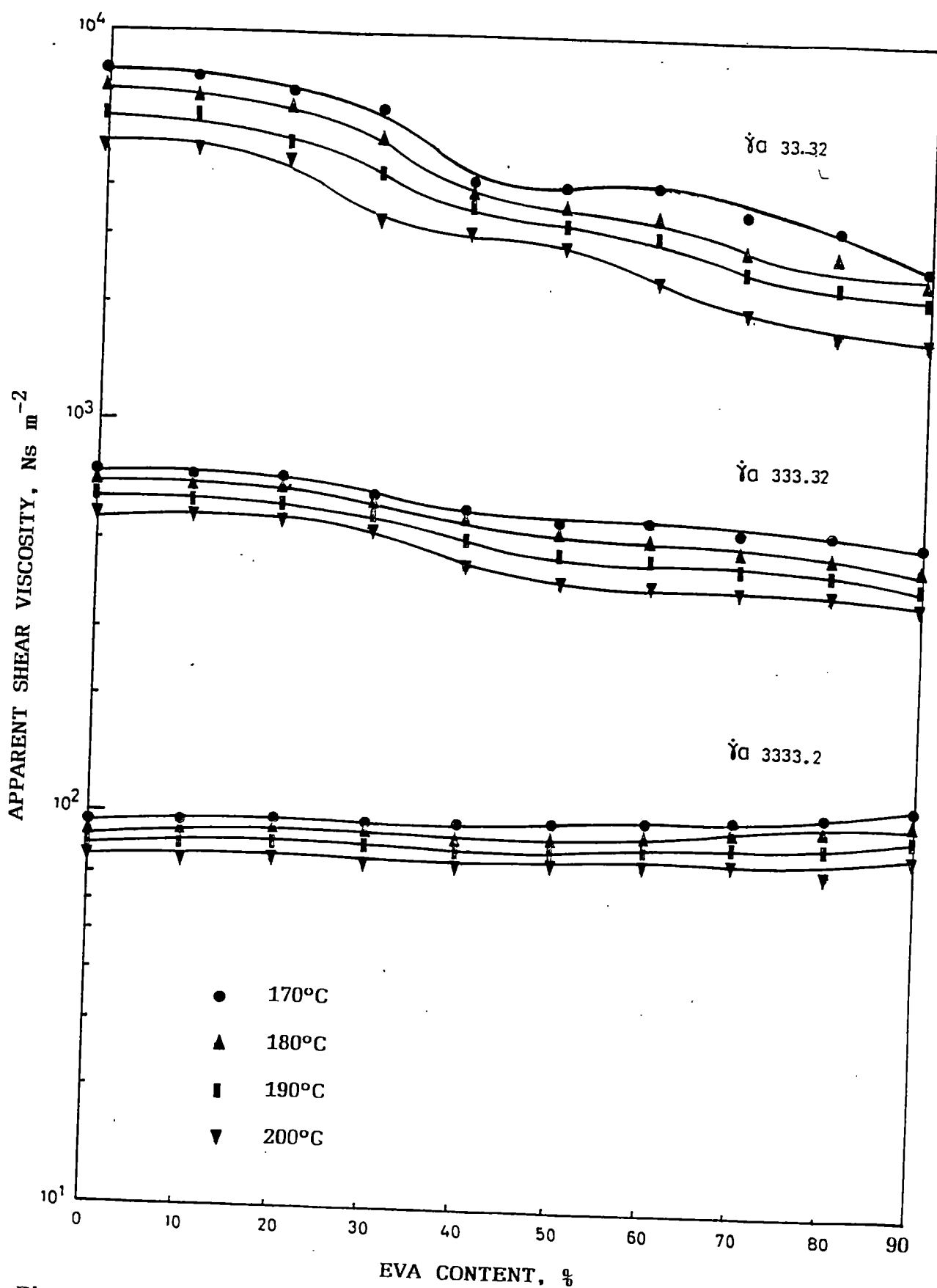
Figure V.8

Effect of temperature and shear rate on the apparent shear viscosity of NR-EVA blends.
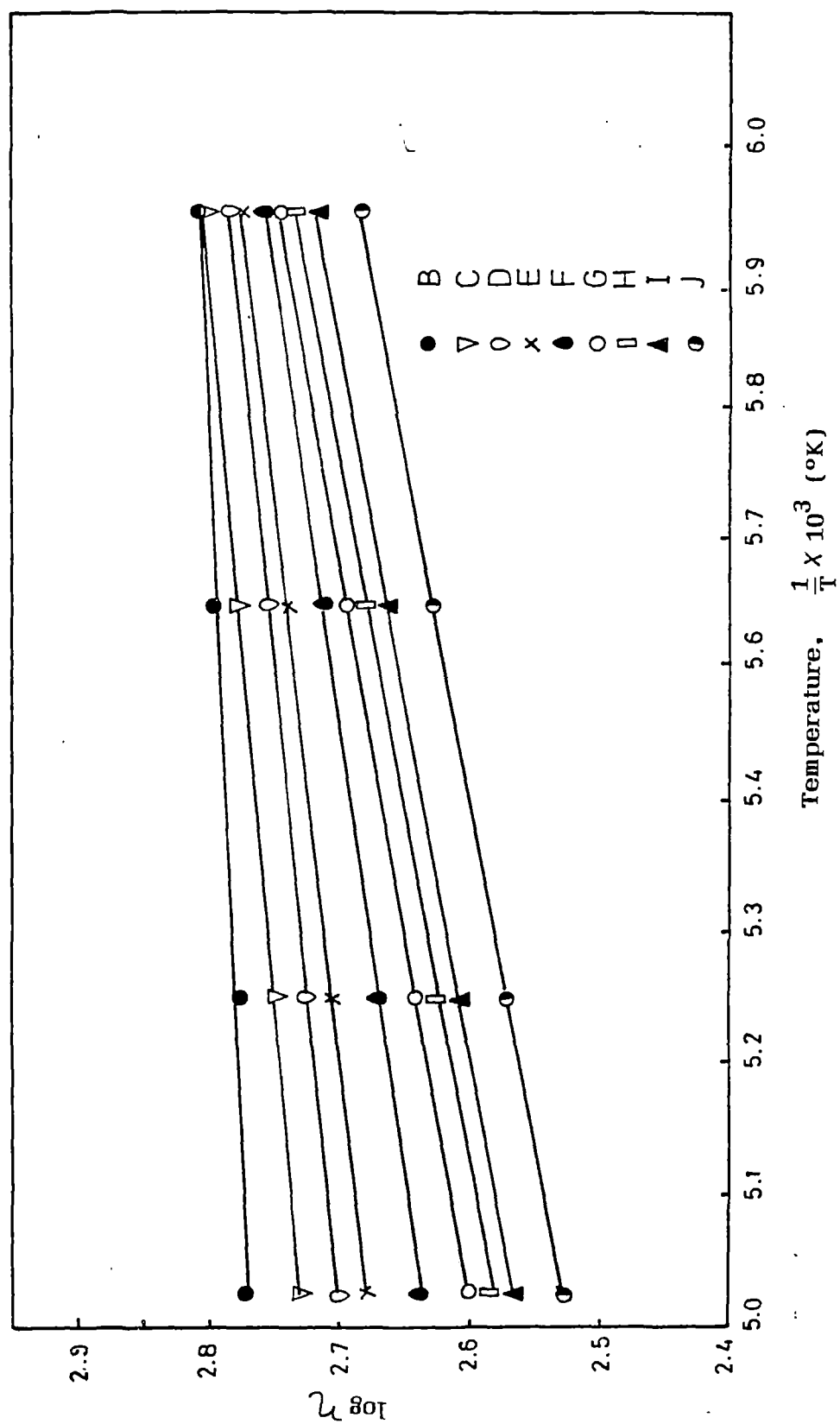
Figure V.9
A plot of $\log \eta$ versus reciprocal of temperature.

TEMPERATURE OF EXTRUSION, 120°C

| SAMPLE | APPARENT SHEAR RATES | |
| No. | 330 s^{-1} | 3330 s^{-1} |

A

B

C

D

E

F

G

H

I

J
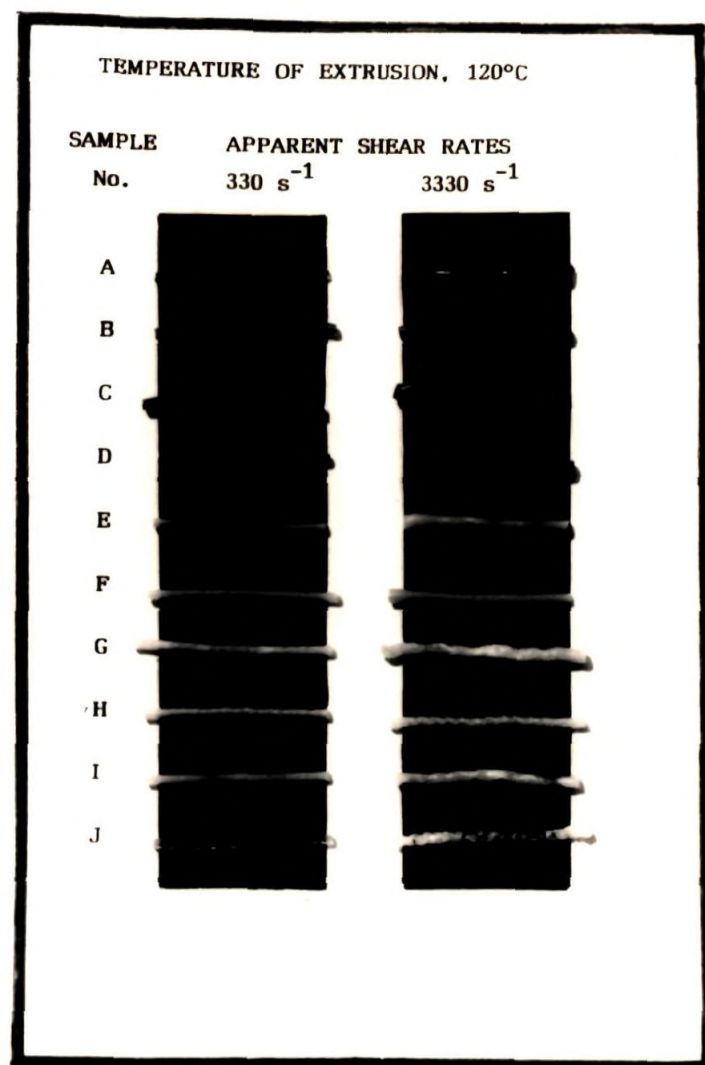
Figure V.10
Effect of shear rate and blend ratio on deformation of extrudates.
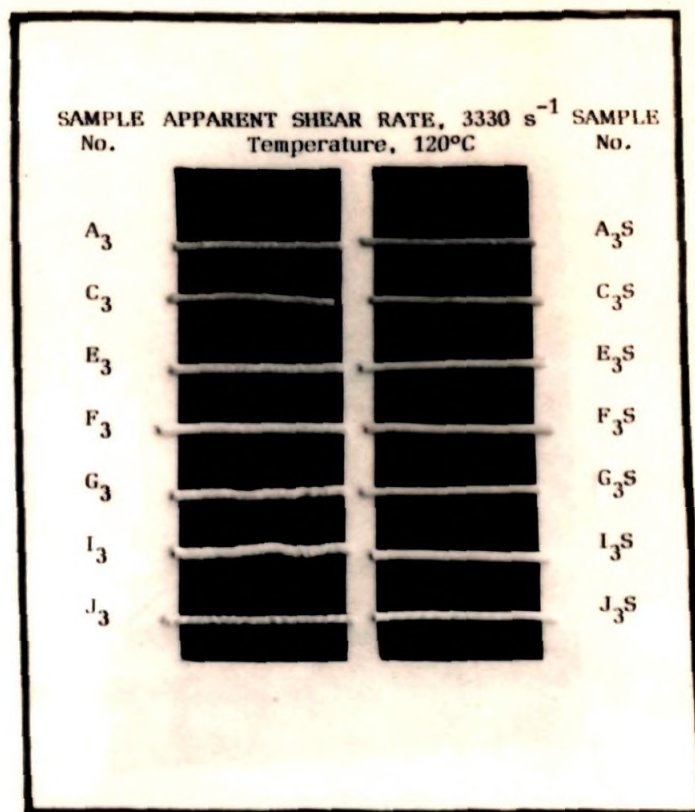
Figure V.11
Effect of blend ratio and silica content
on the deformation of the extrudates.
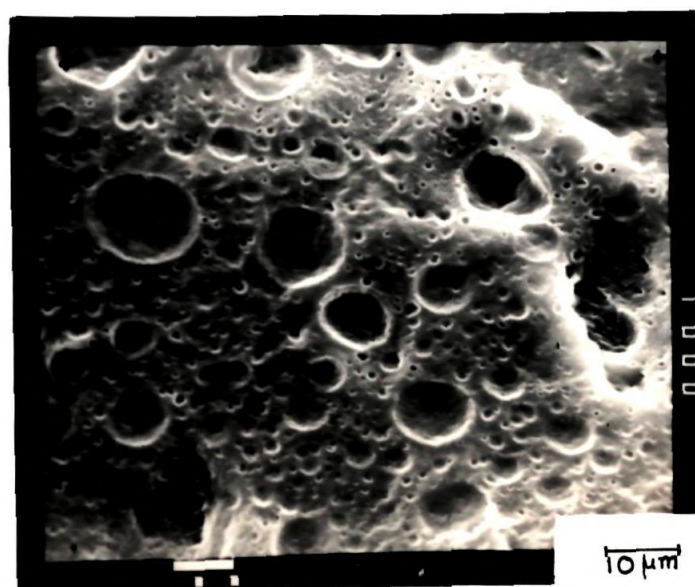
Figure V.12a
Morphology of blend I extruded at a shear
rate of 330 s^{-1}, showing larger particle size

5 μm
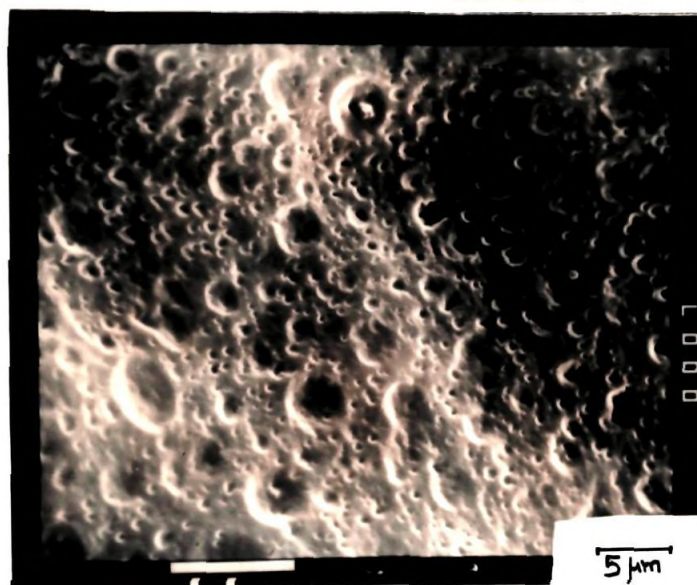
Figure V.12b
Morphology of blend I extruded at a shear
rate of 3330 s^{-1}, showing lower particle
size.

33.3 μm
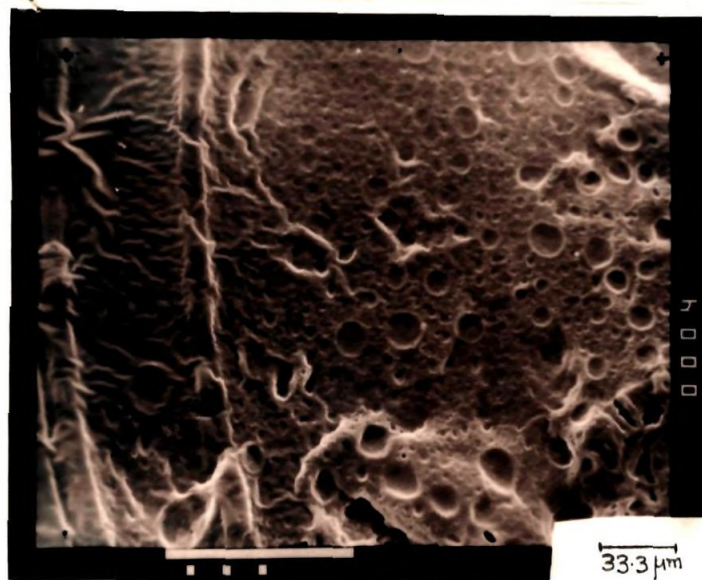
Figure V.12c
Sheath and core structure of blend I.

222 μm

Figure V.13
SEM Photomicrograph of blend H extruded
at a shear rate of 330 s^{-1}.
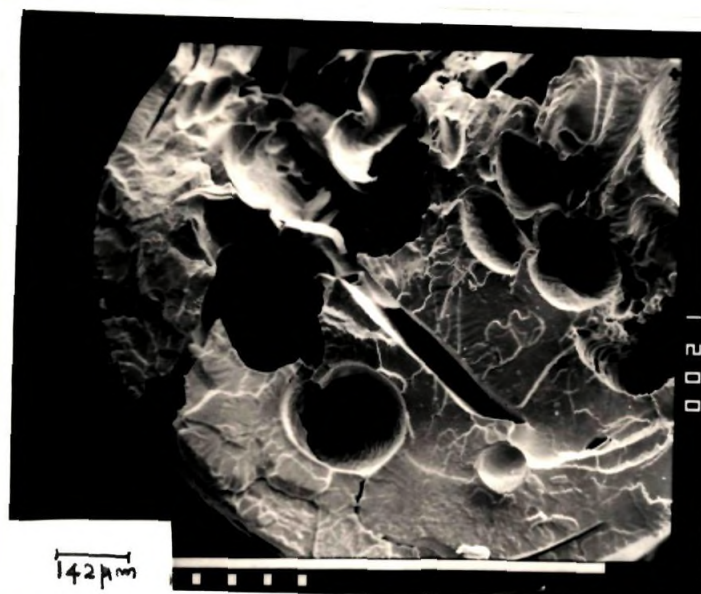
Figure V.14
SEM Photomicrograph of blend G extruded
at a shear rate of 330 s^{-1}.
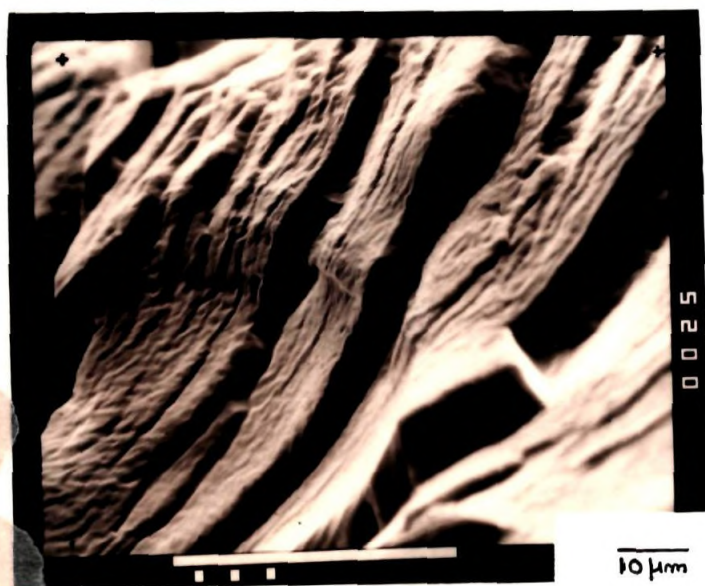
Figure V.15
SEM Photomicrograph of blend F extruded
at a shear rate of 330 s^{-1}.
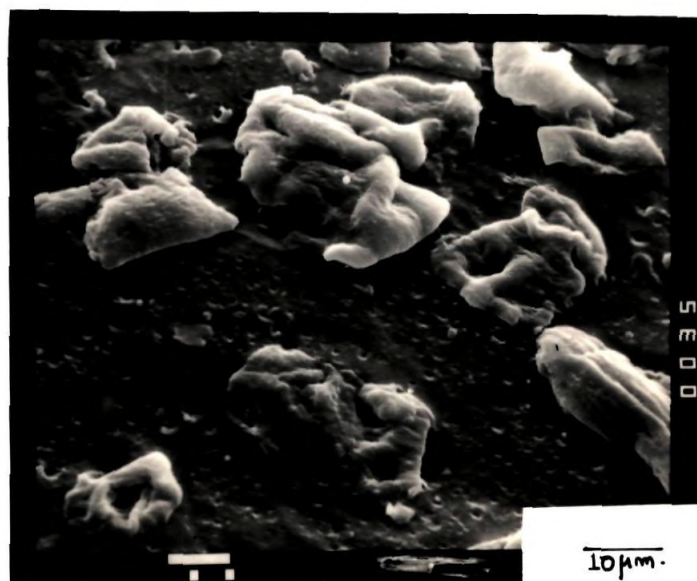
Figure V.16
SEM Photomicrograph of blend D extrud
at a shear rate of 330 s^{-1}.

CHAPTER VI – EFFECT OF BLEND RATIO AND SILICA CONTENT ON

(A) MECHANICAL PROPERTIES AND DEGRADATION

(B) DYNAMIC MECHANICAL PROPERTIES

OF NR-EVA BLENDS.

_____

The results of the above study have been accepted for publication in (1) Kautschuk Gummi Kunststoffe and communicated for publication to (2) Journal of Materials Science.

The reinforcing action of fillers on elastomers depends on factors such as particle size, structure and physico-chemical inter-action of filler with the polymer. However, in blends of elastomers, the reinforcing activity also depends on distribution and dispersion of the filler in each phase of the blend. In this chapter, the effects of precipitated silica on the mechanical, dynamic mechanical and degradation resistance of NR-EVA blends have been evaluated. Blend ratios selected for the evaluation are 100:0, 80:20, 60:40, 50:50, 40:60, 20:80 and 0:100, NR:EVA. The crosslinking system used in the present evaluation is a mixed one, consisting of sulphur and dicumyl peroxide, since it was found to yield better technological properties for the blends (Chapter III). Effects of silica in protecting NR:EVA blends against the action of heat, ozone and γ-radiation were assessed. The results obtained are discussed under two headings.

Part A discusses the effect of precipitated silica on mechanical properties and degradation of NR-EVA blends.

Part B discusses the dynamic mechanical properties of silica filled NR-EVA blends with special reference to the effect of blend ratio and silica content on storage modulus (E'), loss modulus (E") and loss tangent (tan δ) at different temperatures. The experimental techniques for determining the mechanical properties, degradation behaviour and dynamic mechanical measurements are given in Chapter II.

VI.A.1 EFFECT OF SILICA ON TENSILE AND TEAR STRENGTHS

Effect of loading of silica on the tensile strength of NR-EVA blends is shown in Figure VII.A.1. At 45 phr level, silica adversely affected the tensile strength of the blends. However, loading upto 30 phr did not seriously affect the tensile strength of those blends which contained a higher proportion of NR. But in EVA rich blends, silica reduced the tensile strength even at 15 phr loadings. From Figure VI.A.2, it is clear that tear strength increased with increase in proportion of EVA in the blend. Addition of silica increased the tear strength of those blends which had a higher proportion of NR. But in EVA rich blends, tear strength decreased with the addition of silica.

The above observations on tensile and tear strengths of silica filled NR-EVA blends can be explained based on the morphology of the blends and distribution of the filler in each phase of the blend. It is already seen that in NR-EVA blends, EVA also formed a continuous phase when its proportion was 40 per cent or more, due to its lower melt viscosity and that NR remained as dispersed particles when its percentage was 40 or below (Chapter III, Section III.A). It is also well known that silica has high affinity towards polar polymers and preferentially get distributed into the polar component of the blend[119]. Considering the above, it is possible that silica got distributed preferentially in the EVA phase of those

blends in which EVA also formed a continuous phase (blends E to J). V_{ro} and V_{rf} are the volume fractions of rubber in the unfilled and silica filled vulcanisates respectively, swollen in xylene to an equilibriumı state. The weight fraction of filler in the vulcanisate is denoted as z. From the nature of the V_{ro}/V_{rf} versus e^{-z} plots the reinforcing activity of the filler can be ascertained. Identical slopes of the straight lines obtained by plotting V_{ro}/V_{rf} against e^{-z} (Figure VI.A.3) for the silica filled EVA and NR compounds, especially in the region of higher silica loading, indicated that re-inforcing activity of silica in both the polymers is almost same. But it is already established that strong physico-chemical interactions between filler and polymer can reduce the extent of crystallization of the polymer[120]. Hence the basic reason for the lower tensile and tear strengths of the silica filled EVA and blends containing higher proportion of EVA appears to be   lower extent of crystallization of the EVA. For NR and NR rich blends, silica improved the tear strength and tensile strength due to reinforcement of the NR phase.

VI.A.2 MODULUS, HARDNESS AND ABRASION LOSS

The modulus and the hardness values shown in Figures VI.A.4 and VI.A.5, respectively, increased with loading of silica and this effect was more pronounced in blends A to F in which NR remained as a continuous phase. The increase in modulus and hardness is due to reduced elasticity of the filled blends. For NR (compound A)

abrasion loss reduced with loading of silica due to its reinforcing effect, but in blends as well as in pure EVA (B to I and J) addition of silica increased abrasion loss (Figure VI.A.6). This observation again pointed out the fact that the expected property increase due to reinforcement of the EVA phase was offset by the reverse effect caused by the decrease in the extent of crystallization of the EVA phase. This is further supported by the compression set behaviour of the silica filled NR-EVA blends.

VI.A.3 EFFECT ON COMPRESSION SET

Figure VI.A.7 shows the compression set behaviour of silica filled ˙NR-EVA blends. Compression set of NR (compound A) increased with loading of silica filler, which is typical for compounds containing high reinforcing filler. However, this tendency was reversed from blend E onwards in which EVA also showed phase continuity. In these cases, compression set was lower for the blends when filler loading was increased. For crystallizing elastomers, it is reported that compression set values decreased when the crystallizing tendency was reduced[121]. In the present case also, strong physico-chemical interaction between EVA and silica might have adversely affected the extent of crystallization of the EVA phase, which resulted in lower compression set values of the blends, as the filler loading was increased.

VI.A.4   EFFECT ON RADIATION RESISTANCE

Retention of tensile strength of silica filled NR-EVA blends, after exposing the test samples to 20 Mrad of γ-radiation, from a ^{60}Co source, is presented in Figure VI.A.8. As the EVA content increased, resistance to degradation by γ-radiation also increased as evidenced by higher retention of tensile strength. This effect was found to be more pronounced in blends E to I in which EVA formed a continuous phase. Silica enhanced the resistance to degradation by radiation and this effect increased with loading of silica. During irradiation by γ-rays, two types of reactions take place, i.e., degradation and crosslinking of the polymer chains. When the former reaction predominates, the strength of the material is decreased. Precipitated silica is found to favour the second type of reaction, as shown by better tensile retention of silica filled NR, EVA and their blends.

VI.A.5   EFFECT ON OZONE RESISTANCE

Figure VI.A.9 is the photograph of samples exposed to ozonised air for 8 h (top) and 85 h (bottom) respectively. In the unfilled blend (C_3So) small cracks were initiated after 8 h of exposure. This sample developed deep cracks as seen in the photograph after 85 h of exposure. On the other hand, samples C_3S_{15}, C_3S_{30} and C_3S_{45} which contained 15, 30 and 45 phr precipitated silica respectively, did not develop any crack during this period. Addition

of silica increased the modulus of the blend and reduced its elongation. Hence the stress required 'to produce the critical strain, necessary for the ozone attack to take place, might be much higher in silica filled blends.

VI.B.1 DYNAMIC MECHANICAL PROPERTIES OF SILICA FILLED NR-EVA BLENDS

The tan δ values of the unfilled blends as a function of temperature are shown in Figure VI.B.1. It is seen that the tan δ values of pure EVA increased sharply above 75°C and reached a plateau value beyond 95°C. The sharp increase in the tan δ value in this temperature range is associated with the melting of the crystalline segments of the EVA phase. The results on the thermal behaviour of NR-EVA blends described in Chapter IV, Section 1 indicate that the EVA phase has a sharp melting point of 86.7°C The damping curve of EVA has three distinct zones: (a) a rubbery plateau, (b) a melt transition and (c) a viscous plateau. The damping curves of the blends also show a similar trend as that of EVA, although the intensity of transition is lower. This is associated with the decrease in crystallinity of the samples. The damping curve of natural rubber is different from that of EVA and their blends. In this case the curve is almost in parallel to the temperature axis. This is associated with the amorphous nature of the NR phase. The damping curves of systems containing 45 parts of silica filler is shown in

Figure VI.B.2. It is seen that addition of silica decreased the tan δ values substantially except that of natural rubber where a marginal increase in tan δ values can be observed at high temperatures. The sharp decrease in tan δ values of EVA blends is associated with the decrease in the crystallinity of the EVA phase due to the presence of filler. Silica filler has high affinity towards the EVA phase due to its polar nature. Therefore, the crystallinity of EVA is impaired. It can also be noticed that the crystalline transition zone become broader as a result of the addition of filler.

The storage modulus values of unfilled blends are given in Figure VI.B.3. In the case of EVA and the blends, the storage modulus curves have three distinct regions namely, rubbery, transition and viscous regions. It is seen that the storage modulus of high EVA blends decreased sharply with temperature in the rubbery and the transition zone and it levels off in the viscous region. The storage modulus of NR is almost unaffected by temperature. The effect of addition of silica filler on the storage modulus of the blends as a function of temperature is given in Figure VI.B.4. In all cases, addition of silica increased the storage modulus of the blends considerably. The storage modulus of filled NR shows a marginal decrease with increasing temperature. Although the general trend of filled EVA and the blends are similar to that of unfilled systems, the transition region is less predominant than unfilled systems due to the decrease in the crystallinity of the samples.

The loss modulus of the unfilled and filled systems are given in Figures VI.B.5 and VI.B.6, respectively. In the case of unfilled systems, the loss modulus of NR and high NR blend (80:20 NR:EVA) is almost unaffected by temperature. However, the loss modulus of pure EVA and high EVA blends decreased sharply with temperature before they undergo melting. In the viscous region, the loss modulus values are unaffected by temperature. Addition of silica increased the storage modulus of the systems considerably. In the case of EVA and high EVA blends the storage modulus decreased with temperature and the decrease is more sharp in the rubbery region.

The storage modulus of the filled and unfilled blends at a temperature of 30°C as a function of EVA content is presented in Figure VI.B.7. It is seen that the storage modulus increased with the increase of EVA content in all cases. Addition of 15 parts of silica marginally increased the storage modulus. However, at 45 parts of silica loading the storage modulus of the systems showed a very high increase. This is an expected trend in the silica filled systems since silica imparts high stiffness to the polymer matrix. The loss modulus of the blends as a function EVA content is given in Figure VI.B.8. Addition of 15 parts of silica showed a marginal change in loss modulus. There was considerable increase in loss modulus at higher loading of silica for the NR rich blends.
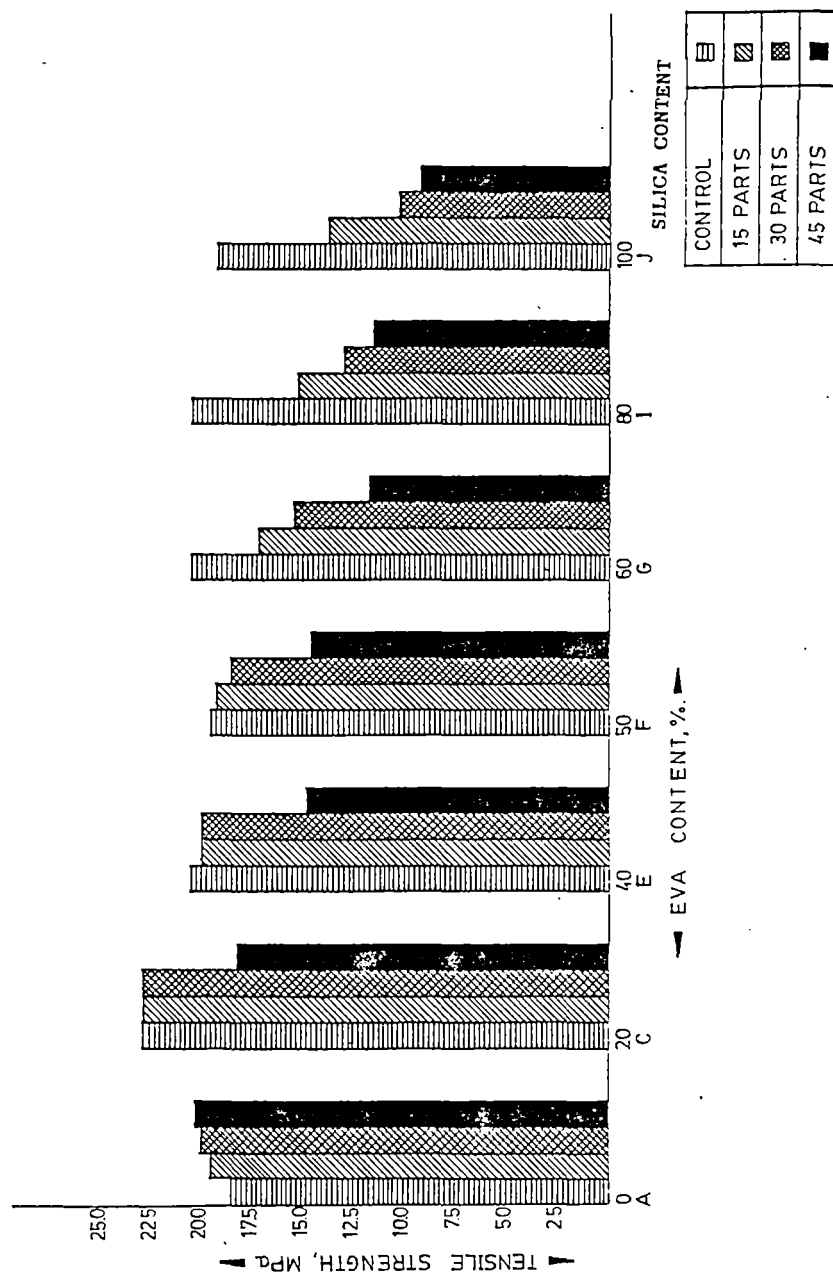
Figure VI.A.1
Change of tensile strength with blend ratio and silica content.
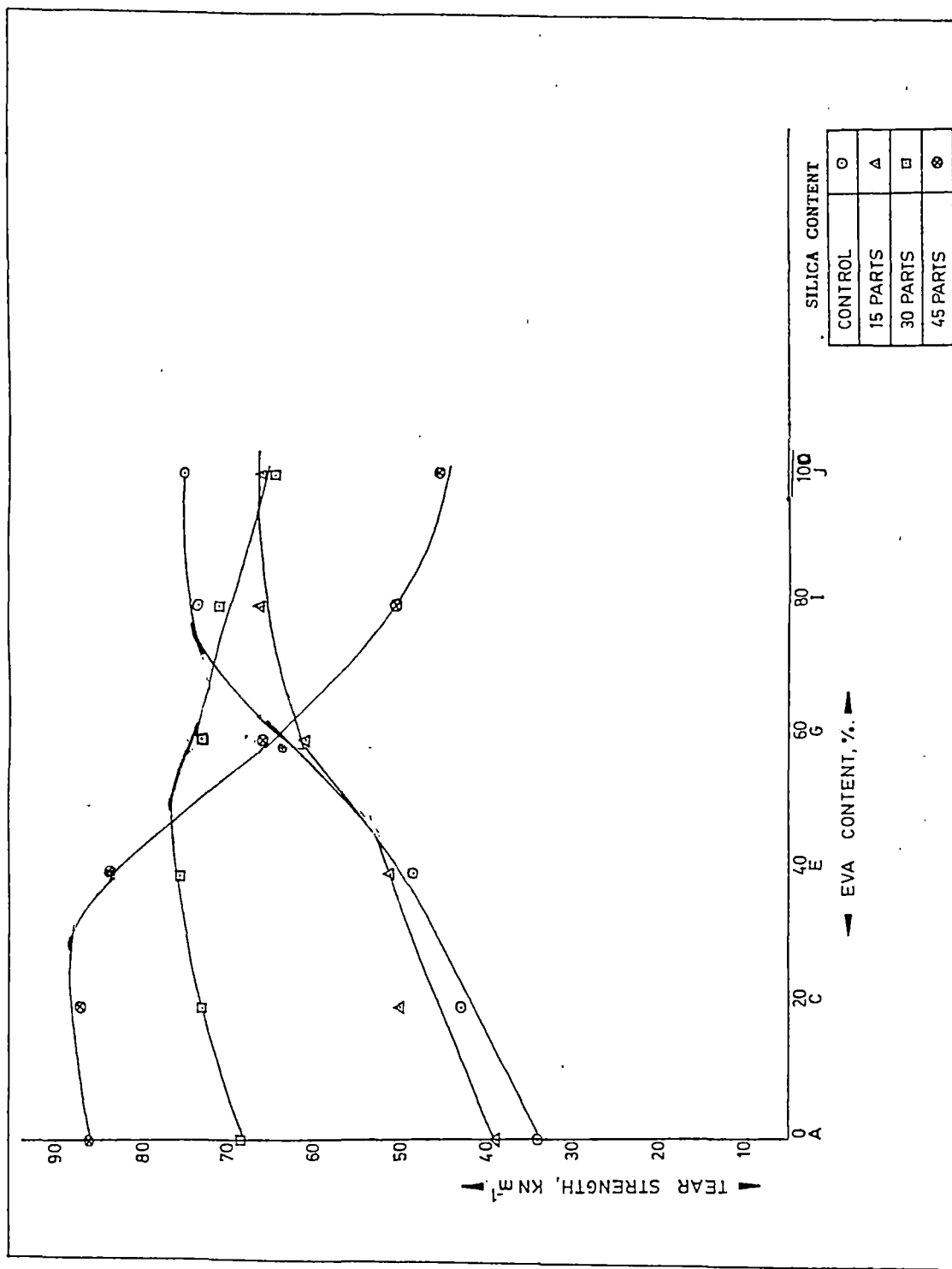
Figure VI.A.2
Change of tear strength with blend ratio and silica content.
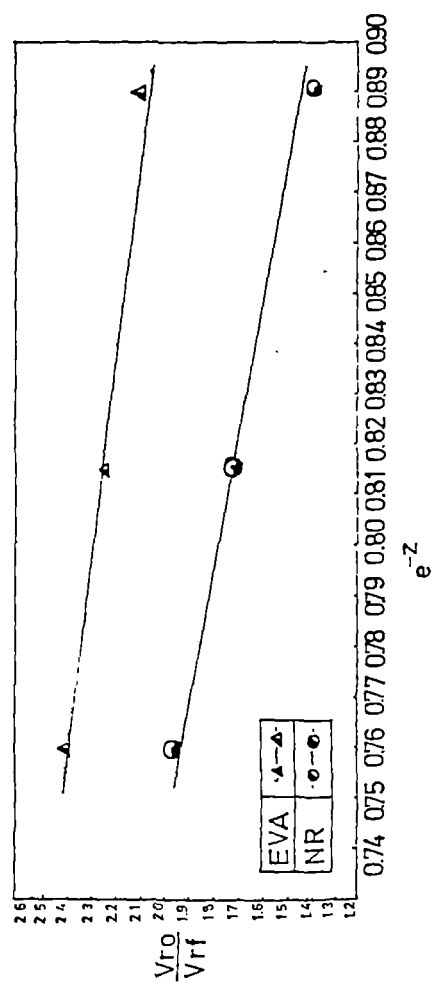
Figure VI.A.3
Plots of V_{ro}/V_{rf} against e^{-z}
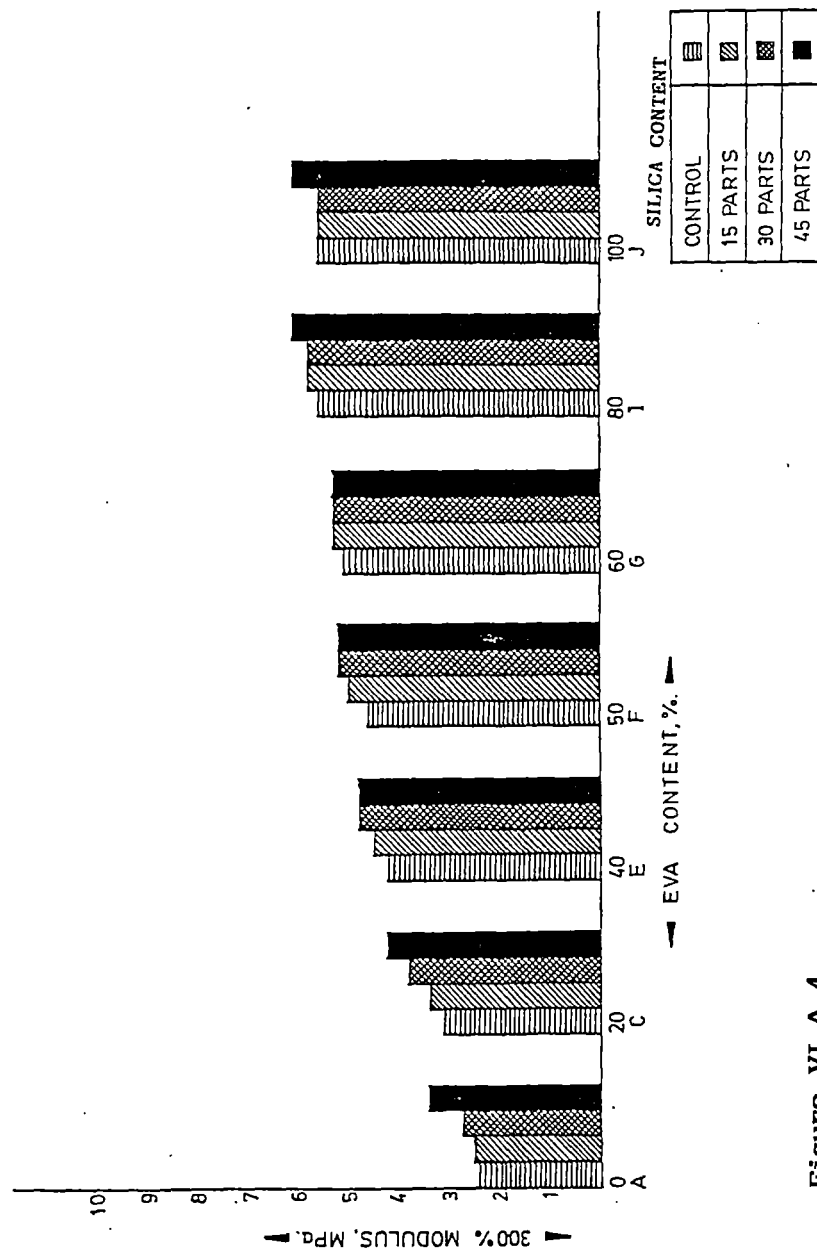
Figure VI.A.4
Change of modulus 300% with blend ratio and silica content.
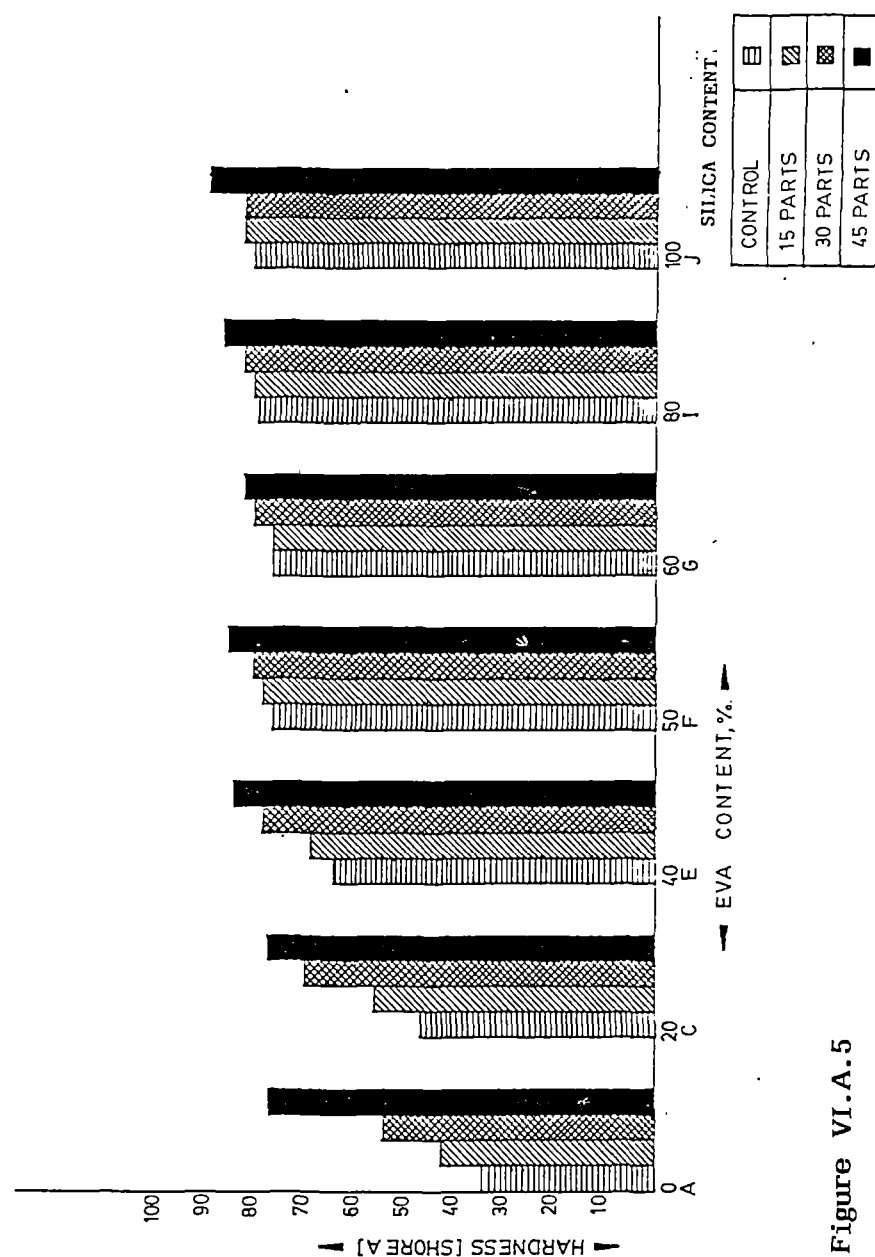
Figure VI.A.5

Change of hardness (Shore A) with blend ratio and silica content.
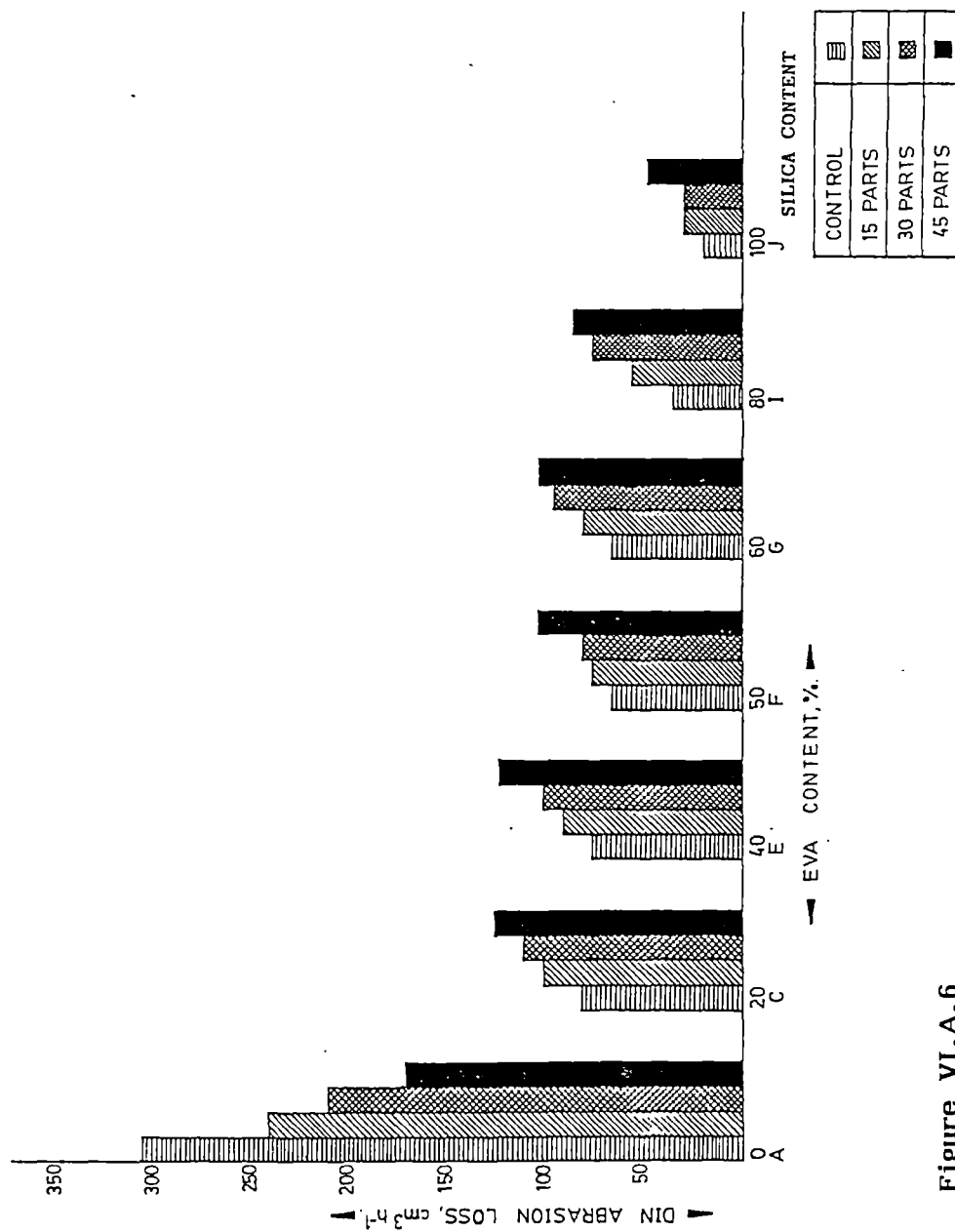
Figure VI.A.6
Change of Din abrasion loss with blend ratio and silica content.
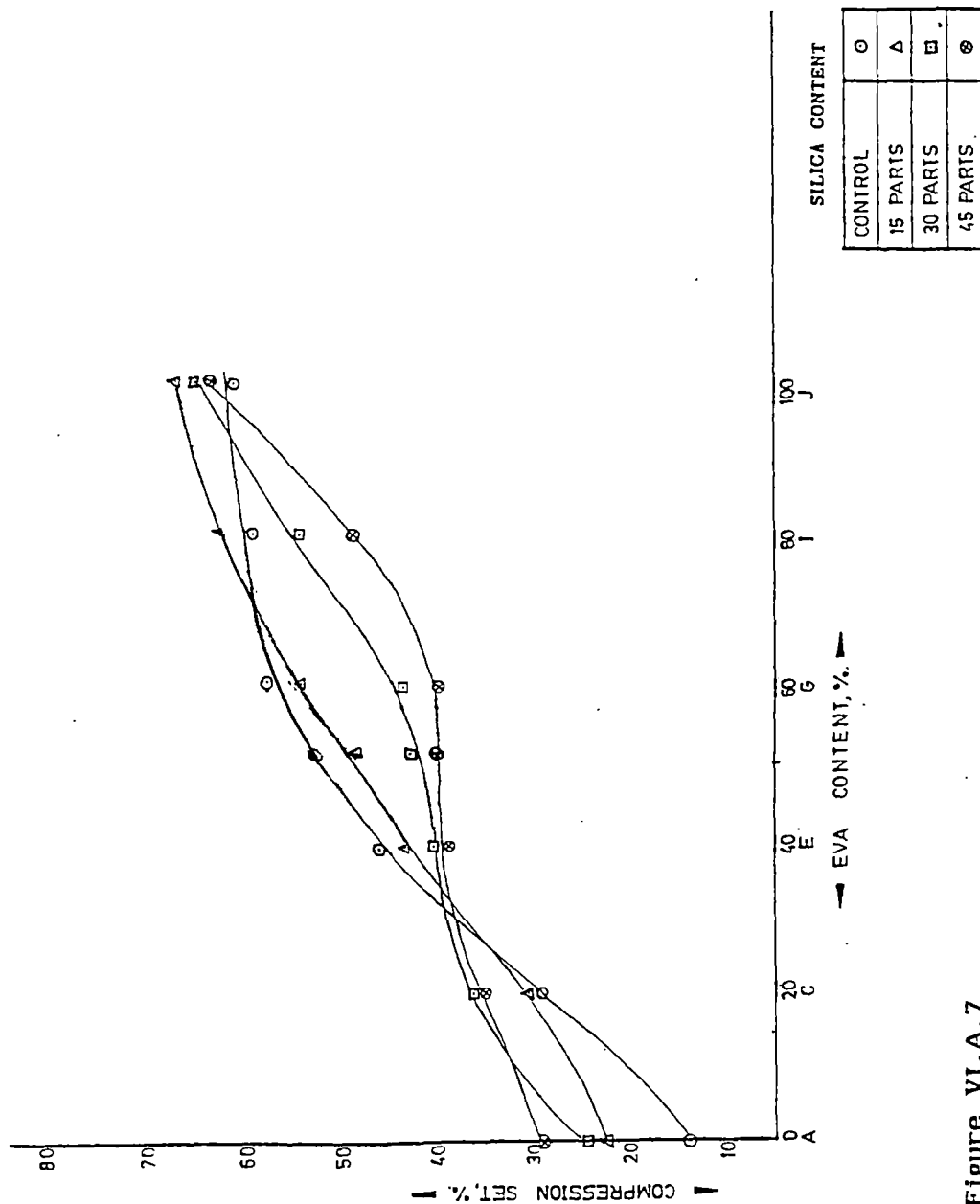
Figure VI.A.7
Change of compression set with blend ratio and silica content.
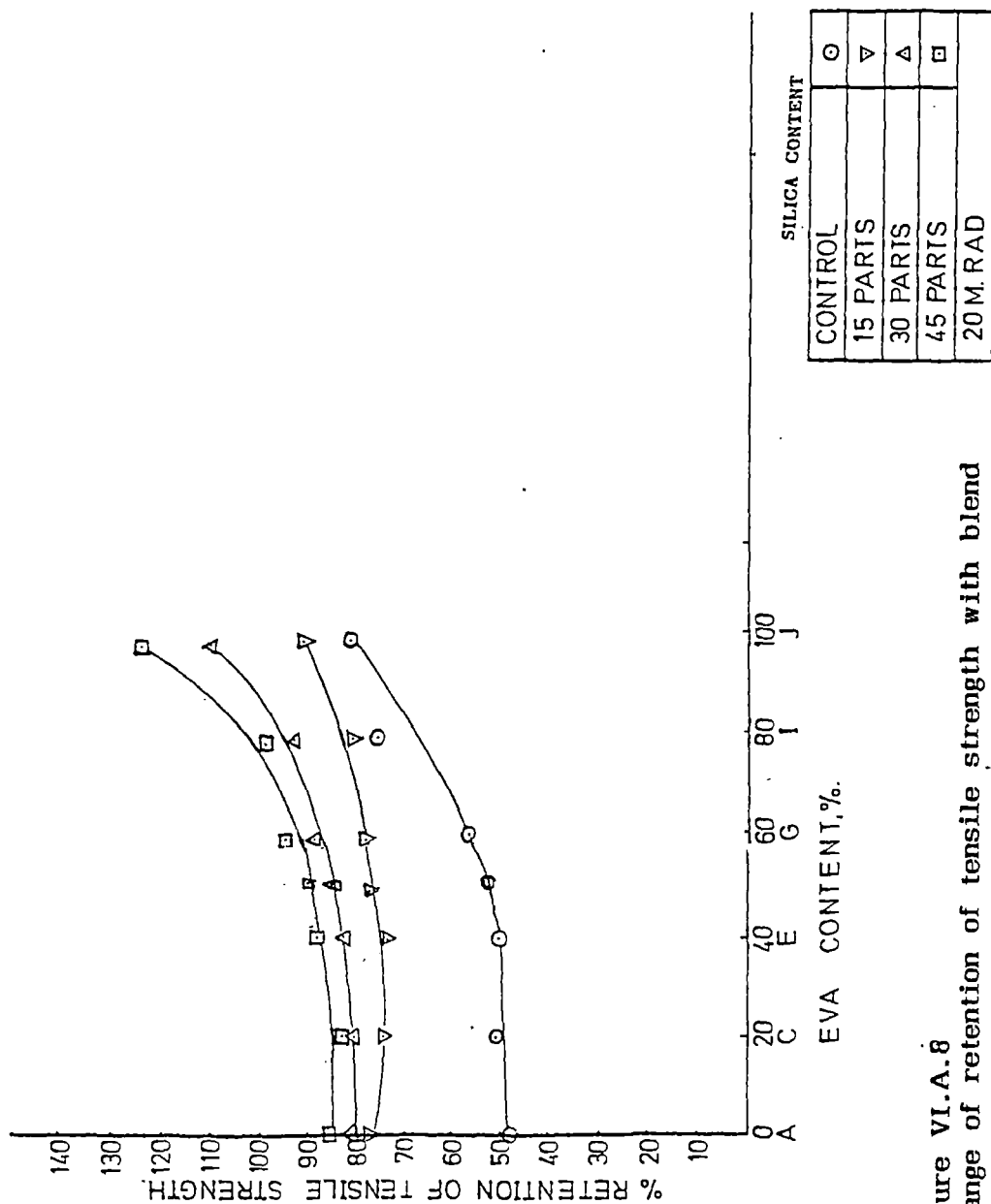
Figure VI.A.8
Change of retention of tensile strength with blend
ratio and silica content.

SILICA CONTENT	
CONTROL	⊙
15 PARTS	▷
30 PARTS	◁
45 PARTS	▣
20 M.RAD	

Figure VI.A.9
Photograph of blend C (80:20 NR:EVA) having different silica content after 8 h and 85 h of exposure to ozonised air.
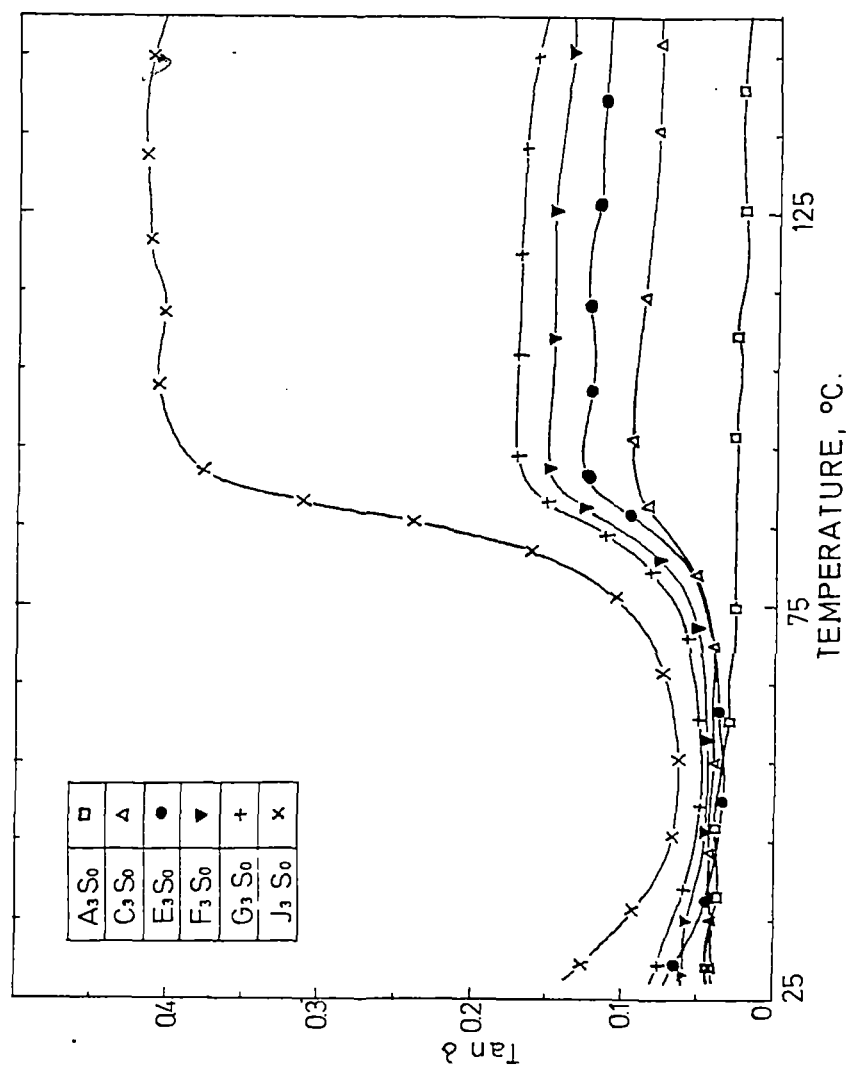
Figure VI.B.1
Effect of temperature on loss tangent of unfilled NR-EVA blends.
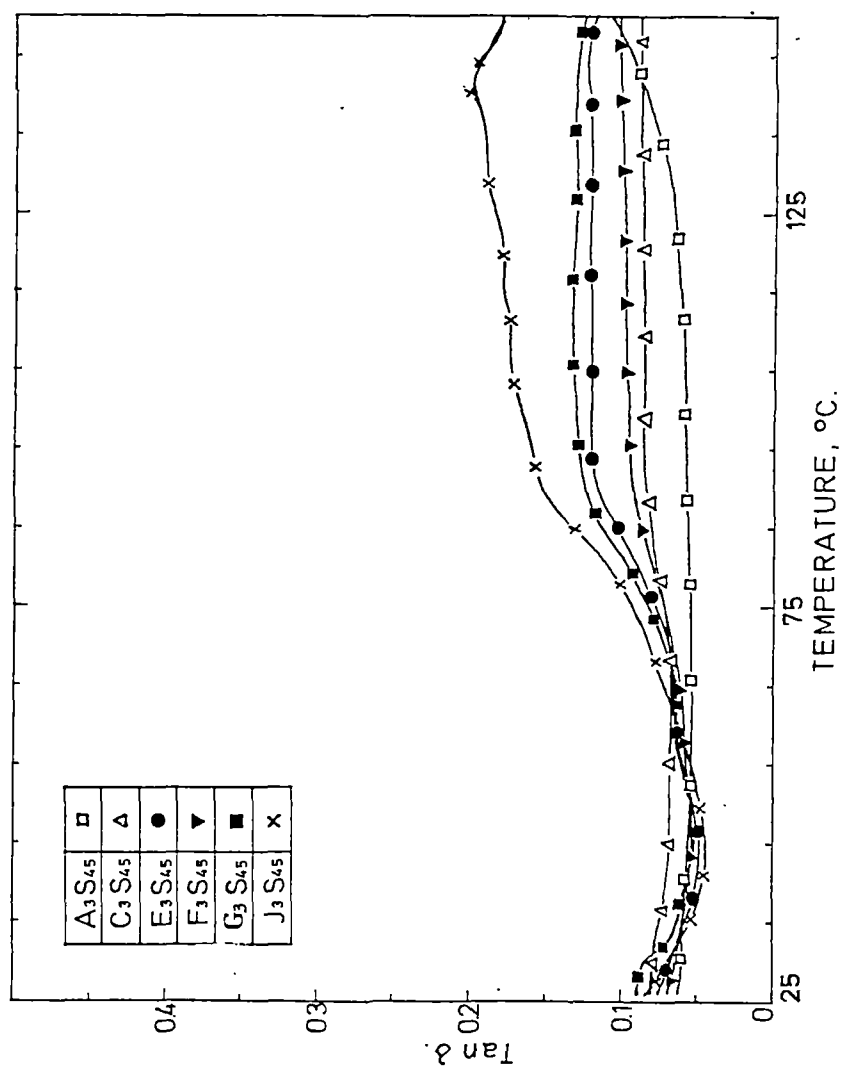
Figure VI.B.2
Effect of temperature on loss tangent of silica filled NR-EVA blends.
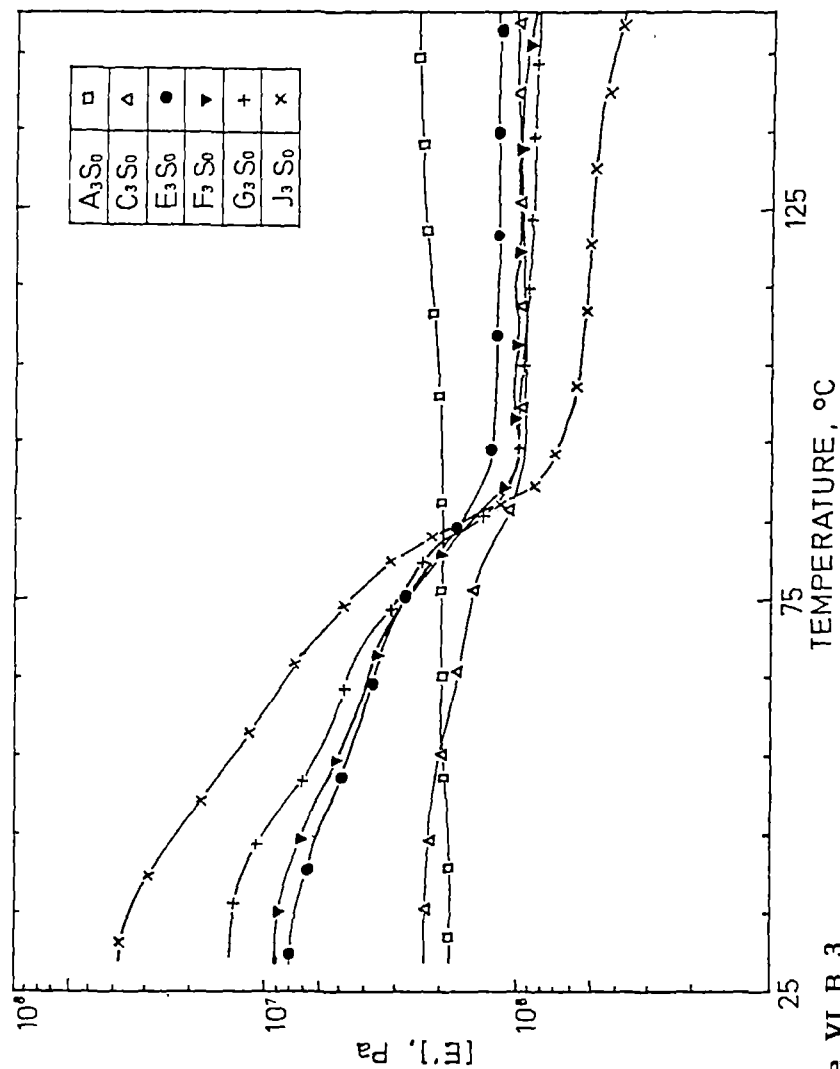
Figure VI.B.3
Effect of temperature on storage modulus of unfilled NR-EVA blends.
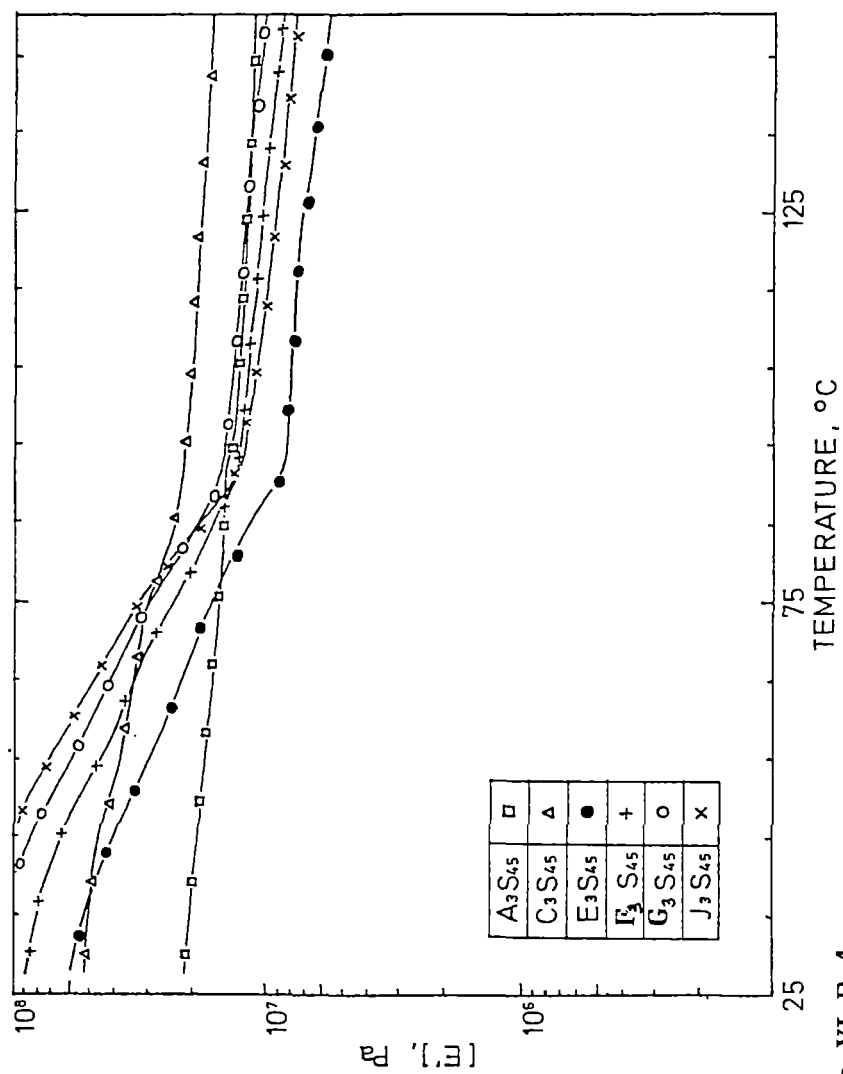
Figure VI.B.4
Effect of temperature on storage modulus of silica filled NR-EVA blends.
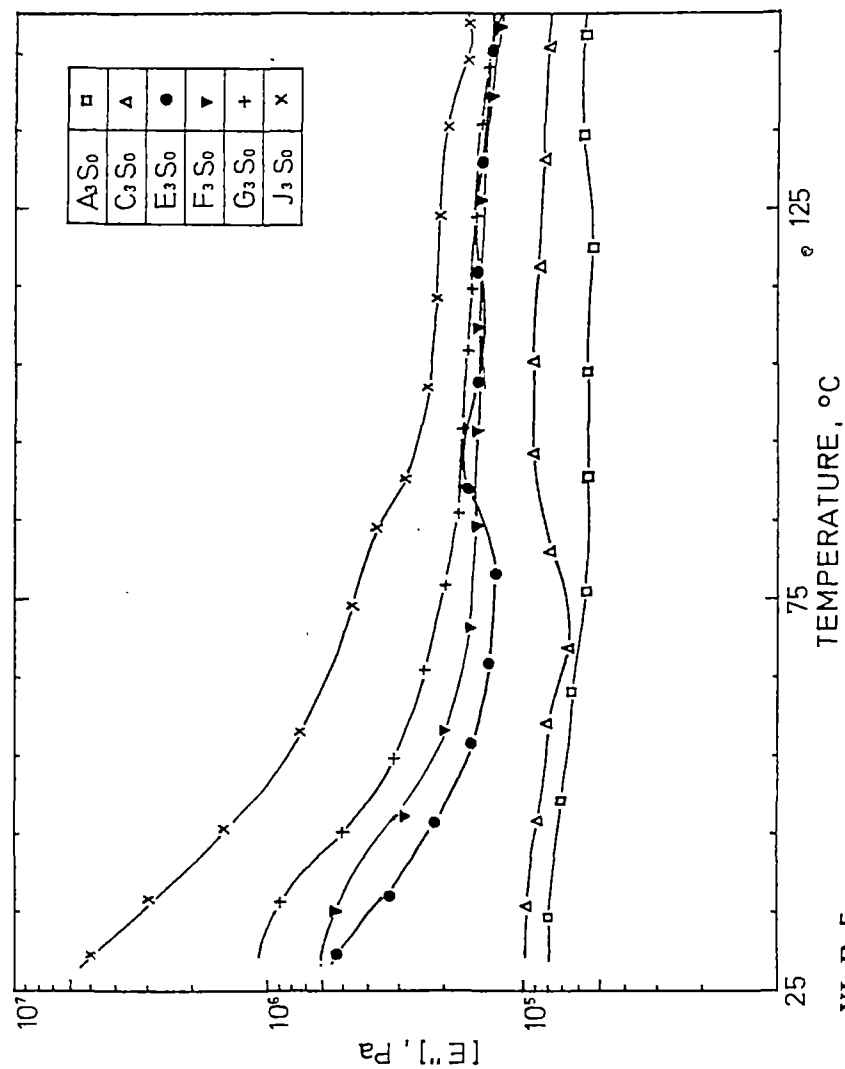
Figure VI.B.5
Effect of temperature on loss modulus of unfilled NR-EVA blends.
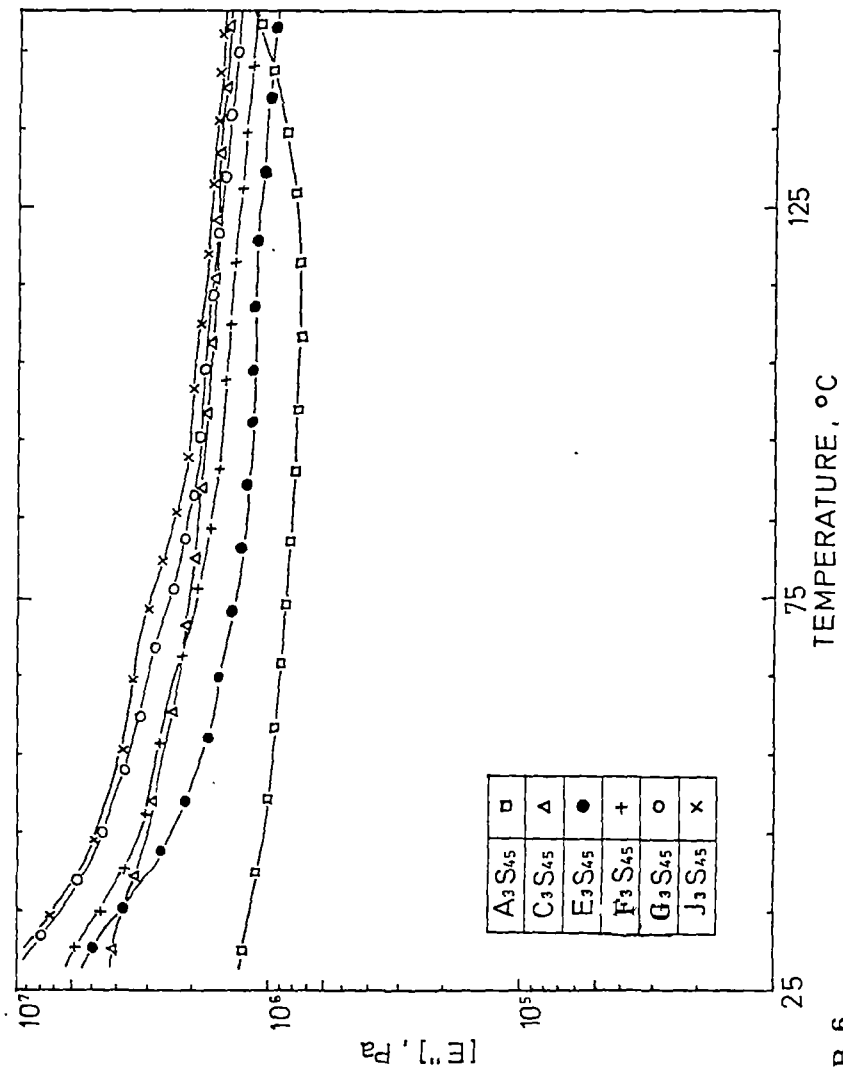
Figure VI.B.6
Effect of temperature on loss modulus of silica filled NR-EVA blends.
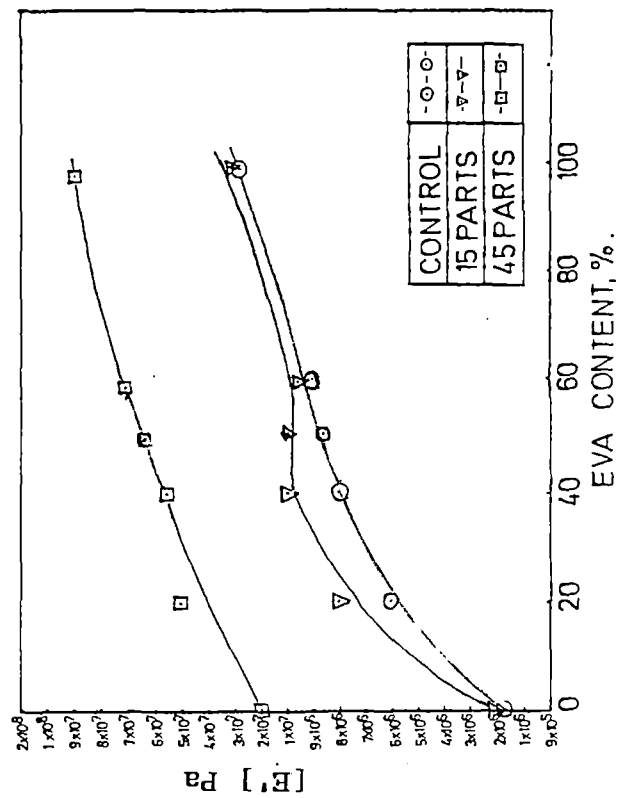
Figure VI.B.7
Effect of EVA content and silica on storage modulus at 30°C.
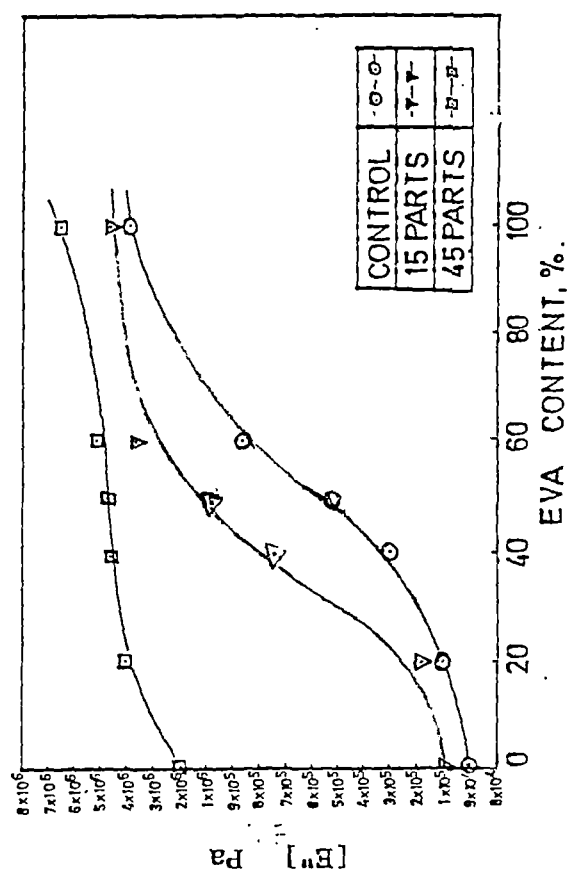
Figure VI.B.8
Effect of EVA content and silica on loss modulus at 30°C.

CHAPTER VII – EFFECT OF BLEND RATIO AND CURE SYSTEM ON THE DEGRADATION OF NR–EVA BLENDS.

Results included in this chapter have been accepted for publication in Polymer Degradation and Stability.

Use of polymeric materials under the influence of degrading agents such as ozonised air, gamma radiation and thermal ageing has increased rapidly during the last few years. Hence it is very important to study the effects of such degrading agents on the performance of elastomers at different conditions. For NR, the resistance to ageing and ozone is poor due to the presence of double bond in the main chain. EVA possesses excellent ageing resistance due to its saturated backbone structure. Hence the behaviour of blends of these elastomers against the action of the various degrading agents is worth examining. The effect of degrading agents on each type of polymer will be different and depends mainly on the chemical structure of the polymer and the type of crosslink system used. Several studies have been reported on the thermo-oxidative ageing of rubbers[122] and on protection of polymers against the action of ozone[123]. The effects of radiation on polymeric materials and their blends have also been reported by several research groups[124].

This chapter discusses the result of the studies on the retention of tensile strength, modulus 300%, and elongation at break, after exposing test sample of NR-EVA blends to different degrading agents such as ozone, heat and gamma radiation. The effects of blend ratio and type of crosslink system in retaining the tensile properties of the blends under the influence of the above degrading agents have been examined. The details of the experimental procedures adopted for the studies on degradation and morphology are given in Chapters II and III, respectively.

VII.1 EFFECT OF THERMAL AGEING

It is well known that during thermal ageing main chain scission, additional crosslink formation and crosslink breakage can take place. There is also the possibility that the existing crosslinks break and a more stable type of crosslink which is immune to further scission can be formed. The relative ratio and magnitude of such reactions that are taking place during ageing govern the amount of change in each property.

The percentage retention of modulus 300% after ageing the test samples of NR-EVA blends containing three different types of cure systems is given in Figures VII.1 to VII.3. From Figures VII.1 and VII.3, it is seen that the percentage retention of modulus increased with period of ageing which indicated that further cross-linking of the blends which contained sulphur and mixed cure systems had taken place. It is interesting to note that the sulphur system showed maximum retention for the blends C to D and the mixed cure system showed maximum retention for blends E to G. In the case of sulphur cure, EVA cannot be vulcanised by sulphur and the sulphur which is dispersed in the EVA phase, slowly migrates to the NR phase as ageing proceeds due to the difference in concentration of free sulphur present in each phase during that time. The decrease in retention of modulus of the 50:50 NR:EVA blend (No. F_1) is due to the degradation of the uncrosslinked EVA which also forms a

continuous phase at this blend ratio. In the case of mixed cure system there was continuous increase in percentage retention of modulus for the blends which contained a higher proportion of NR and this trend was reversed in the case of blends which contained a higher proportion of EVA. This is because NR can be crosslinked both by sulphur and peroxide whereas EVA gets crosslinked by DCP only and the rate of crosslinking in the latter case is very slow. In the case of peroxide system there was decrease in percentage retention of modulus with period of ageing for the blends in which the proportion of NR was high. However, this trend was reversed in the case of blends H_2 to J_2. This indicated that for the blends which contained higher proportions of NR, main chain scission predominated over the crosslinking of the NR phase as the time of ageing is increased. Since EVA has a saturated backbone structure, main chain scission was less and crosslinking reaction predominated as evidenced by gradual increase in retention of modulus as the proportion of EVA is increased.

The percentage retention of tensile strength of the NR-EVA blends decreased with time of ageing for the sulphur (Figure VII.4), peroxide (Figure VII.5) and mixed (Figure VII.6) systems of cure, when the proportion of NR in the blend was high. However, at higher proportions of EVA in the blend, the mixed and peroxide systems of cure did not show much further drop in tensile strength after seven days ageing period. In the case of blends which contained

the peroxide cure system, the retention of tensile strength increased with increase in EVA content. This increase was more evident for blends E_2 to G_2 in which the EVA also formed a continuous phase. In the case of mixed cure system, minimum retention of tensile strength was observed for the blends F_3 and G_3. This difference between the peroxide and mixed cure systems can be due to the higher extent of crosslinking of the blends F_3 and G_3 compared to F_2 and G_2 respectively, due to the continued crosslinking reaction which takes place during ageing. It is possible that the NR phase in blends F_3 and G_3 gets highly crosslinked during ageing because of the presence of a higher dosage of sulphur owing to its preferential migration to the NR phase. As the extent of crosslinking increases, the NR phase becomes less deformable and acts as stress raisers in the EVA matrix, leading to lower tensile values. The observation that the retention of modulus 300% was also high for the blends E_3 to G_3 compared to E_2 to G_2 justifies the above inference.

VII.2 EFFECT OF γ-RADIATION

γ-radiation is a powerful means for crosslinking elastomers. But exposure to higher dosage of it, degrades the polymer. The extent of crosslinking/degradation undergone by each polymer depends on the nature of polymer and the presence of initiators/sensitisers. In the case of NR-EVA blends, it is observed that presence of EVA

increased the percentage retention of modulus 300% after γ-irradiation. This was true for all the three different cure systems examined (Figures VII.7, VII.8 and VII.9). While the NR vulcanisate (A) showed lower retention of modulus with increase in irradiation dosage, EVA vulcanizate (J) showed regular increase in retention of modulus. This observation indicated that while NR undergoes degradation, EVA gets crosslinked during γ-ray exposure. It has already been reported that EVA undergoes brittle type fracture during tensile failure, after exposure to γ-radiation, due to continued crosslinking[125]. The NR rich blends in general showed maximum retention of modulus after exposing them to 20-30 Mrad of radiation. This is probably because at these doses, the degradation level was much lower compared to the extent of crosslinking undergone by both NR and EVA phases. On exposure to 50 Mrad of radiation, it is noticed that the retention of modulus was always lower for the NR rich blends, while the EVA rich blends maintained a higher retention at this dosage (Figures VII.8 and VII.9). This change in pattern of radiation resistance of the blends was associated with a change in morphology of the blends. At blend ratio 60:40 EVA:NR (blend G) the NR phase remained as dispersed phase only (Figure III.1). Since the continuous matrix of EVA undergoes crosslinking reaction the modulus retention is increased with increase in exposure to γ-rays.

The retention of tensile strength after exposure of the NR-EVA blends to γ-radiation is shown in Figures VII.10, VII.11 and VII.12,

for the sulphur, peroxide and mixed cure systems, respectively. From Figures VII.10 and VII.11, it is seen that as the EVA content in the blend is increased, the retention of tensile strength is increased for the blends which contained sulphur and peroxide cure systems. But, when a mixed type of cure system was used, higher retention of tensile strength was noticed only for those blends which contained a higher proportion of EVA. In the case of all the three types of cure systems, higher doses of γ-radiation gave only lower percentage retention of tensile strength. This could be due to the degradation of the NR phase in NR rich blends and excessive crosslinking of the EVA when it formed a continuous phase.

VII.3 EFFECT OF EXPOSURE TO OZONE

Unsaturated elastomers, especially those containing activated double bonds in the main chain, are severely attacked by ozone, resulting in deep cracks in a direction perpendicular to that of the applied stress. Protection against ozone attack can be achieved by blending the unsaturated elastomers with those containing a saturated main chain. The morphology of the blends plays a vital role on the extent of protection imparted by the latter type of elastomers.

The photographs of the NR-EVA blends after exposure to ozonised air containing 50 pphm ozone concentration are shown in Figures VII.13 to VII.16. The samples at the top side of the photograph are those taken out after 8 hours of exposure and the bottom

ones are those exposed for 85 hours. From the photographs it is clearly evident that the ozone resistance of the blends increased as the proportion of EVA in the blend is increased. In the case of blends which contained 40 per cent or more of EVA (blends E, F, G etc), no crack was observed even after exposing the samples in ozonisea air for periods beyond 85 hours. The morphology of the blends described in Chapter III indicated that at 40 per cent concentration of EVA in the blend, it also formed a continuous phase. It is possible that EVA which has a saturated backbone structure formed a protective layer during processing of the blends, due to its lower melt viscosity, resulting in complete protection against ozone attack. Blends B to D, in which the EVA remained as dispersed particles, also showed wide difference in intensity of the cracks formed. The intensity of the cracks, both after 8 hours and 85 hours of exposure, decreased for the samples from A to D. This is due to the increase in critical stress of the blends from B to D because of the presence of the dispersed particles of EVA, which has a crystalline structure. The nature of crosslink system also was found to have a profound influence on the ozone resistance of the blends. This effect became highly prominent as the proportion of EVA in the blend increased. In all the samples from .A to D, the peroxide cure system gave cracks of lower intensity compared to the other two types of cure systems (A_2, B_2, C_2, D_2 less than A_1, B_1, C_1, D_1 and A_3, B_3, C_3, D_3, respectively). This could be due to the

presence of less flexible carbon-carbon crosslinks formed during peroxide cure, which increased the stress required to produce the critical strain encountered in the ozone attack.
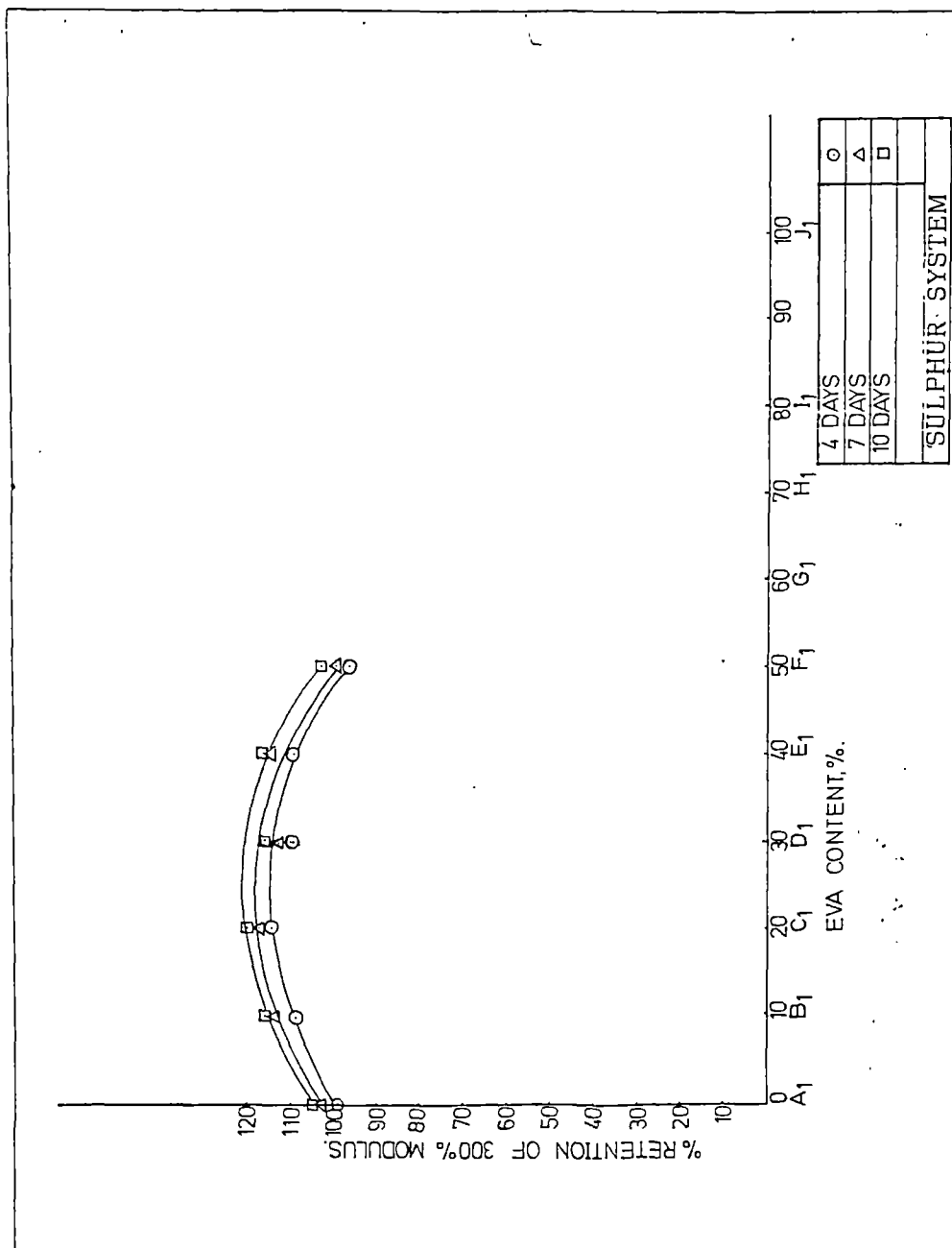
Figure VII.1
Plots of retention of 300% modulus of sulphur cured blends after thermal ageing.
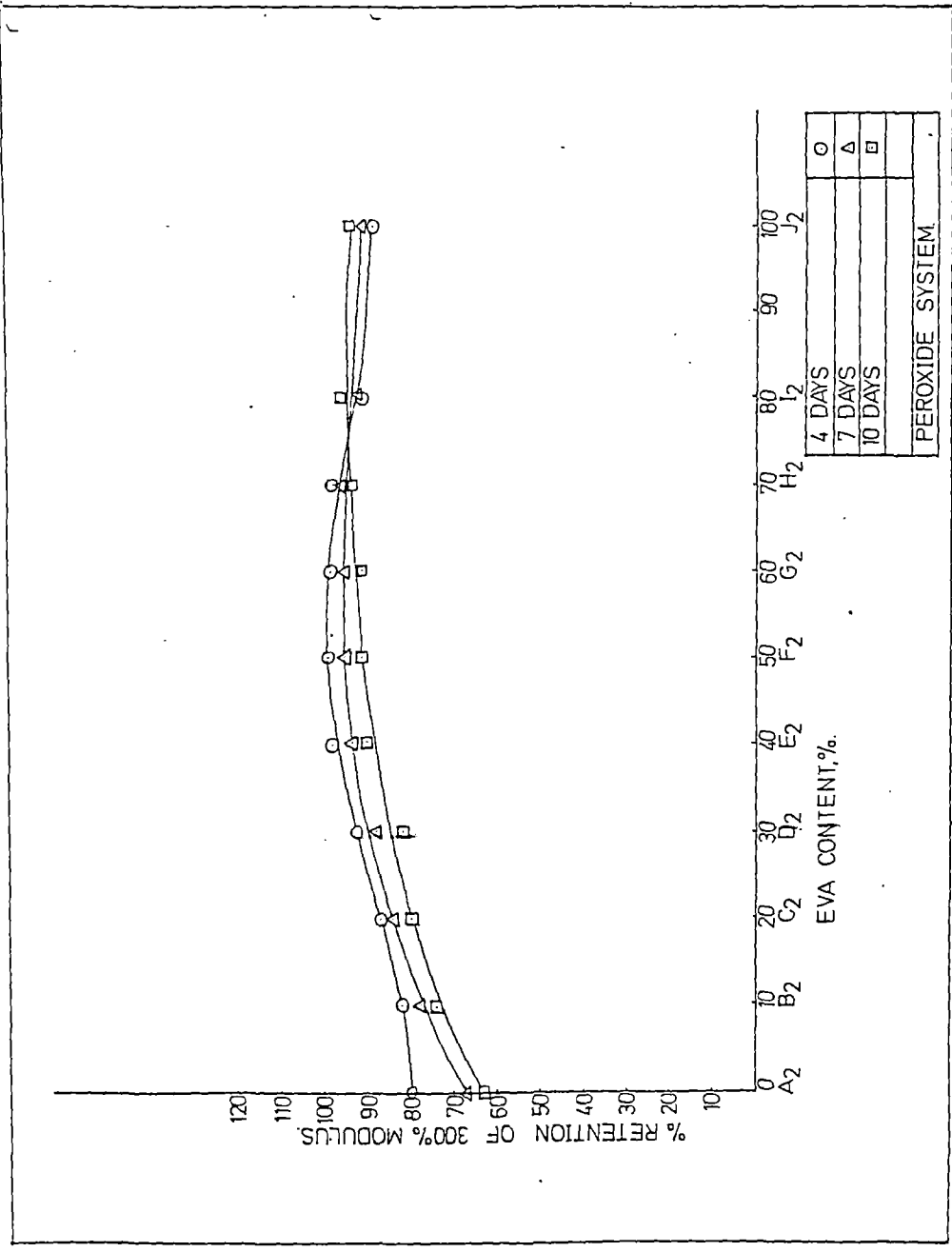
Figure VII.2
Plots of retention of 300% modulus of peroxide cured blends
after thermal ageing.
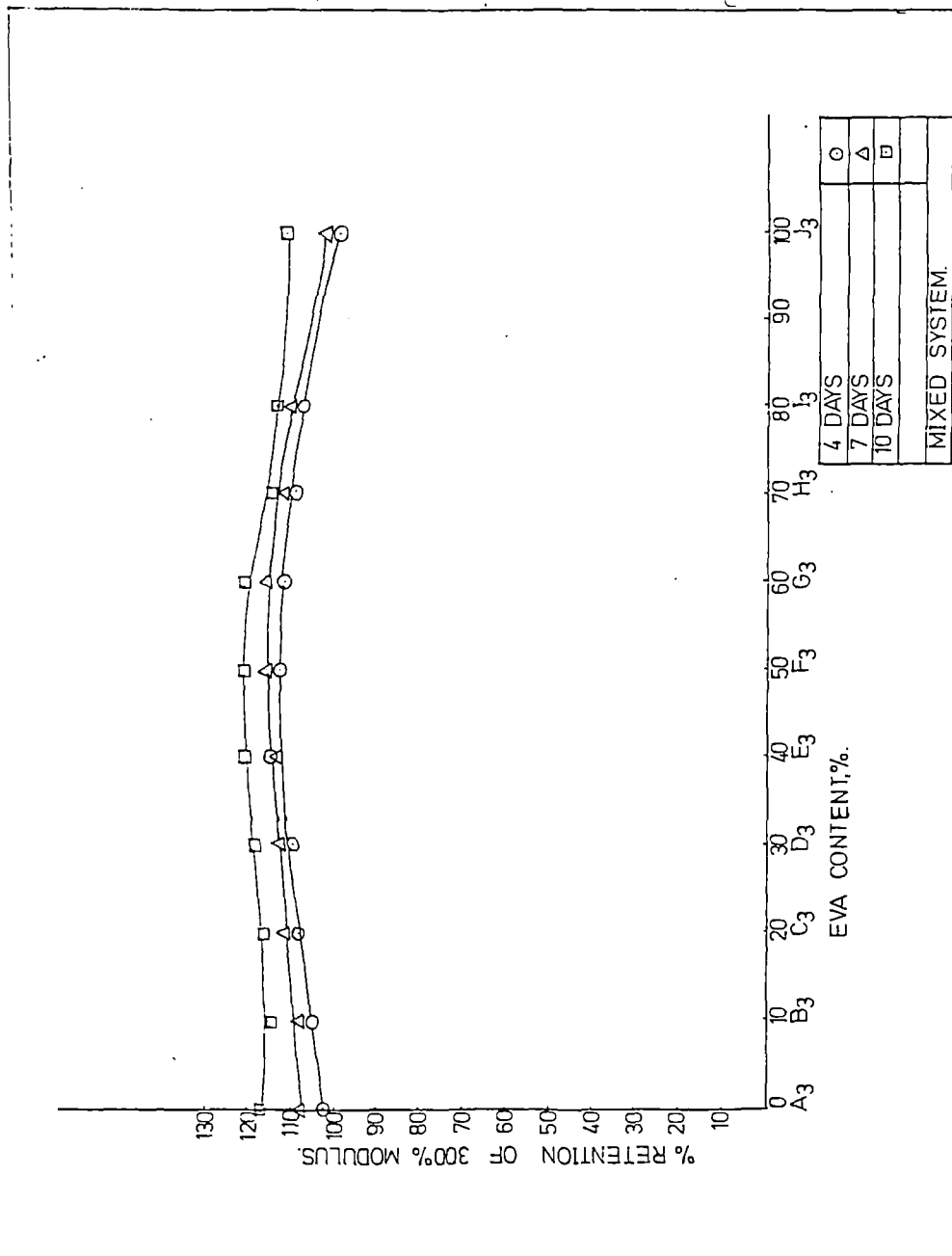
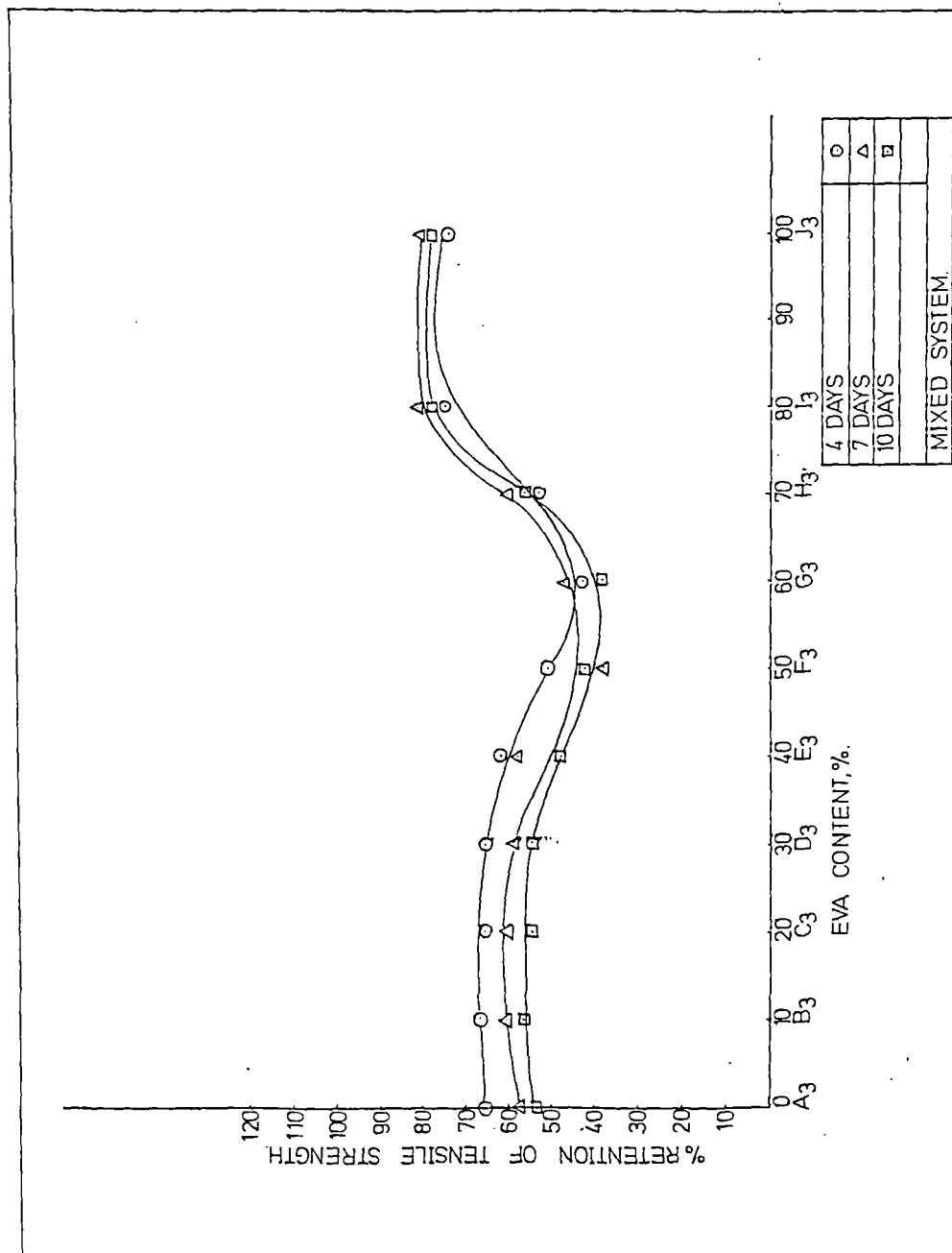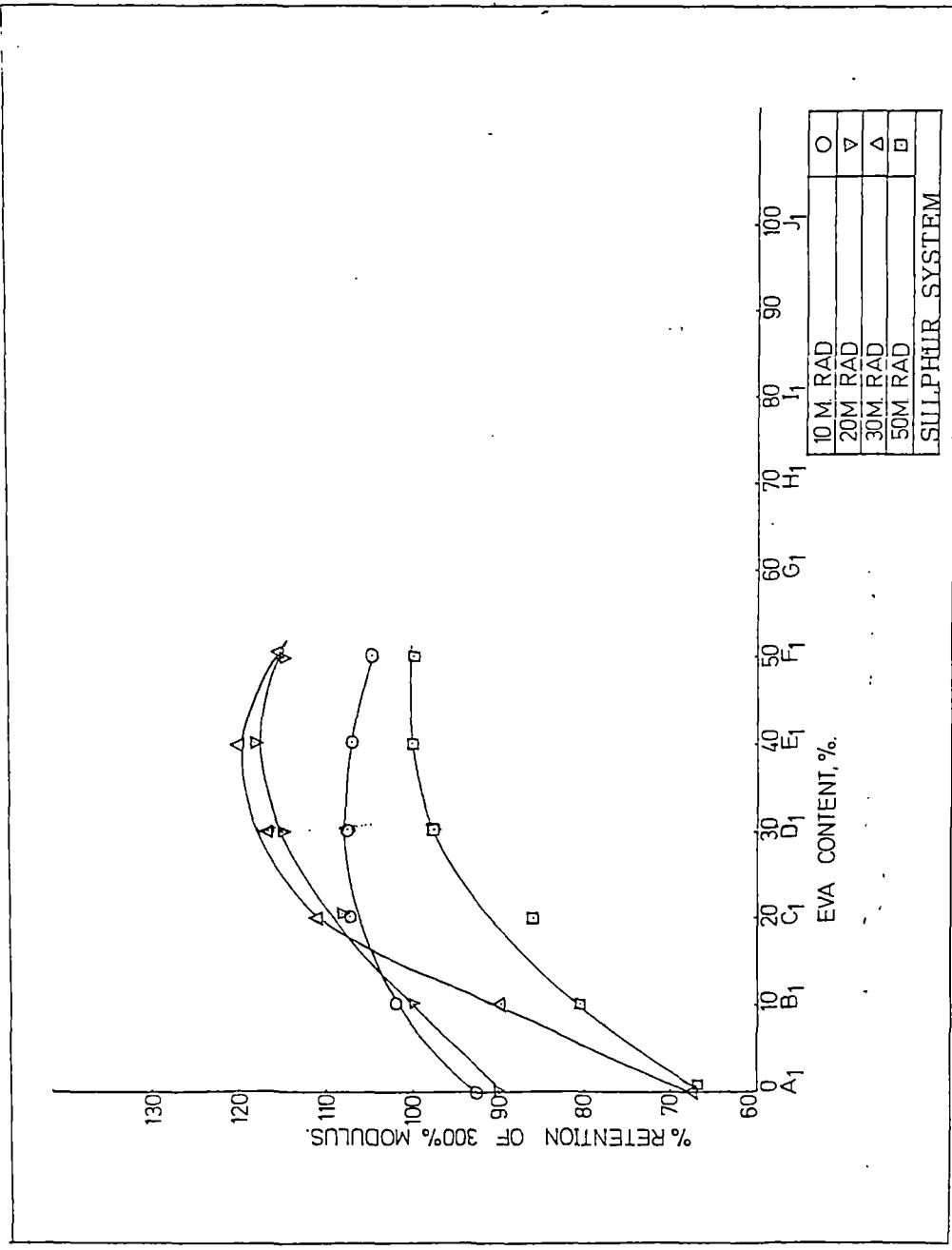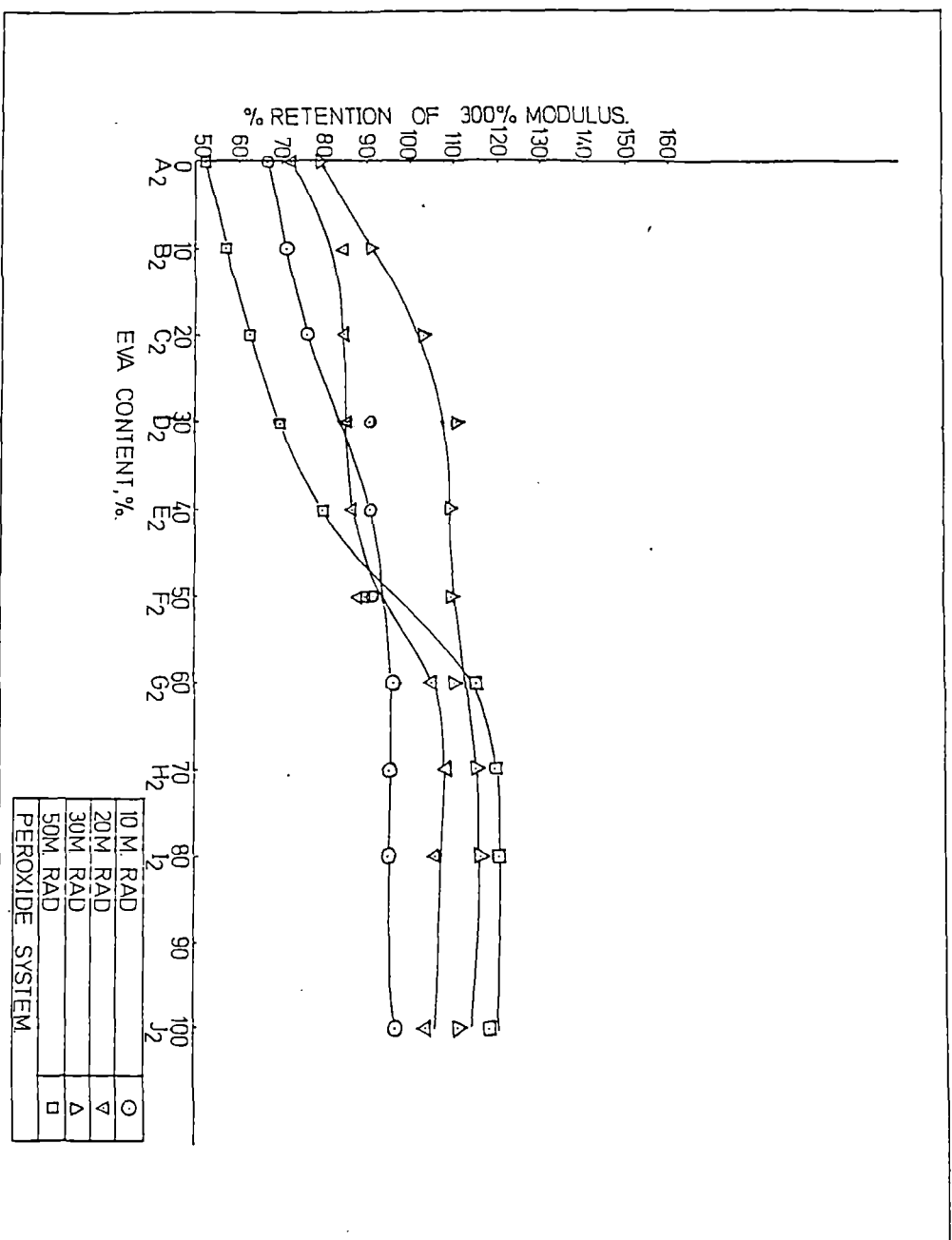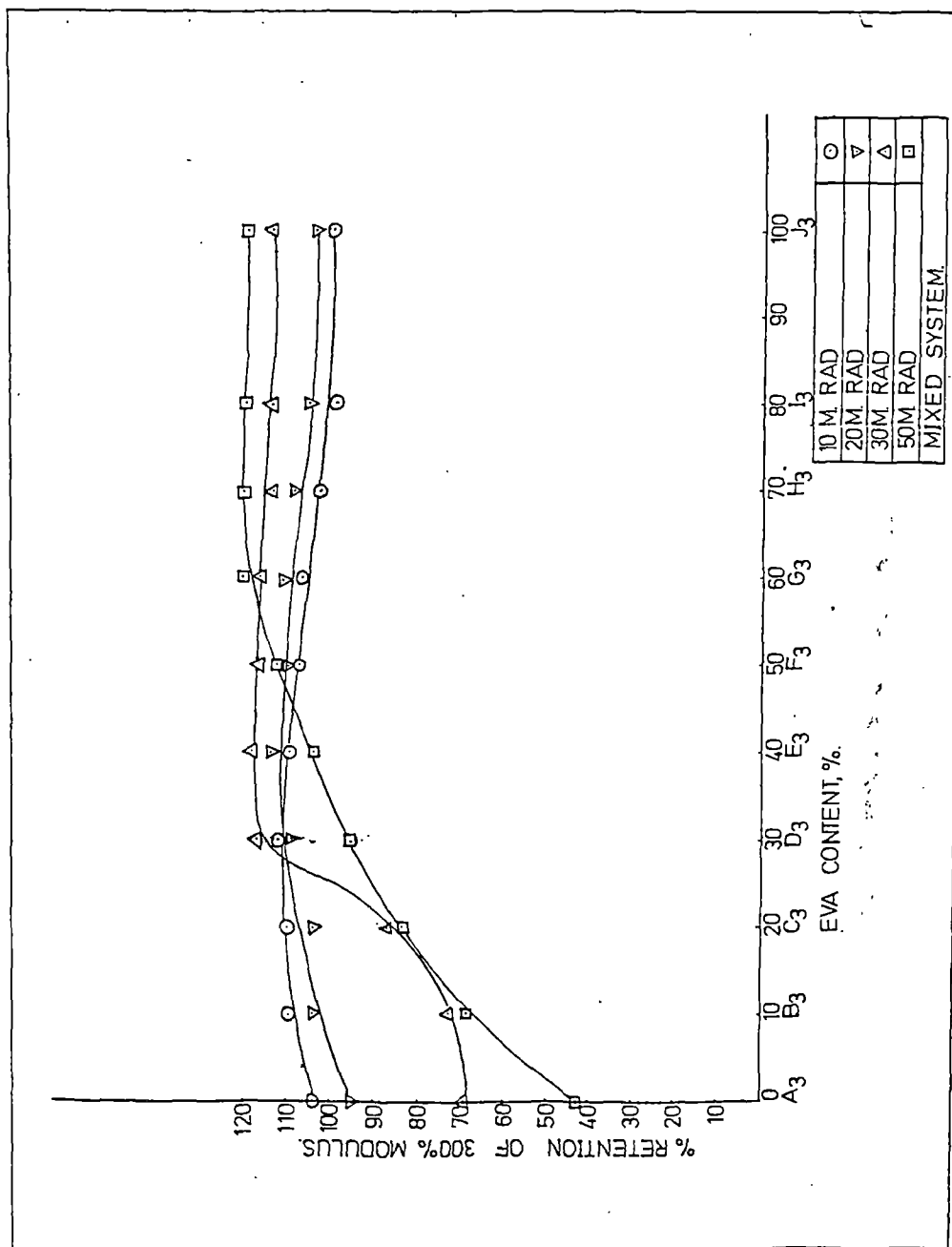Figure VII.3
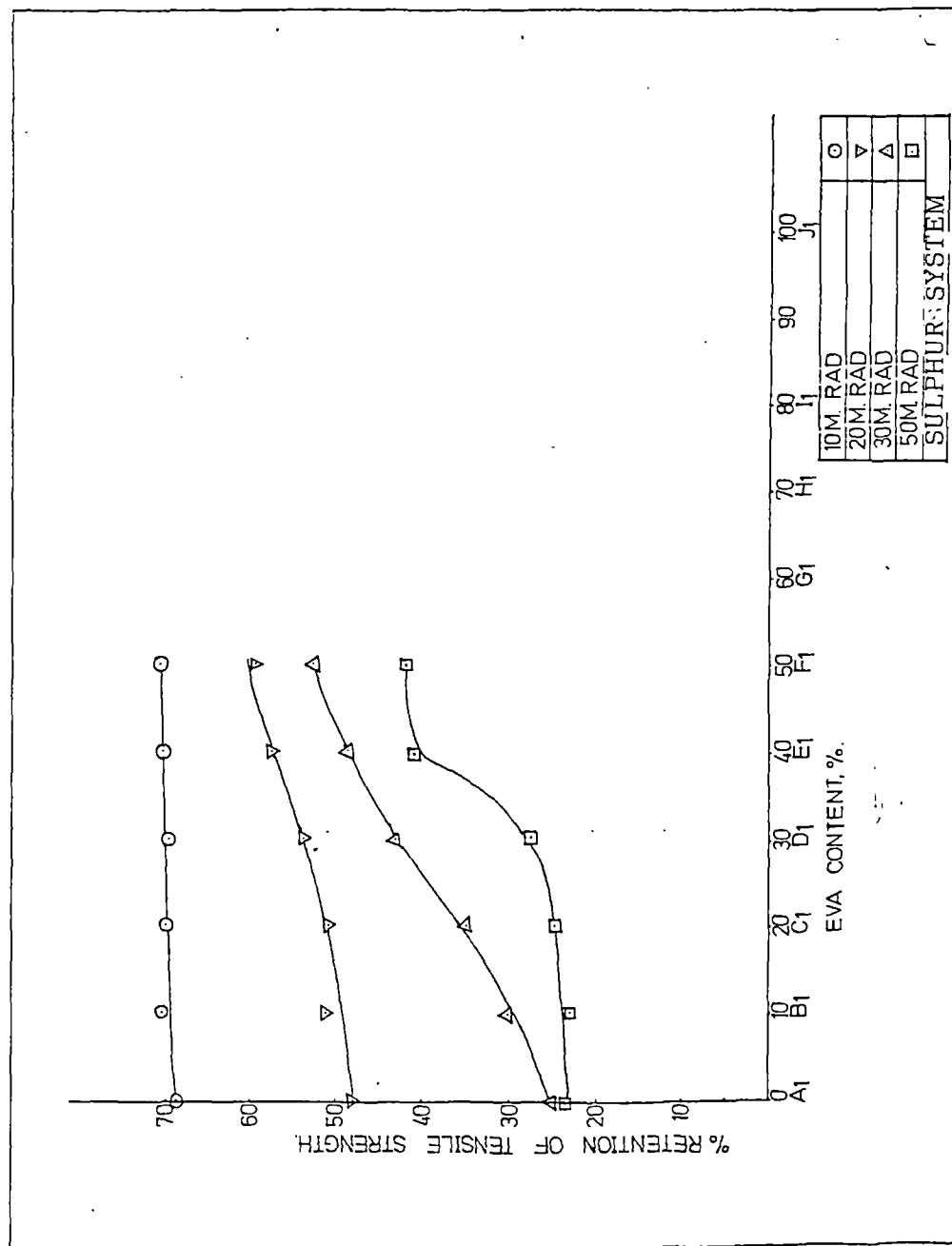Plots of retention of 300% modulus of mixed cureblends
after thermal ageing.
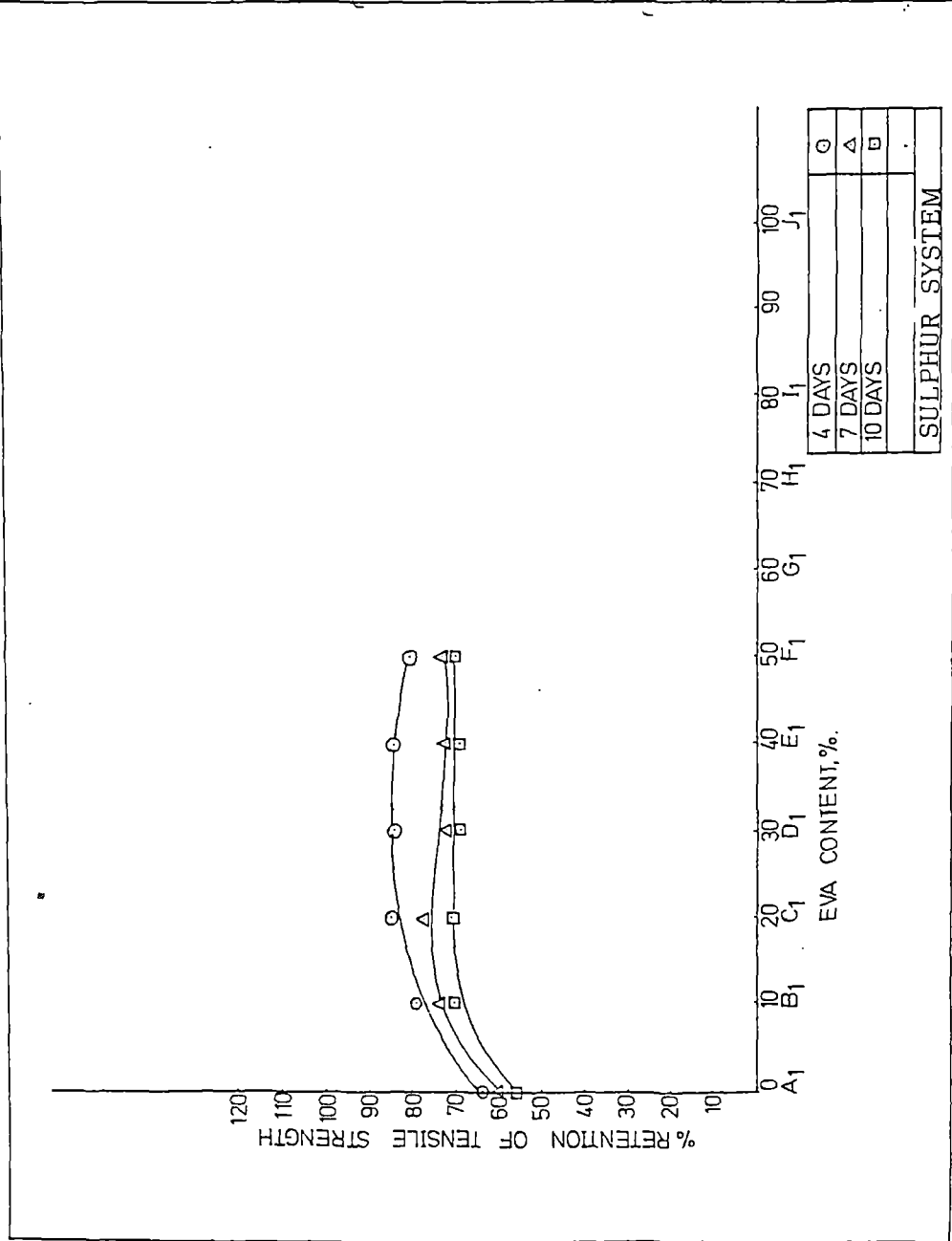
Figure VII.4
Plots of retention of tensile strength of sulphur cured blends
after thermal ageing.
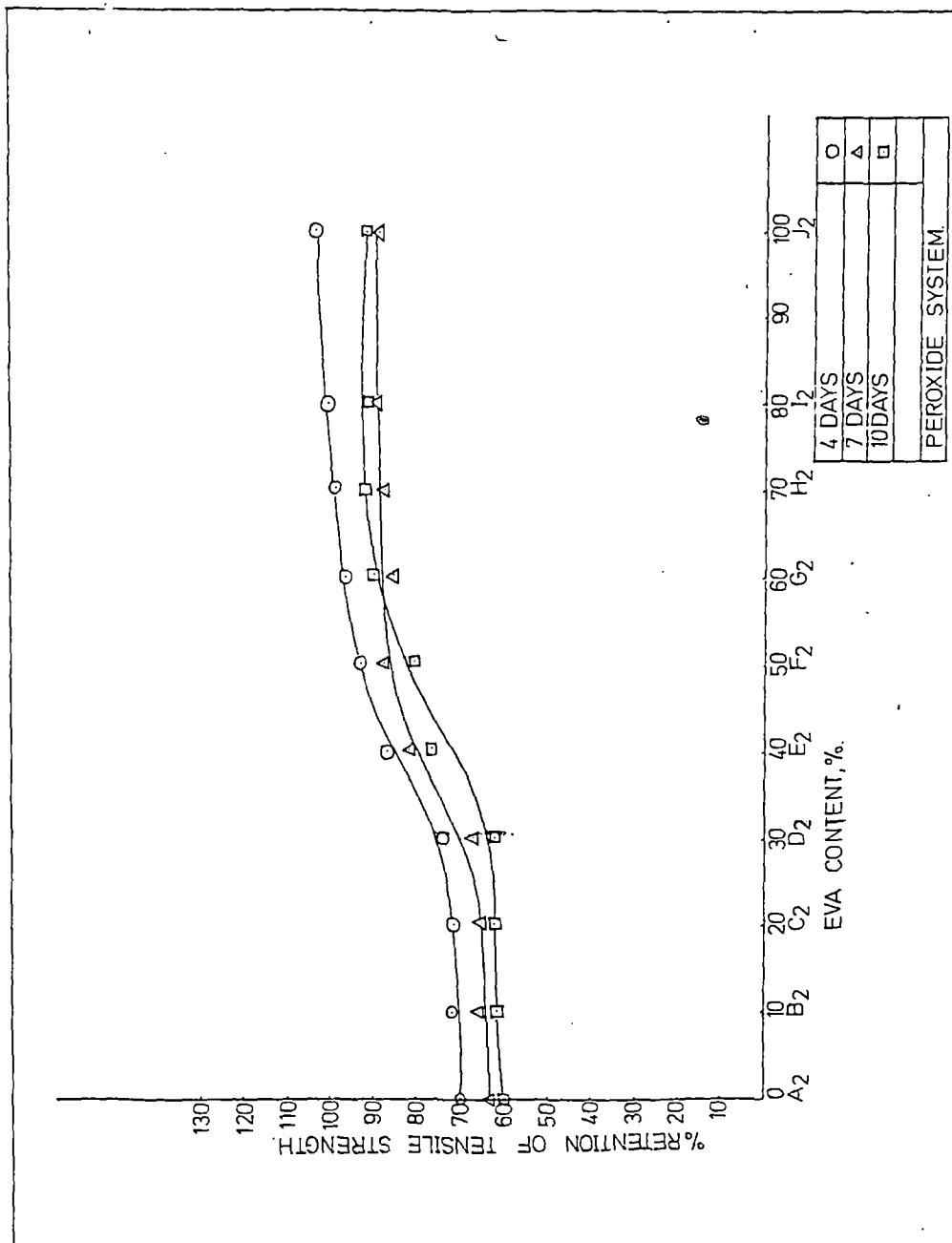
Figure VII.5
Plots of retention of tensile strength of peroxide cured blends
after thermal ageing.

Figure VII.6
Plots of retention of tensile strength of mixed cure blends
after thermal ageing.

Figure VII.7
Plots of retention of 300% modulus of sulphur cured blends
after γ-irradiation.

Figure VII.8
Plots of retention of 300% modulus of peroxide cured blends
after γ-irradiation.

Figure VII.9
Plots of retention of 300% modulus of mixed cure blends after γ-irradiation.

Figure VII.10
Plots of retention of tensile strength of sulphur cured blends
after γ-irradiation.
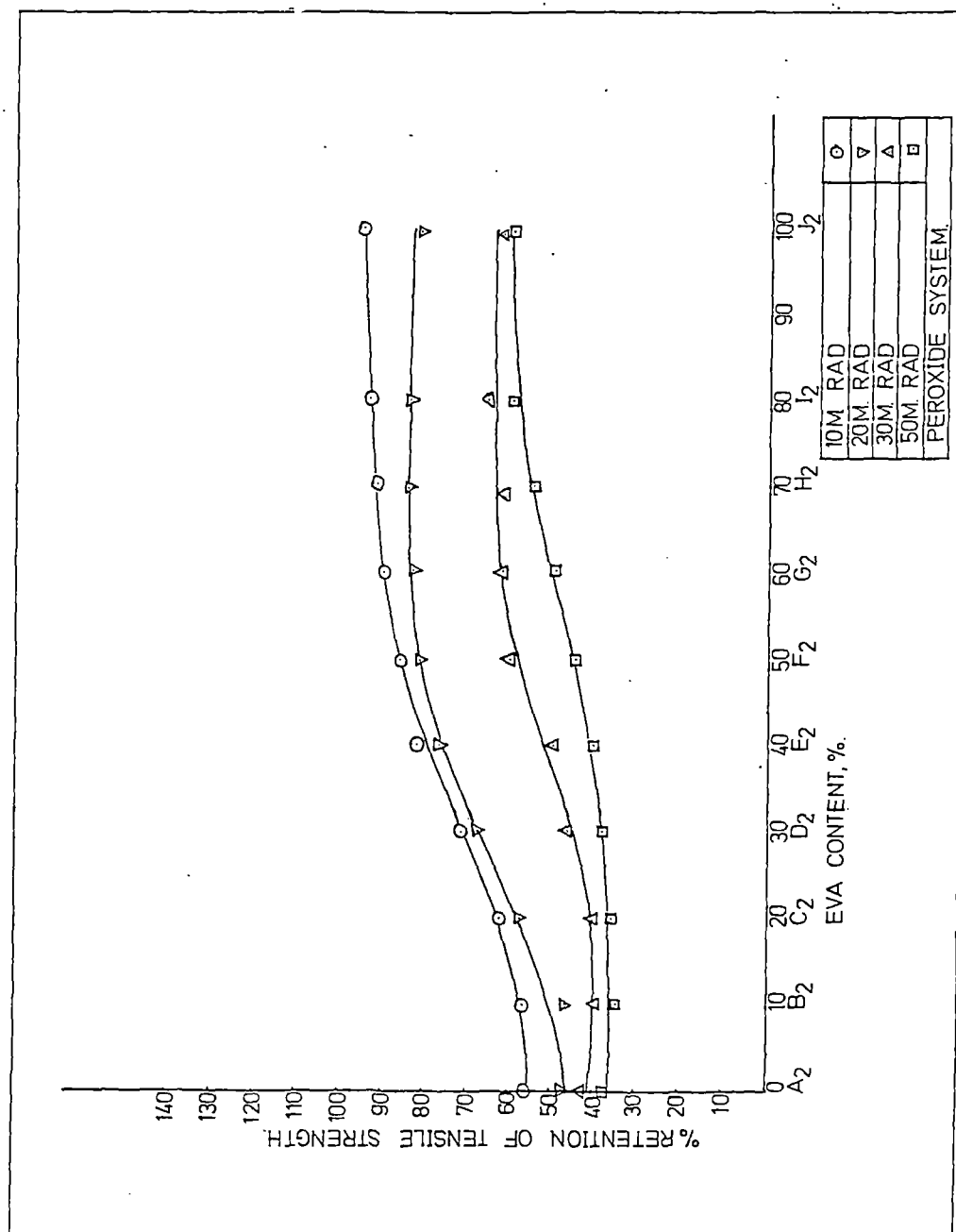
Figure VII.11
Plots of retention of tensile strength of peroxide cured
blends after γ-irradiation.
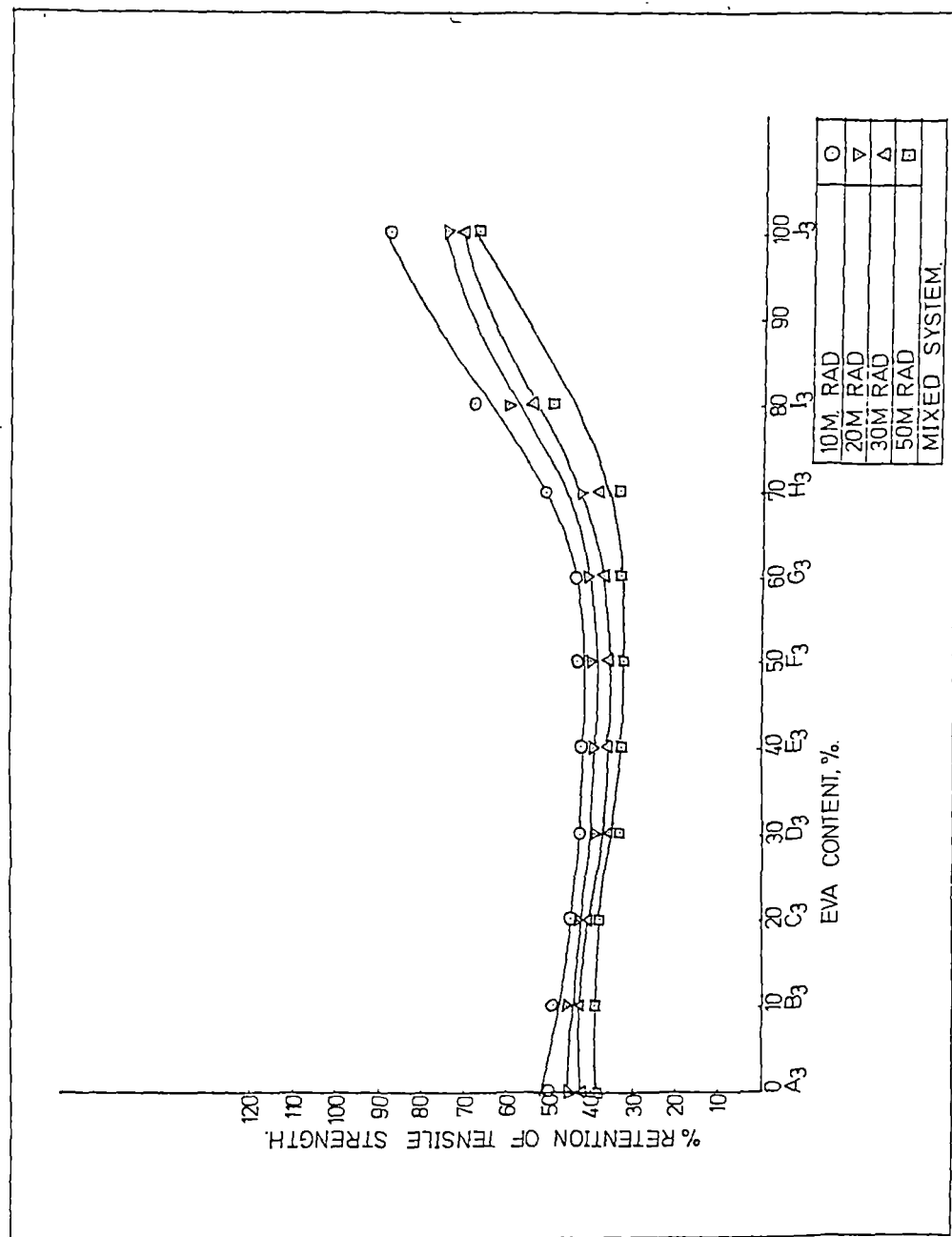
Figure VII.12
Plots of retention of tensile strength of mixed cure blends
after γ-irradiation.
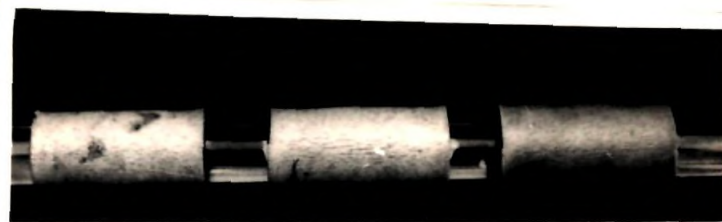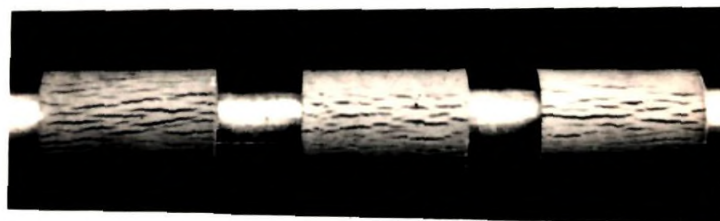
Figure VII.13
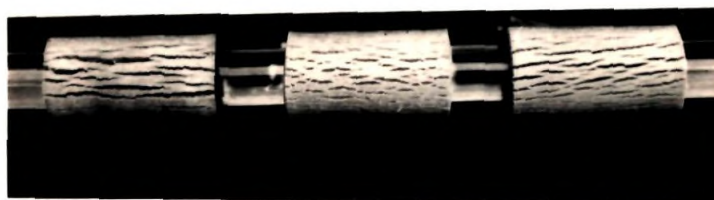Photograph of NR vulcanisates after 8 h
and 85 h exposure.
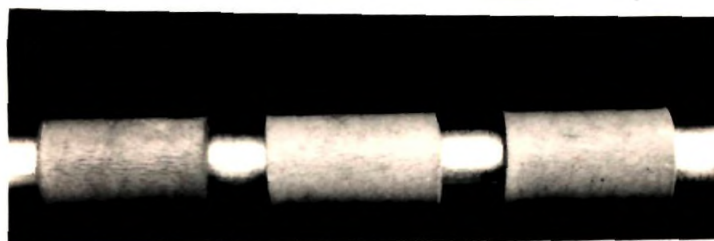
Figure VII.14
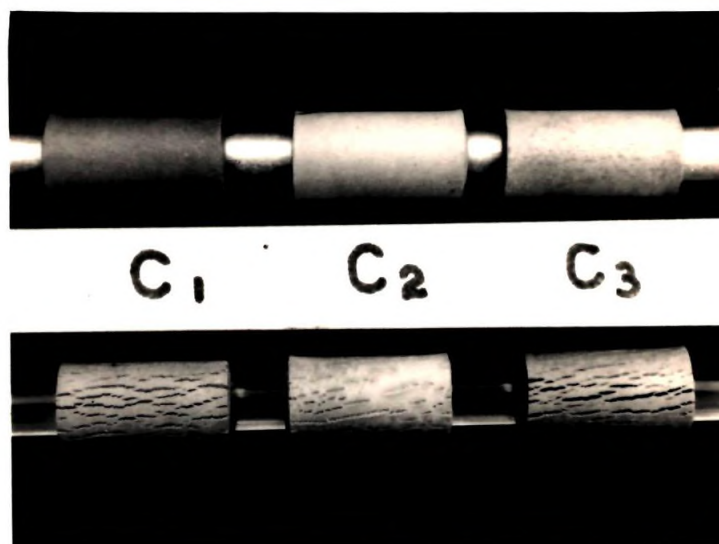Photograph of blend B (90:10 NR:EVA)
after 8 h and 85 h exposure.

Figure VII.15
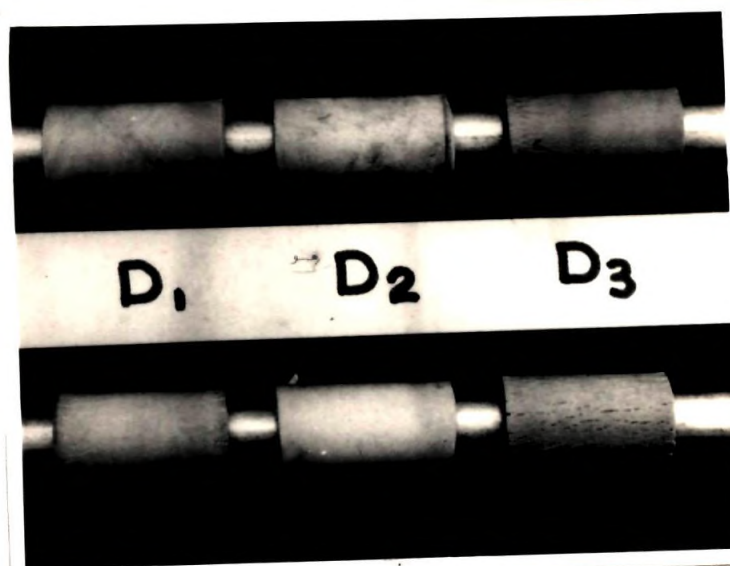Photograph of blend C (80:20 NR:EVA) after 8 h and 85 h exposure.

Figure VII.16
Photograph of blend D (70:30 NR:EVA) after 8 h and 85 h exposure.

CHAPTER VIII - EFFECT OF BLEND RATIO AND FILLERS ON THE CELL
STRUCTURE AND PROPERTIES OF MICROCELLULAR SOLES
FROM NR-EVA BLENDS.

The results included in this chapter have been accepted for present-
ation at the International Natural Rubber Conference, scheduled for
5-8 February 1992, Bangalore, India.

Various types of polymers and their blends are used in foot-wear to achieve specific combination of properties such as light weight, wearing comfort, stiffness and durability. Conventionally a blend of natural rubber (NR) or styrene-butadiene (SBR) with high styrene resin (SBR 1958) is used for making microcellular soles. Supply of styrene for the production of SBR is reported to be decreasing[126]. Attempts have been going on to develop a substitute for SBR 1958 in footwear application. A promising alternative for SBR 1958 in microcellular soles appears to be ethylene-vinyl acetate copolymer (EVA), which possesses an overall balance of properties.

This chapter discusses the effect of blend ratio and fillers on the mechanical properties of microcellular soles based on NR-EVA blends. Scanning electron microscopic observations were made on microcellular sheets to study the variation in cell structure with blend ratio and type of filler. The details of the experimental procedures adopted for studying the mechanical properties and for scanning electron microscopic observations are given in Chapter II.

For preparing microcellular sheets, blends having NR:EVA ratios 50:50, 40:60, 30:70, 20:80 and 0:100 were used. These blends are designated as F, G, H, I and J, respectively (Table VIII.1). The effect of fillers was evaluated in blend G only. This was because, for DCP cured NR-EVA blends, better technological properties were shown by those blends which contained a higher proportion of EVA

(Chapter III). The concentration of blowing agent was varied so as to get the same expansion for the microcellular sheets prepared from various blends. Linear expansion of the sheets before post-curing was controlled to about 100 per cent of the mould dimensions.

VIII.1 CELL STRUCTURE

VIII.1.1 Effect of blend ratio on cell structure

Figures VIII.1 to VIII.5 are the photomicrographs of the cut edges of the microcellular sheets prepared from blends F to J, respectively, as seen under a scanning electron microscope. From these figures, it is evident that as the proportion of EVA in the blend is increased, the size of the cells becomes larger and the cells attain a more uniform structure. The larger cell size of the EVA rich blends is due to the lower melt viscosity of such blends which facilitates increased blowing with unit weight of the blowing agent. The non-uniformity of the cells in those blends in which the proportion of EVA is reduced can be due to the non-uniform distribution of blowing agent between EVA and NR phases. In the NR phase, distribution of the blowing agent can be less due to its non-polar nature. But the dispersion of the blowing agent in this phase will be better since the viscosity of the blend increases as the proportion of NR is increased. This will lead to smaller size for the cells formed in such blends. The non-uniformity in cell structure of such blends can also be due to the difference in extents of blowing of the two phases.

VIII.1.2   Effect of filler on cell structure

Figure VIII.6 is the photomicrograph of the microcellular sheet in which china clay was used as the filler. Comparing with figure VIII.2, which contained the same loading of precipitated calcium carbonate, it is seen that the china clay filled compound gave a slightly larger cell size. The uniformity of cell structure is almost identical. From the rheographs of calcium carbonate and china clay loaded compounds it is seen that the compound containing the former has a higher viscosity (Figure VIII.7). Hence in this compound the blowing agent will be more finely dispersed which will result in smaller cell size for the expanded sheet.

VIII.2   PHYSICAL PROPERTIES

VIII.2.1   Relative density and shrinkage

The relative density decreased with increase in EVA content and the extent of decrease was higher when EVA content increased from 50 to 70 per cent (Figure VIII.8). Further increase of EVA content did not cause any appreciable change in relative density. But shrinkage of microcellular sheets showed steady increase with increase in proportion of EVA in the blend. In microcellular soles, shrinkage that occur on post-curing or long term storage is due to loss of gases by diffusion process. The larger cell size and reduced wall thickness of the cells facilitate diffusion of gases from blends

having higher proportions of EVA. The combined effects of high permeability and faster diffusion of gases in high EVA blends are reflected in higher shrinkage of such blends.

VIII.2.2 Hardness and compression set

Hardness of the microcellular soles decreased and the compression set increased with increase in EVA content (Figure VIII.9). The increase in compression set is due to the residual thermoplastic nature of EVA.

VIII.2.3 Abrasion loss and split tear

The increase of EVA content in the blend enhanced the abrasion resistance and split tear strength of the microcellular sole (Figure VIII.10). These two properties are very important as far as the service life of the product is concerned. The factors which contribute to the improvement in these properties are uniform cell structure of the sole having higher proportion of EVA and the crystalline nature of EVA. Uniform cell structure helps to take up higher loads by equal distribution of the applied force. Crystalline regions in EVA impart high tear resistance to the product by arresting/diverting the propagation of the tear path.

VIII.2.4 Effect of filler on properties

The effects of china clay and precipitated calcium carbonate

on the physical properties of the microcellular soles were evaluated, by varying the filler content. All other ingredients, including the blowing agent were kept at the same dosage as that for compound G, except the oil content which was varied in proportion to the filler level. Diethylene glycol (DEG) was added in those compounds which contained china clay as the filler.

Figure VIII.11 shows the effect of loading of china clay and calcium carbonate on expansion of the moulded sheets. Filler loading reduced the expansion of the sheets and this effect was almost identical for both the fillers. However, calcium carbonate showed better expansion ratio than clay. Compression set of the microcellular sheets increased with filler loading (Figure VIII.12). In this case, the behaviour of both the fillers are almost identical. However, calcium carbonate showed comparatively lower set. The split tear strength (Figure VIII.13) was also better for the calcium carbonate loaded sheets. But the relative increase in split tear with loading was less for calcium carbonate loaded microcellular sheets. Figure VIII.14 shows the effect of filler on shrinkage of expanded sheets. Shrinkage was more for the calcium carbonate loaded compounds at higher filler loadings. This is due to the fact that these sheets had higher expansion ratios compared with clay loaded samples. However, at 45 phr level, the calcium carbonate loaded compound showed lower shrinkage. Hardness (Figure VIII.15) and relative density (Figure VIII.16) also increased with filler loading. Both

these properties were lower for the sheets containing calcium carbonate since these sheets had higher expansion than those containing china clay. Abrasion loss decreased with increase in filler loading (Figure VIII.17). But in this case, calcium carbonate loaded sheets showed higher abrasion loss than china clay loaded samples. Comparatively less increase in split tear and higher abrasion loss of the calcium carbonate loaded sheets is due to higher expansion of the sheets. These two properties depend very much on the strength of the matrix. When expansion is higher, the actual volume of the matrix to take up the load will be lower.

FORMULATION OF COMPOUND MEETING BIS SPECIFICATIONS

With an understanding of the changes in properties with blend ratio and filler loading, a formulation which can yield microcellular sheets that meet Bureau of Indian Standard specifications for Hawai sheets, was developed. The formulation developed and the properties of the sheets prepared using the same are given in Tables VIII.1 and VIII.2, respectively.

Table VIII:1.   Formulation to meet BIS specifications.

Polymer (blend consisting of 40% NR and 60% EVA)	100.0
Zinc oxide	3.5
Stearic acid	1.0
Zinc stearate	2.0
Styrenated phenol type of antioxidant	1.0
Dicumyl peroxide*	4.0
Calcium carbonate	90.0
Paraffinic oil	3.6
Azodicarbonamide	4.0

*40 per cent active.

Table VIII.2.   Physical properties.

		NR-EVA	BIS Specifications limit
1.	Relative density	0.45	0.4 to 0.5
2.	Hardness (Shore A)	46.0	45±5
3.	Change in hardness after ageing at 100°C for 24 hours	+2	+5 -0
4.	Split tear strength (N)	53	50
5.	Shrinkage, 100±1°C, 1 h (%)	2.9	3.0
6.	Flex resistance: Kilocycles to crack initiation	$\langle$ 400	$\langle$ 60
7.	DIN abrasion loss 5 N load (mm^3)	440	--
8.	Compression set (%)	23	25
9.	Room temperature shrinkage at 27°C for 2 weeks (%)	1.3	1.5
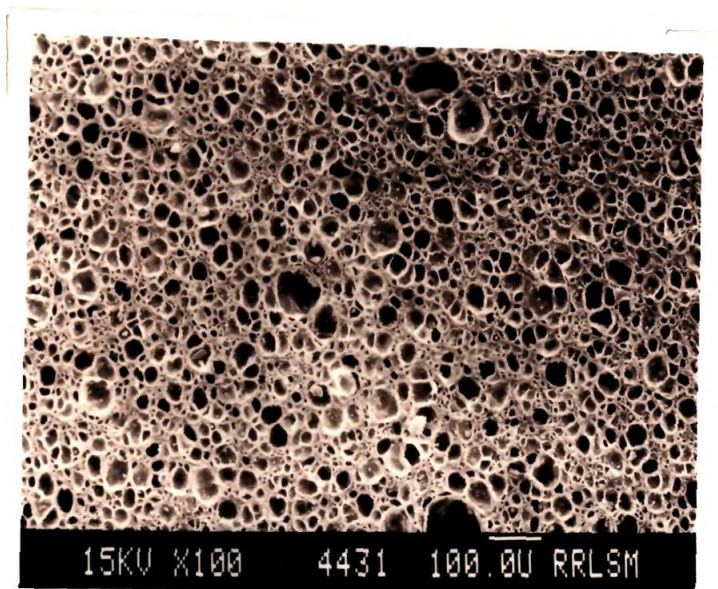
Figure VIII.1
Photomicrograph of NR:EVA (50:50) blend.
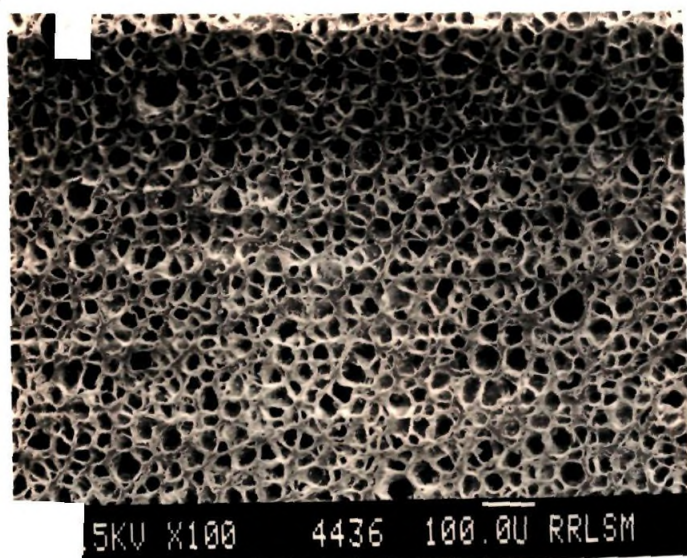
Figure VIII.2
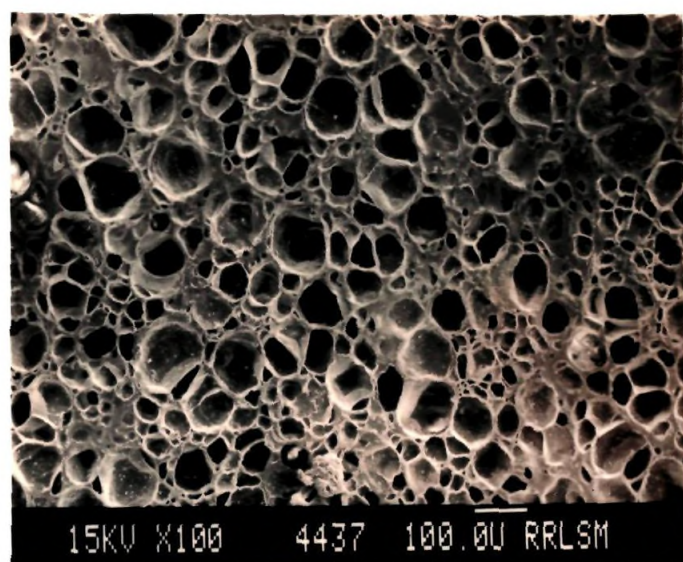**Photomicrograph of NR:EVA (40:60) blend.**

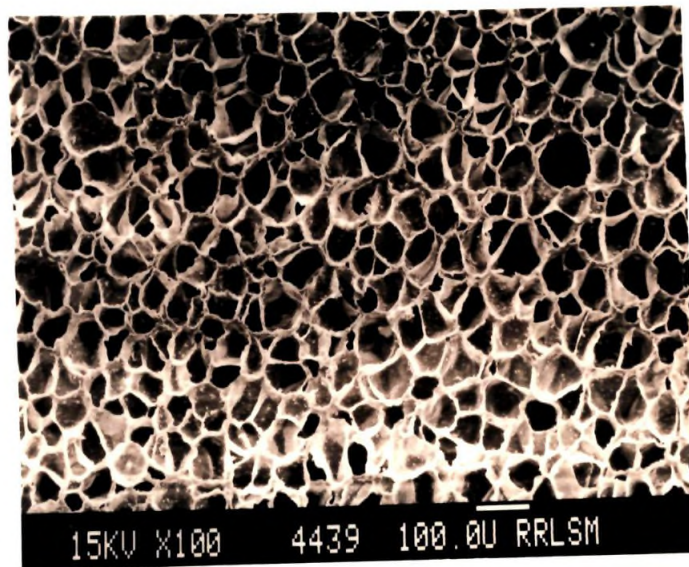
Figure VIII.3
Photomicrograph of NR:EVA (30:70) blend.

Figure VIII.4
Photomicrograph of NR:EVA (20:80) blend.
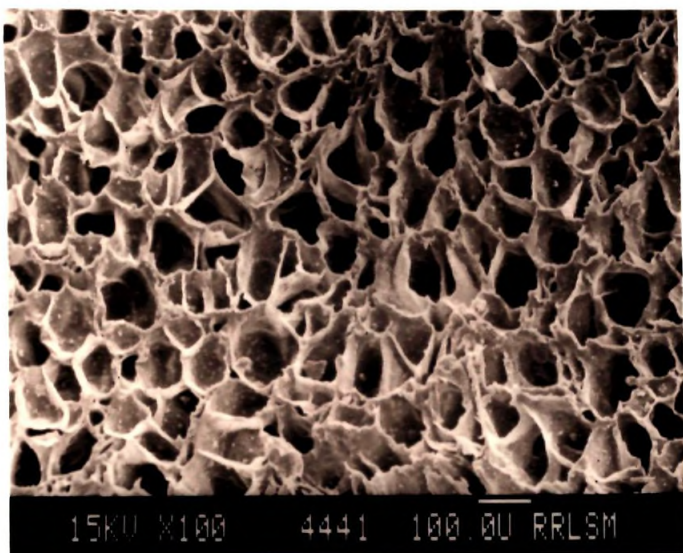

Figure VIII.5
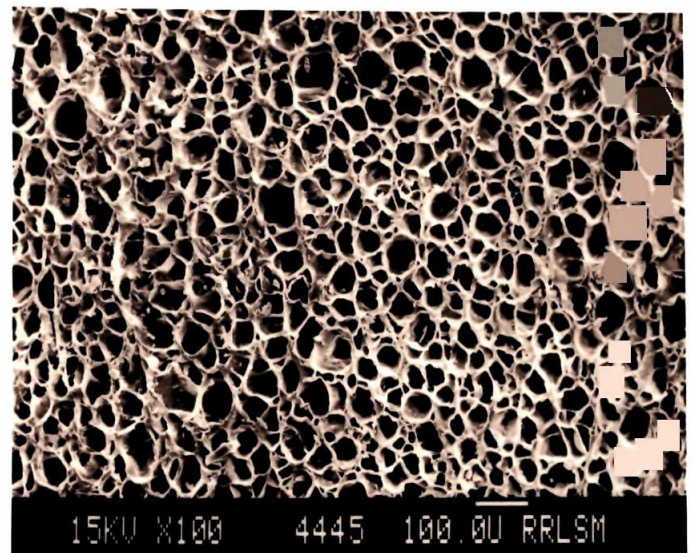**Photomicrograph of NR:EVA (0:100) blend.**

Figure VIII.6
Photomicrograph of NR:EVA (40:60)
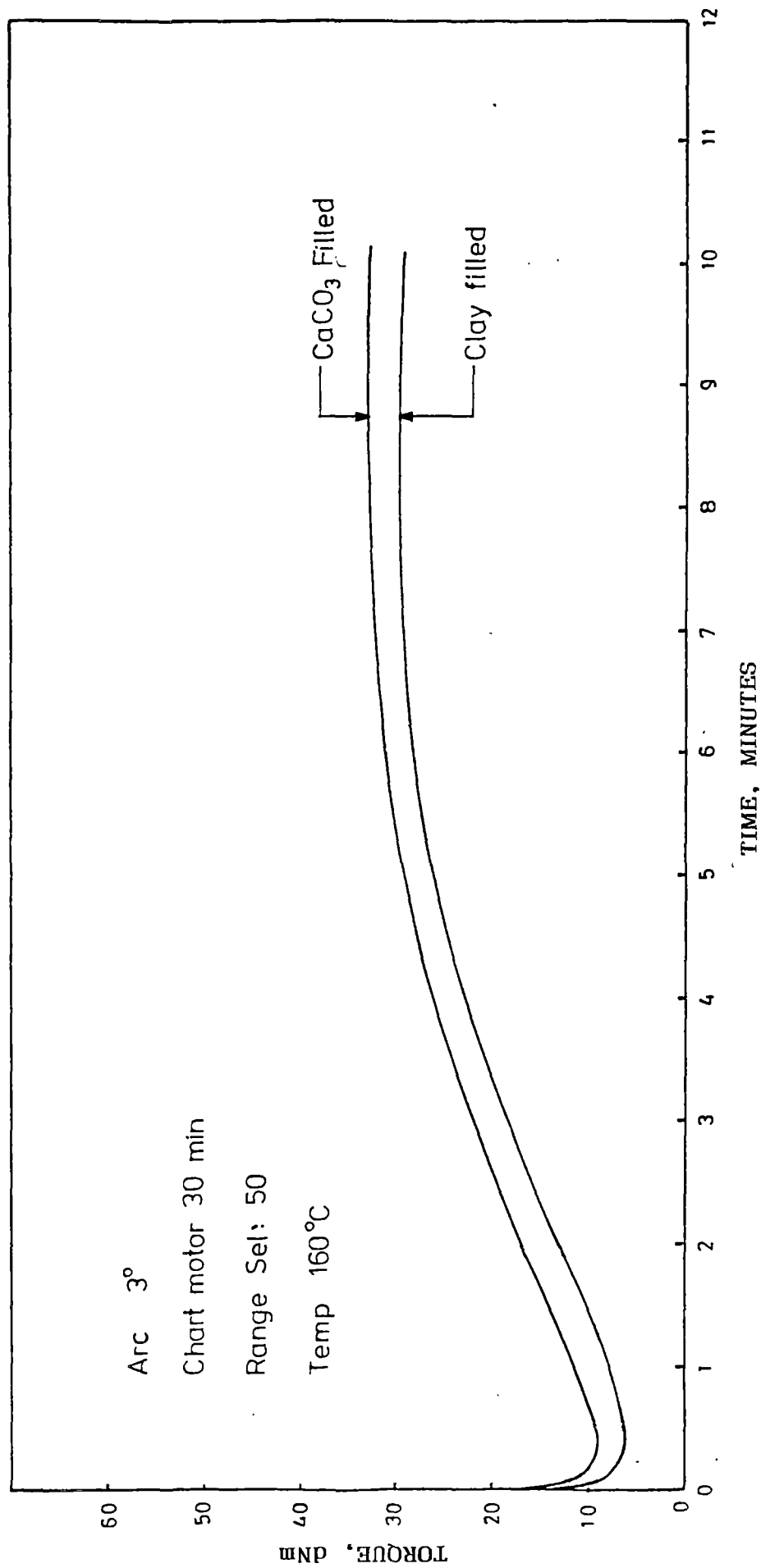**clay filled blend.**

Figure VIII.7
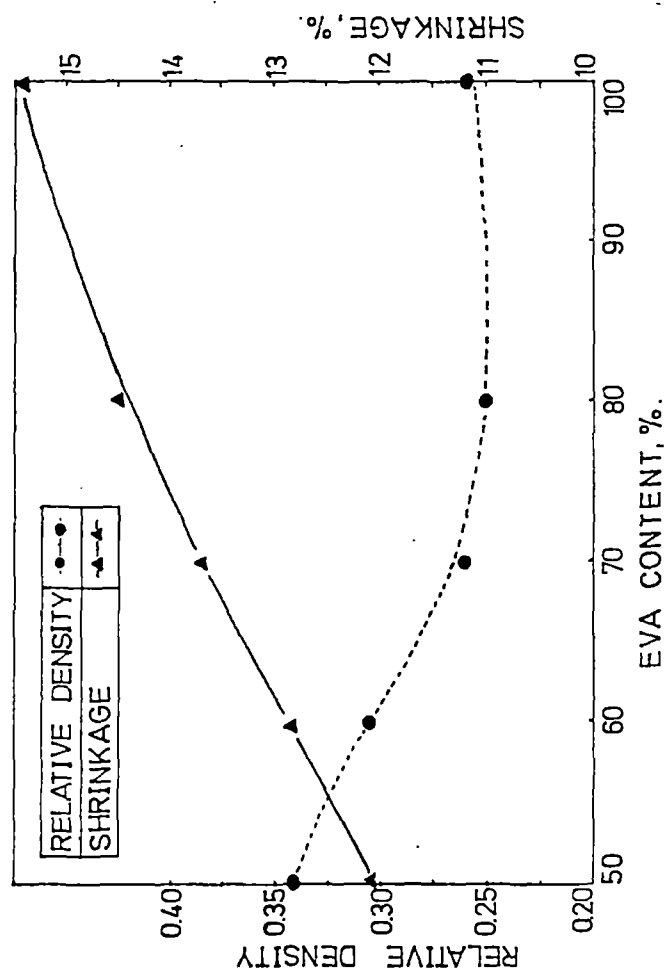Rheographs of calcium carbonate and china clay filled compounds.

Figure VIII.8
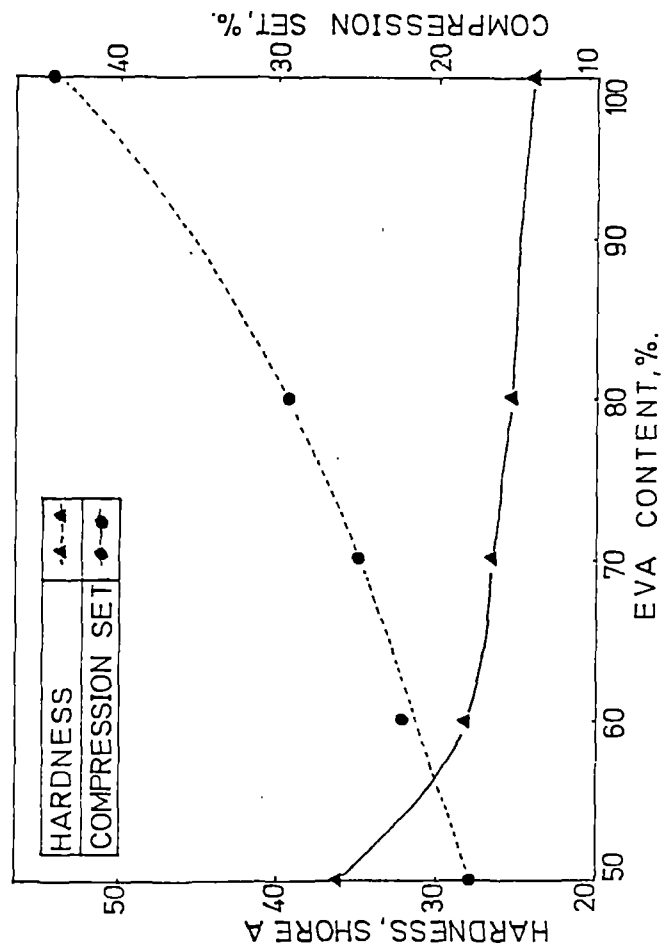Variation of relative density and shrinkage with EVA content.

Figure VIII.9
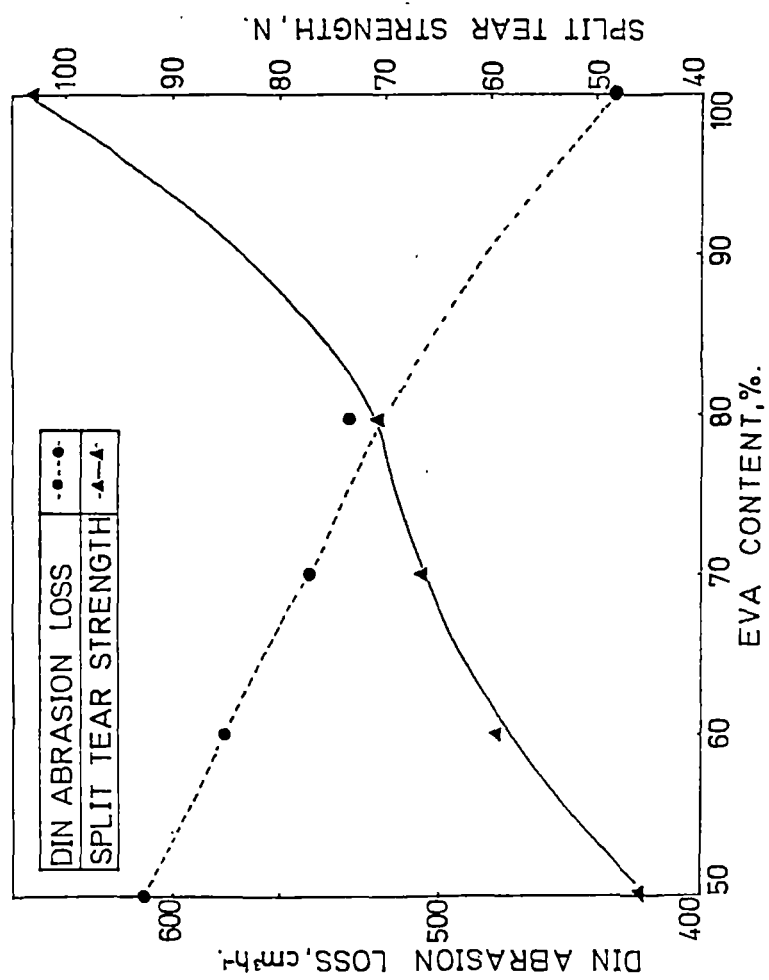Variation of hardness and compression set with EVA content.

Figure VIII.10
Variation of abrasion loss and split tear strength with EVA content.
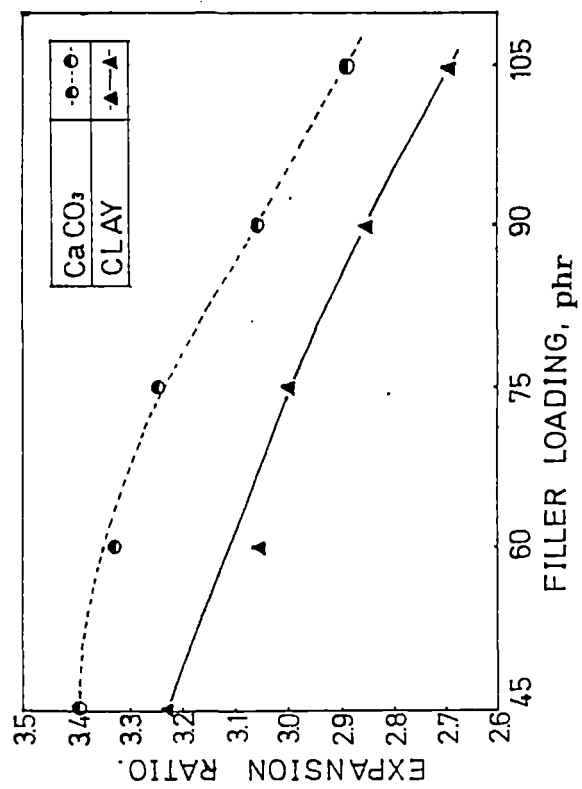
Figure VIII.11
Effect of china clay and calcium carbonate on expansion.

Figure VIII.12
Effect of china clay and calcium carbonate on compression set.

Figure VIII.13
Effect of china clay and calcium carbonate on split tear strength.

Figure VIII.14
Effect of china clay and calcium carbonate on shrinkage.

Figure VIII.15
Effect of china clay and calcium carbonate on hardness.
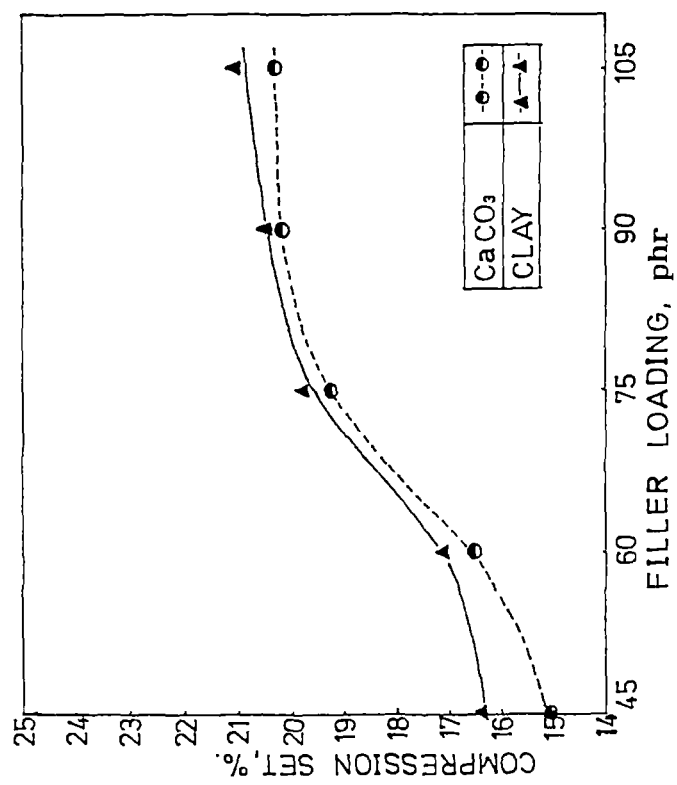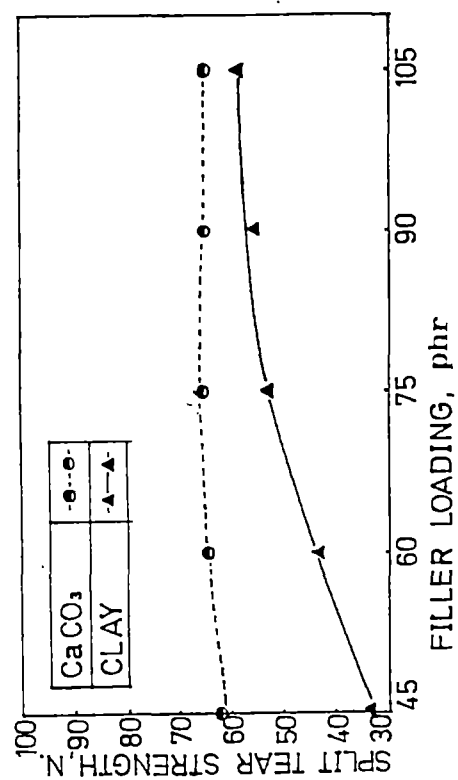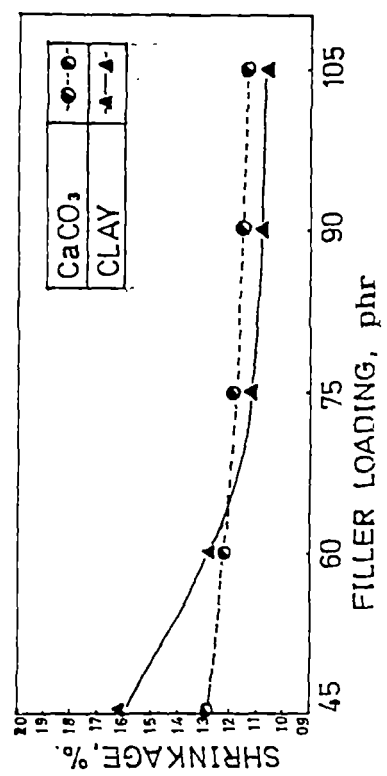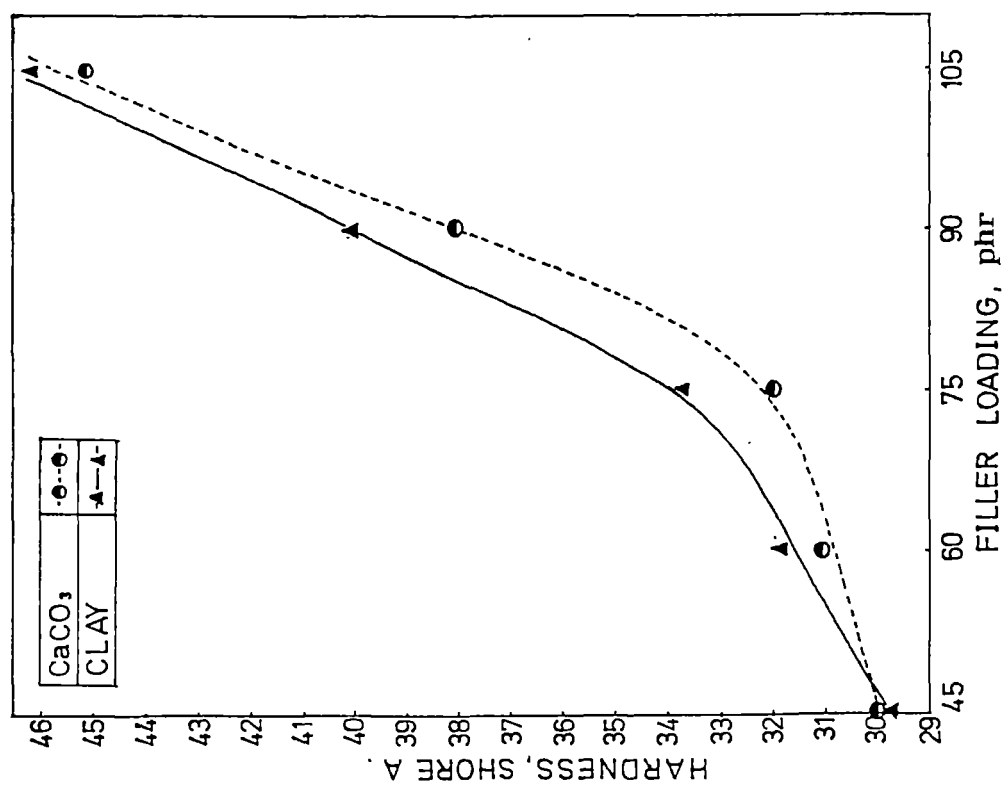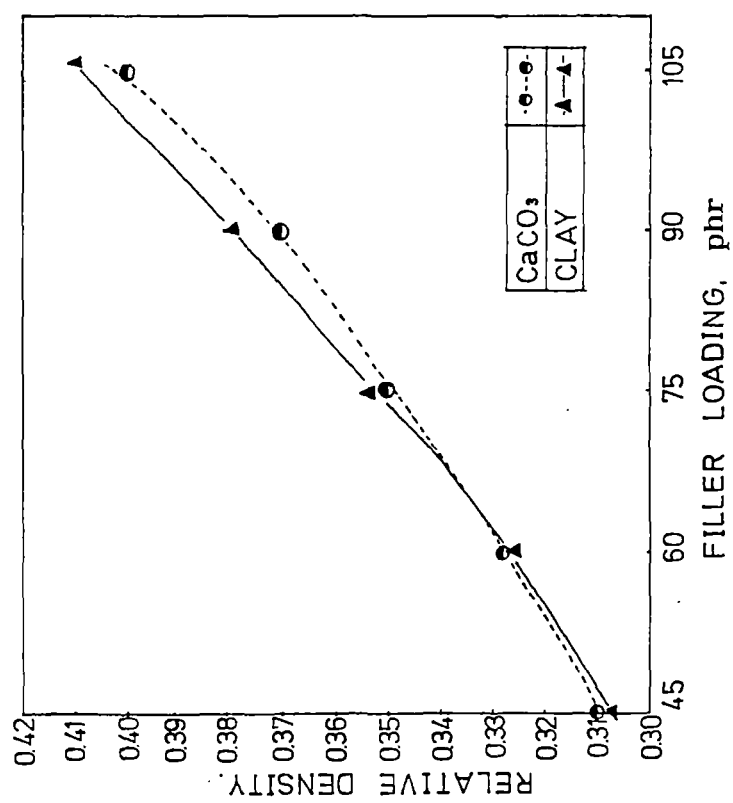
Figure VIII.16
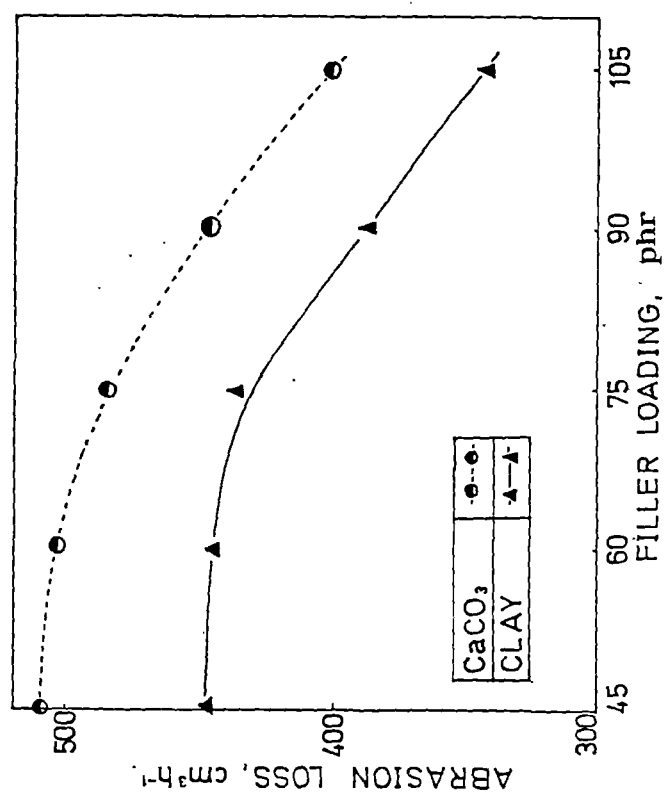Effect of china clay and calcium carbonate on relative density.

Figure VIII.17
Effect of china clay and calcium carbonate on abrasion loss.

SUMMARY AND CONCLUSIONS

SUMMARY AND CONCLUSIONS

All rubbers have shortcomings in one or more properties. Thus there are technical reasons for blending two rubbers in order to achieve the right compromise. Processing difficulties may also be overcome by blending. Appreciable difference in price of different rubbers emphasizes economic reasons for blends. In developing a useful blend, there is a need to understand which elastomers can be successfully blended and what underlying factors influence the results.

The data presented in this thesis consist of the results of a systematic study conducted on the morphology, vulcanisation kinetics, melt flow behaviour, miscibility behaviour, effect of fillers and degradation behaviour of NR-EVA blends. The effects of blend ratio and filler on the cell structure and properties of microcellular soles based on NR-EVA blends have also been investigated. Emphasis has been given for studying the effect of different crosslinking systems on the above characteristics of the blends. It is expected that these blends can be advantageously used in many applications such as footwear, tubings, cables, automobile components, etc.

The thesis consists of eight chapters. The first chapter deals with various aspects of elastomer blends and a review of the earlier

work done in the field of elastomer blends. The scope and objectives of the present work are also given in this chapter. Types of commercially available elastomer blends, problems associated with blend formation, necessity for blending elastomers and the major advantages of elastomer blends have been reviewed. The melt flow behaviour, morphology of blends and methods to characterise the polymer blends have also been discussed in this chapter.

The second chapter contains a detailed account of the experimental procedures adopted for the preparation of the blends and the test samples. The description of the testing procedures and the details of the equipment used are included in this chapter. The characteristics of the materials used for the study are also described in this chapter.

The third chapter describes the effect of blend ratio on morphology and the effect of three cure systems on the vulcanisation kinetics and technical properties of NR-EVA blends. The morphology of NR-EVA blends was such that the EVA formed the dispersed phase where its proportion was below 40 per cent and NR formed the dispersed phase when its proportion was 40 per cent or below. In the range of 40:60 and 50:50 EVA:NR both polymers formed continuous phases leading to an interpenetrating network structure. Blending of EVA with NR increased the tear resistance, modulus, hardness and abrasion resistance and adversely affected the compression set

and rebound resilience of NR, at all proportions. Morphology-property relationship has been made. In NR-EVA blends a mixed cure system consisting of DCP and sulphur gave better technological properties than DCP alone, especially at high proportion of NR. The activation energy and cure time were found to be lower in the case of mixed cure blends.

Chapter four discusses miscibility and crystallization behaviour of NR-EVA blends. The thermal behaviour, crystallinity and dynamic mechanical properties of the blends have been investigated with special reference to the effect of blend ratio and crosslinking systems. The DSC and DMTA results showed that the blends are incompatible in crosslinked and in uncrosslinked state. The predominant crosslinking of natural rubber phase as a result of the addition of sulphur or mixed crosslinking agent could be analysed by the shift in the glass transition temperature of the natural rubber phase towards higher temperatures. Addition of NR to EVA decreased the crystallinity of the EVA, as evidenced by the DSC and X-ray analysis.

The effects of blend ratio, crosslinking systems, silica content and temperature on the melt flow behaviour of NR-EVA blends are reported in chapter five. The extrudate morphology of the blends at different shear rates has also been reported in this chapter. All systems showed pseudoplastic behaviour as evident

from the decrease in viscosity with increase in shear stress. The decrease of viscosity of the blends with the increase of temperature was prominent at low shear rates. At lower shear stress ($<3 \times 10^5$ N/mm^2), the viscosity of the blends appeared to be non-additive function of the viscosity of the homopolymers. This behaviour was observed at the lower proportion of the EVA phase ($<40\%$) where it formed a dispersed phase in the continuous NR matrix. The observed anomaly has been explained due to the structural build up of EVA particles in the NR matrix at lower shear region.

Extrudate morphology of the blends showed that at higher shear forces the NR domains are broken down into smaller particles. The stratification of the extrudates with NR forming the core region and EVA as the sheath was observed. This is associated with the migration of low viscosity EVA phase towards the periphery of the extrudate.

The sixth chapter consists of the results of the studies on the effect of silica on mechanical and dynamic mechanical properties of NR-EVA blends. Precipitated silica improved the tear strength and did not affect the tensile strength when the proportion of NR in the blend was higher. Addition of silica adversely affected the technological properties, except compression set of blends having higher proportions of EVA. Silica was found to impart resistance to degradation by γ-radiation and ozone, for NR-EVA blends. Tan δ

values of unfilled blends increased as a function of temperature. Addition of silica decreased the tan δ values. Addition of silica increased the storage modulus. The loss modulus of filled and unfilled blends decreased with temperature. In the case of EVA and high EVA blends the storage modulus decreased with temperature and the decrease was more sharp in the rubbery region.

The seventh chapter describes the degradation behaviour of NR-EVA blends. The effect of blend ratio and the type of crosslinking system on thermal ageing, γ-radiation and ozone resistance of the blends have been evaluated. It is observed that blends containing higher proportion of EVA show better thermal ageing and γ-radiation resistance. It is also noted that mixed cure system gives lower retention of tensile strength after thermal ageing and γ-irradiation. But modulus 300% is better for this system. The ozone resistance of peroxide cured vulcanisate was better than that of the other cure systems. The morphological studies discussed in the third chapter help to explain the degradation behaviour of the blends.

The eighth chapter of the thesis describes the effects of blend ratio and fillers on the cell structure and properties of micro-cellular sheets made from NR-EVA blends. The concentration of blowing agent was adjusted so as to get the same expansion in all the blends. Higher proportions of the EVA in the blend enhanced the abrasion resistance and split tear strength of microcellular sheets based on

NR. As the proportion of EVA is increased compression set and shrinkage are increased. The change in properties with increasing EVA content is basically due to the characteristics of EVA and the accompanying change in cell structure of the microcellular sheet. Among china clay and calcium carbonate fillers, the latter one imparted higher expansion and split tear strength and gave lower set and abrasion resistance.

REFERENCES

1. I. Frenta, "Elastomers and Rubber Compounding Materials" Elsevier, New York, 1989.

2. D.R. Paul and J.W. Barlow, J. Macromol. Sci-Rev. Macromol. Chem: Page 31, [18(1)], 109 (1980).

3. T. Inone, Nippon Gomu Kyokaishi, 1, 20 (1981).

4. C.S.L. Baker and I.R. Wallance, J. Nat. Rubb. Res., 1(4), 270 (1986).

5. N.M. Mathew, J. Polym: Sci: Polym: Lett., 22, 135 (1984). 1984).

6. S. Akhtar, B. Kuriakose, P.P. De and S.K. De, Plast. Rubber Process. Appl., 7(1), 11 (1987).

7. L.M. Glanville and P.W. Milner, Rubber Plast. Age, 48, 1059 (1957).

8. J.F. Svetlik, E.F. Ross and D.T. Normann, Paper presented at the meeting of the Division of Rubber Chemistry, American Chemical Society, Chicago, Illinois, September 2-4, 1964.

9. C.A. Mc Call and H.K.J. de Decker, Fr. 1,422,275 (June 17, 1966).

10. R. Grimberg, Ind Usoara, 13, 339 (1966).

11. W.C. Flannigan, Rubber Age, 101(2), 49 (1969).

12. R.N. Kienle, E.S. Dizon, T.J. Brett and C.F. Eckert, Rubb. Chem. Technol., 44, 996 (1971).

13. T.H. Meltzer and W.J. Dermondy, J. Appl. Polym. Sci., 8, 773 (19640.

14. T.H. Meltzer and W.J. Dermoundy, J. Appl. Poly. Sci., **8,** 791 (1964).

15. M.S. Sutton, Rubber World, **149(5),** 62 (1964).

16. K. Stake, T. Wada, T. Sone and M. Hamada, J. Inst. Rubber Ind., **4,** 102 (1970).

17. D.D. Dunnom and H.K. de Decker, Rubber World, **151(6),** 108 (1965).

18. B. Topcik, Mater. Plast. Elast., **35,** 201 (1969).

19. T. Kyu and J.M. Saldanha, Macromolecules, **21,** 1021 (1988).

20. M. Takenaka, T. Izumitai and T. Hashimoto, Macromolecules, **20,** 2257 (1987).

21. H. Meier and G.R. Strobol, Macromolecules, **20,** 649 (1987).

22. S. Danesi and R.S. Porter, Polymer, **19,** 448 (1978).

23. B. Kuriakose and S.K. De, Polym. Eng. Sci., **25,** 630 (1985).

24. M. Baer, J. Appl. Polym. Sci., **16,** 1109 (19720.

25. K.C. Dao, Polymer, **25,** 1527 (1984).

26. C.K. Riew, E.H. Rowe and A.R. Siebert, "Advances in Chemistry" Ser. 154, American Chemical Society, Washington DC (1976).

27. S. Miller, Proceedings Int. Conf. Toughening of Plastics, Paper 8, Plastics and Rubber Institute, London (1978).

28. S. Cimmino, L.D'Orazio, R. Greco, M. Manglio, M. Malirconico, C. Macarella, E. Martuscelli, R. Palumbo and G. Ragosta, Polym. Eng. Sci., **24,** 48 (1989).

29. D. Yang, B. Zhang, Y. Yang, Z. Fang, G. Sun and Z. Feng. Polym. Eng. Sci., **24,** 612 (1984).

30. G. Demma, E. Martuscelli, A. Zanetti and M. Zorzetto, J. Mat. Sci., **18,** 89 (1983).

31. B. Kuriakose, S.K. De, S.S. Bhagawan, R. Sivaramakrishnan and S.K. Athithan, J. Appl. Polym. Sci., **32,** 5509 (1986).

32. D. Klempner and K.C. Frisch, Polym. Sci. Technol., **10** and **11** (1980).

33. L.H. Sperling, Polym. Sci. Technol., **4** (1974).

34. R. Alex, P.P. De and S.K. De, J. Polym. Sci. Lett. Ed., **27,** 361 (1989).

35. R. Alex, P.P. De and S.K. De, Polym. Commun., **31,** 118 (1990).

36. J.L. Leblanc, Plast. Rubber Process Appl., **2,** 361 (1982).

37. G.J. Van Amerongin, Rubb. Chem. Technol., **37,** 1065 (1964).

38. V.A. Shershenv, Rubb. Chem. Technol., **55,** 537 (1982).

39. M.G. Huson, W.J. Mc Gill and R.D. Wigget, Plast. Rubber Process Appl., **5,** 319 (1985).

40. R.F. Bauer and A.H. Crossland, Rubb. Chem. Technol., **61,** 585 (1988).

41. J.R. Gardner, Rubb. Chem. Technol., **41,** 1312 (1968).

42. J.R. Gardner, Rubb. Chem. Technol., **42,** 1058 (1969).

44. J.R. Gardner Rubb. Chem. Technol., **43,** 370 (1970).

44. A.K. Bhowmick and S.K. De, Rubb. Chem. Technol., **53,** 960 (1980).

45. K.C. Baranwal and P.N. Son, Rubb. Chem. Technol., **47,** 88 (1974).

46. K. Hashimoto, M. Miura, S. Takagi and H. Okamoto, Int. Polym. Sci. Technol., **3**, 84 (1976).

47. A.Y. Coran, Rubb. Chem. Technol., **61**, 281 (1988).

48. J.E. Callan, W.M. Hess and C.E. Scott, Rubb. Chem. Technol., **44**, 814 (1971).

49. J.E. Lewis, M.L. Devney and J.E. Whittington, Rubb. Chem. Technol., **42**, 892 (1969).

50. B.G. Corman, M.L. Devney and J.E. Whittington, Rubb. Chem. Technol., **43**, 1249 (1970).

51. M.H. Watters and D.N. Keyte, Trans. Inst. Rubber Ind., **38**, T.41 (1962).

52. G.N. Avgeropoulos, F.C. Weissert, P.H. Biddison and G.G.A. Bohm, Rubb. Chem. Technol., **49**, 93 (1976).

53. O. Olabisi, L.M. Robeson and M.T. Shaw, "Polymer Miscibility", Academic Press, New York, 1979.

54. D.R. Paul and J.W. Barlow, "Multiphase Polymers", American Chemical Society, Washington DC, 1979.

55. G. Kerrult, H. Blumel and H. Weber, Kautsch. Gummi Kunststoffe, 22, 413 (1969).

56. M.E. Woods and J.A. Davison, Rubb. Chem. Technol., **49**, 112 (1976).

57. W.H. Wittington, Rubber Ind., **9**, 151 (1976).

58. V.A. Shershnev, Rubb. Chem. Technol., **55**, 537 (1982).

59. S.V. Usachev, N.D. Zakharov, V.N. Kuleznev and A.B. Vetoshkin, Int. Polym. Sci. Technol., **7(2)**, T/48 (1980).

60. N. Parasiewicz and R. Gacznski, Int. Polym. Sci. Technol., **6(8)**, T/95 (1979).

61. W. Parasiewicz and R. Gaczynski, Reports from the Rubber Symposium, Gottwaldov (September, 1975).

62. A.P. Plochocki, "Polymer Blends", Vol. 2, D.R. Paul and S. newmann, Eds., Ch. 21, Academic Press, New York, 1978.

63. V.L. Flot and R.W. Smith, Rubb. Chem. Technol., **46**, 1193 (1973).

64. J.L. White, Rubb. Chem. Technol., **50**, 163 (1977).

65. L.A. Goettler, J.R. Richwine F.J. Wille, Rubb. Chem. Technol., **55**, 1448 (1982).

66. L.F. Ramos-de Valle, Rubb. Chem. Technol., **55**, 1341 (1982).

67. S. Thomas, B.R. Gupta and S.K. De, Paper presented at the 33rd IUPAC International Symposium on macromolecules, Montreal July 8-13, 1990.

68. J.S.R. News, **5(6)**, 1 (1967).

69. M. Shundo, M. Imoto and Y. Minoura, J. Appl. Polym. Sci., **19**, 939 (1966).

70. W.M. Hess, C.E. Scott and J.E. Callon, Rubb. Chem. Technol., **40**, 371 (1967).

71. R.W. Smith and J.C. Andries, Rubb. Chem. Technol., **47**, 64 (1974).

72. P.A. Marsh, A. Voet and L.D. Price, Rubb. Chem. Technol., **40**, 359 (1967).

73. O. Glatter and O. Kratky, "Small-Angle X-ray Scattering", Academic Press, New York, 1982.

74. J.S. Higgins and R.S. Stein, J. Appl. Crystallogr., **11**, 346 (1978).

75. V.J. Mc Briert and D.C. DOuglass, Macromol. Rev., **16**, 295 (1981).

76. B. Albert, R. Jerome, P.ℎ Teyssie, G. Smith, N.G. Boyle and V.J. Mc Brierty, Macromolecules, **18**, 388 (19850.

77. T. Nishi, Rubb. Chem. Technol., **51**, 1075 (1978).

78. D.G. Cory, J.C. de Boer and W.S. Veeman, Macromolecules (in press).

79. F. Amrani, J.M. Hung and H. Morawetz, Macromolecules, **13**, 649 (1980).

80. H. Morawetz, Science, **240**, 172 (1988).

81. R. Gelles and C.W. Frank, Macromolecules, **15**, 1486 (1982).

82. J.L. Halary, J.M. Ubrich, J.M. Nunzi, L. Monnerie and R.S. Stein, Polymer, **25**, 956 (1984).

83. J.M. Ubrich, F.B. Cheikhlarbi, J.L. Halary, L. Monnerie, B.J. Baurer and C.C. Han, Macromolecules, **19**, 810 (1986).

84. G.H. Fredrickson and E. Helford, Macromolecues, **19**, 2601 (1986).

85. G.W. Gɪlby, "Development in Rubber Technology-3, Thermoplastic Rubbers", Applied Science Publishers, London, 1982, p.101-144.

86. E. Kovacs and D. Kallo, Int. Polym. Sci. Technol., **8(6)**, T/23 (1981).

87. G. Menzel, Kunststoffe, **69**, 480 (1979).

88. M. Matsuo, Japan Plastics, **2**, 6 (1968).

89. B. Terselins and B. Ranby, Pure Appl. Chem., **53**, 421 (1981).

90. T.S. Kowronski, J.F. Rabek and B. Ranby, Polym. Eng. Sci., **24**, 278 (1984).

91. S. Thomas, B.R. Gupta and S.K. De, Kaustsch. Gummi Kunststoffe **40**, 665 (1987).

92. M.L. Addonizio, L.D'Orazio and E. Martucelli, Polymer, **32**, 109 (1991).

93. C.S.L. Baker, W.G. Hallan and I.F. Smith, N.R. Technol., **5**, 4 (1974).

94. C.S.L. Baker, W.G. Hallan and I.F. Smith, N.R. Technol., **5**, 29 (1979).

95. A. Subramanyam, Proce. of RRIM, Planters Conference, Kuala Lumpur, 255 (1971).

96. A. Subramanyam, Rubb. Chem. Technol., **45**, 346 (1972).

97. E.B. Bagely, Trans. Soc. Rheol., 355 (1961).

98. B. Ellis and G.N. Welding, Rubb. Chem. Technol., **37**, 563 (1964).

99. W.D. Bascom, Rubb. Chem. Technol., **50**, 327 (1977).

100. N.M. Mathew and S.K. De, Polymer, **23**, 632 (1982).

101. G.J. Van Amerongen, Rubb. Chem. Technol., **37**, 1065 (1964).

102. G.M. Bristow and R.F. Tiller, Kautsch. Gummi Kunststoffe, **23(2)**, 55 (1970).

103. J.A.C. Harwood, "Rubber Technology and Manufacture", Butter-worths, London, 1985, p.56.

104. W. Hoffmann, "Vulcanisation and Vulcanising Agents", Maclaren and Sons Ltd., London, 207 (1967).

105. A.Y. Coran, "Hand book of Elastomers in New Developments and Technology", Marcel Dekker, New York, 249 (1988).

106. E. Martuscelli, Polym. Eng. Sci., **24**, 563 (1984).

107. C.E. Locke and D.R. Paul, Polym. Eng. Sci., **13**, 308 (1973).

108. N. Roy Choudhury, T.K. Chaki, A. Dutta and A.K. Bhowmick, Polymer, **30**, 2047 (1989).

109a. J.A. Brydson, "Flow Properties of Polymer Melts", 2nd ed., George Godwin, London, 1981.

109b. A.J. Tinker, Rubb. Chem. Technol., **63**, 503 (1990).

110. R.A. Mendelson and F.L. Finger, J. Appl. Polym., **19**, 1061 (1975).

111. C.D. Han and Y.W. Kinn, J. Appl. Polym. Sci., **18**, 2589 (1974).

112. H. Munstedt, Polym. Eng. Sci., **21**, 259 (1981).

113. T.Fujimura and K.Iwakura, Kobunshi Roubunshu, **31**, 671 (1979).

114. R.I. Tanner, J. Polym. Sci.,., A-2 **14(8)**, 2067 (1970).

115. N. Nakajimma and E.A. Collins, J. Rheol., **22**, 547 (1978).

116. T.C. Yu and C.D. Han, J. Appl. Polym. Sci., **17**(1973).

117. J.H. Southern and R.L. Ballman, Appl. Polym. Symp., **20**, 175 (1973).

118. S. Thomas, B.R. Gupta and S.K. De, J. Appl. Polym. Sci., **34**, 2053 (1987).

119. A. Stevenson, Kautsch. Gummi Kunststoffe, **37**, 105 (1984).

120. S. Thomas, Int. J. Polym. Meter., **12**, 1 (1987).

121. L. Baker, NR Technol., **18(1)**, 13 (1987).

122. J.R. Dunn, Rubb. Chem. Technol., **51**, 686 (1978).

123. S.D. Rozumovsku and G.E. Zai Kov, Developments in Polymer Stabilization, Applied Science Publishing Co. London, 1982.

124. H.R. Anderson, Rubb. Chem. Technol., **34**, 228 (1961).

125. S. Thomas, B.R. Gupta and S.K. De, Poly. Deg. & Stab., **18**, 189 (1987).

126. R. Elliot, Rubber Age, **1U(2)**, 60 (1974).

LIST OF PUBLICATIONS FROM THIS WORK

1. Vulcanisation kinetics and properties of NR-EVA blends. Indian Journal of Natural Rubber Research, **3(2)**; 77 (1990).

2. Studies on the effect of blend ratio and cure system on the degradation of natural rubber - ethylene-vinyl acetate copolymer blends. Polymer Degradation and Stability (accepted for publication).

3. Studies on the effect of blend ratio and cure system on X-ray, thermal, dynamic mechanical properties and microscopy of natural

•   rubber - ethylene-vinyl acetate copolymer blends. Polymer (communicated).

4. Melt rheology and elasticity of natural rubber - ethylene-vinyl acetate copolymer blends. Polymer Engineering & Science (communicated).

5. Effect of blend ratio and shear stress on the extrudate morphology of natural rubber - ethylene-vinyl acetate copolymer blends. Journal of Materials Science Letters (communicated).

6. Effect of silica on dynamic mechanical properties of NR-EVA blends. Journal of Materials Science (communicated).

7. Effect of silica on mechanical properties and degradation of NR-EVA blends. Kautschuk Gummi Kunststoffe (accepted for publication).

8. Studies on microcellular sheets from NR-EVA blends. Effects of blend ratio and fillers. Accepted for presentation at the International Natural Rubber Conference, 1992, Bangalore, India.